

**Fundamental and Applied Studies of Electrochemical Methods for the Detection of  
Polyanion and Polycation Species**

by

Andrea K. Bell-Vlasov

A dissertation submitted in partial fulfillment  
of the requirements for the degree of  
Doctor of Philosophy  
(Chemistry)  
in The University of Michigan  
2014

**Doctoral Committee:**

Professor Mark E. Meyerhoff, Chair  
Associate Professor Bart Bartlett  
Professor Kristina I. Hakansson  
Assistant Professor Kenichi Kuroda

*“It’s opener there, in the wide open air”*

*~Dr. Seuss*

©Andrea K. Bell-Vlasov

---

2014

## **DEDICATION**

This Work is Dedicated To:

My husband, Anton

My parents, Maryann and Terry

My sister, Angela

My best friends, Regina and Nicole

My Savior

Who provide love and encouragement in all my endeavors

## ACKNOWLEDGEMENTS

So many amazing people have impacted my life during my time spent at the University of Michigan, and I feel incredibly fortunate to have had the opportunity to cultivate relationships and share new experiences with them all. First and foremost, I would like to thank my advisor and academic father, Dr. Mark Meyerhoff, for his support and encouragement. He helped me realize what I am capable of and never allowed me to accept anything less than what came from my maximum efforts. He gave me courage to go into the professional world by reminding me “We all put our pants on one leg at a time”. His guidance and direction has been essential to my successes in my graduate career, which have ultimately improved the quality of the rest of my life. For this I am deeply grateful.

Thank you to Dr. Kristina Hakansson, Dr. Bart Bartlett, and Dr. Kenichi Kuroda for serving on my dissertation committee. I appreciate your helpful comments and suggestions, and all of the time you spent reading my thesis and attending my meetings.

I would like to thank Dr. Kebede Gemene, for teaching me everything he knew about the pulstrode. He also taught me patience and his support has been present even after his departure from our group. I must thank him for taking all of my long phone calls and answering my questions, regardless of his busy schedule. Thank you Dr. Lajos Hofler for teaching me the basics of potentiometry and how to do great research. He

taught me how to find the answers I needed to move forward and challenged me to think for myself.

The last five years I have spent working with truly amazing graduate students and undergraduates, and it is a great privilege to have been able to build relationships with them. Thank you to current and former graduate students Lin Wang, Jun Yang, Qinyi Yan, Laura Zimmerman, Natalie Crist, Wenyi Cai, Bo Peng, Liz Brisbois, Si Yang, Alex Wolf, Alex Ketchum, Zheng Zheng, Hang Ren, Joanna Zajda, Yaqi Wo, and undergraduate students Ananth Balijapalli, Dakota Suchyta, Alessandro Colletta, Tim Sippell and Ian VonWald. I would also like to thank the visiting professors and post docs who have contributed to my knowledge and experience here at U of M: Dr. Yu Qin, Dr. Lachlan Yee, Dr. Kun Liu, Dr. Gary Jensen, Dr. Dipankar Koley, Dr. Arun Agarwal, Dr. Xeuwei and Dr. Gergely Lautner. I am thankful for all of the lab gatherings, conversation, sharing of ideas, and support.

Thank you to Natalie Crist, who was my shoulder to lean on, especially on the hardest days, for being my partner in crime, and a true friend. Thank you to Si Yang and Bo Peng for introducing me to the world of Asian cuisine and providing unconditional friendship. Thank you to Joanna Zajda, a great gym partner, and a friend for life. I appreciate her hard work, expertise, and kindness. I thank Dr. Gary Jensen for his friendship and his ability to challenge me, not only in science, but also in all things. Thank you to Laura Zimmerman for her advice and for spiritual support. Thank you to Zheng Zheng, Ananth Balijapalli, Alex Wolf, Dr. Qin, and Alessandro Colletta for your hours spent editing chapters of my thesis. You have contributed to the success of this written dissertation and I am grateful.

Thank you to Roy Wentz, the department glass blower who made countless glass diffusion cells for me. His in depth spiritual conversations gave me much needed opportunity to escape my stress for a short while. Thank you to Patti Fitzpatrick for her dedication to making sure to order all of the chemicals I needed for my projects and supplies for the lab. She is truly a kind and patient woman for dealing with all of our questions on the constantly changing ordering systems.

I have also made lasting friendships with people who have helped me maintain my sanity here at the University of Michigan. Thank you to Heidi Alvey, who was always there when I needed her, for our grocery outings, late night T.V. sessions, and for standing up in my wedding and being a part of the best day of my life. Thank you to Laura Radecki and Yitian Chen for changing my life and introducing me to power lifting. I appreciate their great efforts to help me succeed in my lifting goals, especially Laura, who was committed to providing us with the best workouts ever.

Finally, I thank my family. They have seen me at my best and my worst and have supported me unconditionally. Thank you to my mom, Maryann. I wouldn't have made it this far without her in everything I have accomplished in life. She has been my driving force. Thank you to my dad, Terry, whose sound advice has kept me calm and focused. He has always known when I needed grounding. Thank you to my sister, Angela, and my two best friends, Regina and Nicole, for always being there to listen and to help me, and for being my personal cheerleaders. Thank you to Mick, for his unconditional and blind love. I love you all so much. Finally, I thank my husband, Anton, my true companion, who has always believed in me, wiped my tears away, and helped me to press on when I didn't think I could. I love you.

## TABLE OF CONTENTS

<b>DEDICATION</b> .....	ii
<b>ACKNOWLEDGEMENTS</b> .....	iii
<b>LIST OF FIGURES</b> .....	ix
<b>LIST OF TABLES</b> .....	xv
<b>ABSTRACT</b> .....	xvi
<b>CHAPTER 1 - INTRODUCTION</b> .....	1
<b>1.1 Ion-Selective Electrodes</b> .....	1
<b>1.2 Potentiometric Polyion Selective Electrodes</b> .....	3
1.2.1 <i>Equilibrium Response</i> .....	5
1.2.2 <i>Quasi-Steady State Response</i> .....	7
1.2.3 <i>Transport Studies</i> .....	8
<b>1.3 Chronopotentiometry and Polyion Sensitive Pulstrode</b> .....	10
1.3.1 <i>Pulstrode for Polycation Sensing</i> .....	12
1.3.2 <i>Pulstrode for Polyanion Sensing</i> .....	15
1.3.3 <i>Chronopotentiometric Detection of Protamine: Improving Detection Limits</i> ..	16
<b>1.4 Statement of Research</b> .....	17
<b>1.5 References</b> .....	21
<b>CHAPTER 2 - REVISITING THE RESPONSE MECHANISM OF POLYMERIC MEMBRANE BASED HEPARIN ELECTRODES</b> .....	23
<b>2.1 Introduction</b> .....	23
<b>2.2 Experimental</b> .....	27
2.2.1 <i>Membrane Preparation</i> .....	27
2.2.2 <i>Transport Cell Set-up</i> .....	27
2.2.3 <i>Impedance Measurements</i> .....	28
2.2.4 <i>Sample Preparation</i> .....	28
<b>2.3 Results and Discussion</b> .....	29
2.3.1 <i>Theory</i> .....	29
2.3.2 <i>Impedance Spectroscopy</i> .....	34
2.3.3 <i>Fractionation of Heparin</i> .....	35
2.3.4 <i>Electrochemical Characterization and Determination of Diffusion Coefficients for Fractionated Heparin in Plasticized PVC Films Doped with TDMAC Using Classic Potentiometry and Impedance Spectroscopy</i> .....	36
<b>2.4 Conclusions</b> .....	39
<b>2.5 References</b> .....	41
<b>CHAPTER 3 - DETECTION OF OVERSULFATED CHONDROITIN SULFATE CONTAMINANT/ADULTERANT IN COMMERCIALY AVAILABLE</b>	

<b>HEPARINS: A PRACTICAL APPLICATION OF POTENTIOMETRIC POLYANION SENSITIVE POLYMERIC MEMBRANE ELECTRODES</b> .....	42
<b>3.1 Introduction</b> .....	42
<b>3.2 Experimental</b> .....	45
3.2.1 <i>Polyion Sensor Preparation</i> .....	45
3.2.2 <i>Measurements in Commercial Lots of Heparin</i> .....	47
<b>3.3 Results and Discussion</b> .....	48
<b>3.4 Conclusions</b> .....	51
<b>3.5 References</b> .....	53
<b>CHAPTER 4 - POLYION SELECTIVE POLYMERIC MEMBRANE BASED PULSTRODE AS A DETECTOR IN FLOW-INJECTION ANALYSIS</b> .....	54
<b>4.1 Introduction</b> .....	54
<b>4.2 Experimental</b> .....	56
4.2.1 <i>Reagents</i> .....	56
4.2.2 <i>Preparation of Ion-Exchanger Salt</i> .....	56
4.2.3 <i>Membrane Preparation</i> .....	57
4.2.4 <i>Electrodes</i> .....	57
4.2.5 <i>Measurements</i> .....	57
4.2.6 <i>FIA Systems</i> .....	59
<b>4.3 Results and Discussion</b> .....	60
<b>4.4 Conclusions</b> .....	70
<b>4.5 References</b> .....	71
<b>CHAPTER 5 - MONITORING ENZYMATIC REACTIONS USING POLYMERIC MEMBRANE-BASED POLYION SELECTIVE PULSTRODES</b> .....	72
<b>5.1 Introduction</b> .....	72
<b>5.2 Experimental</b> .....	74
5.2.1 <i>Reagents</i> .....	74
5.2.2 <i>Preparations of Ion-Exchanger Salt</i> .....	74
5.2.3 <i>Membrane Preparation</i> .....	74
5.2.4 <i>Electrodes</i> .....	75
5.2.5 <i>Measurements</i> .....	75
<b>5.3 Results and Discussion</b> .....	76
5.3.1 <i>Mechanistic Response</i> .....	76
5.3.2 <i>Hexametaphosphate Measurements</i> .....	78
5.3.3 <i>Digestion of Hexametaphosphate by Acid Phosphatase</i> .....	79
5.3.4 <i>Enzyme Inhibitor Measurements</i> .....	82
<b>5.4 Conclusions</b> .....	84
<b>5.5 References</b> .....	85
<b>CHAPTER 6 - POLYION SELECTIVE POLYMERIC MEMBRANE-BASED PULSTRODE FOR THE DETECTION OF HIGH CHARGE DENSITY SPECIES IN HEPARIN PREPARATIONS</b> .....	86
<b>6.1 Introduction</b> .....	86
<b>6.2 Experimental</b> .....	87
6.2.1 <i>Reagents</i> .....	87
6.2.2 <i>Preparation of Ion-Exchanger Salts</i> .....	88

6.2.3 Polymeric Membrane Preparation .....	88
6.2.4 Electrodes .....	88
6.2.5 Measurements Using Polymeric Membrane Configuration .....	89
<b>6.3 Results and Discussion</b> .....	89
<b>6.4 Conclusions</b> .....	98
<b>6.5 References</b> .....	99
<b>CHAPTER 7 - CONCLUSIONS AND FUTURE DIRECTIONS</b> .....	100
7.1 Summary of Results and Contributions .....	100
7.2 Future Work.....	103
7.3 References.....	110

## LIST OF FIGURES

- Figure 1.1:** Scheme of ion-selective membrane. Target ion activity is constant within the aqueous inner filling solution phase, therefore the membrane potential changes in response to change of the target ion concentration in the aqueous sample phase. 2
- Figure 1.2:** Overall potentiometric responses to (A) chondroitin sulfate, (B) heparin, and (C) dextran sulfate at 1 mg/mL. Approximate  $\Delta\text{EMF}$  for each polyion are as follows; (A)  $\sim$ -35 mV, (B)  $\sim$ -50 mV, and (C)  $\sim$ -100 mV. Measurements were made in separate solutions in a background of 120 mM NaCl in phosphate buffer, pH 7.4. 6
- Figure 1.3:** Sensor response to concentrations of heparin and OSCS within the analytical working range of the polyion sensor. 8
- Figure 1.4:** Polyanion extraction from the sample phase into the membrane phase. (A) Polyanion added to the sample phase and (B) Polyion extraction into the membrane phase to make a cooperative ion-pair with TDMA<sup>+</sup>, where the phase boundary potential,  $\Delta\Phi_{\text{pb}}$ , at the sample/membrane interface decrease. 9
- Figure 1.5:** Conventional three-electrode set-up for pulstrode: Working electrode housing the sensing membrane, a platinum counter electrode, and a double-junction reference electrode. 11
- Figure 1.6:** (A) Current-time behavior and (B) potential-time behavior, where I is the galvanostatic pulse, II is the open circuit zero current pulse where data is sampled and averaged over the last 10% of the pulse period, and III is the potentiostatic pulse. (C) Structures of lipophilic salt species used to prepare polyion sensing pulstrode membrane. 13
- Figure 1.7:** Membrane configurations during each pulse of pulstrode system; Pulse I denotes the direction of the ion-flux under an anodic current pulse, Pulse II shows the membrane during open circuit measurement where the ion-exchanger forms a complex with the target analyte, and Pulse III demonstrates the voltage pulse where 14

ions that were pulled in during Pulse I are expelled. Ion notations are as follows:  $P^{z-}$  is polyanion,  $A^-$  is the interfering ion ( $Cl^-$ ), and  $I^+$  is the counterion ( $Na^+$ ),  $R^+$  is the anion of the lipophilic ion-exchanger salt ( $TDMA^+$ ) and  $R^-$  is the cation of the lipophilic ion-exchanger salt.

- Figure 2.1:** Sketch of transport cell set-up. Ag/AgCl wires were used for reference and working electrodes and cells were stirred throughout the data acquisition period. The ISM is the ion-selective polymer membrane containing TDMACl that is sensitive to heparin. 28
- Figure 2.2:** a) Finite-element simulation of the potential response curve of a 100  $\mu m$  membrane. The membrane is conditioned in 50 mM interfering ion (chloride) solution. At 0 h the primary ion (heparin) concentration is set to 5 mg/mL in the sample solution. Arrows show the range used for the linear regression. b) Concentration profiles of heparin in the membrane at 10, 20, 40, 80, 160, 320, 640, and 1280 min after the addition of 5 mg/mL in the sample solution. 31
- Figure 2.3:** Results of gel electrophoresis of various heparin preparations; (A) contains fractionated heparin, (B) contains unfractionated heparin, and (C) contains enoxaparin (low molecular weight heparin). Heparins were introduced onto the gel at the left of the figure (left side negative(-), right side positive(+)). Gel was run at 16 W for 1.5 h. 36
- Figure 2.4:** Dynamic potentiometric response curves of ion-selective membranes containing TDMACl with thicknesses of 60.1  $\mu m$ , 76.5  $\mu m$ , 180.5  $\mu m$ , and 193.5  $\mu m$ , from left to right, respectively, after addition of 5 mg/mL of heparin to the frontside of the membrane. 37
- Figure 2.5:** (A) Potentiometric response curve of a 300  $\mu m$  ion-selective membrane. (B) Bulk resistance of the ion-selective membrane, the dots are the experimental results, the solid line is the theoretical response curve based on Equation 7. Note: The potentiometric curve in Figure 2.5A was generated from the same membrane used to map resistance as function of time in Figure 2.5B. Potentiometric curves in Figure 2.4 were generated from different membranes. 39
- Figure 3.1:** Different glycosaminoglycans and their respective potential changes in a background solution of 120 mM NaCl/10 mM phosphate buffered saline. 44

- Figure 3.2:** Polyion sensor arrangement where the conditioned polyion selective sensor, made from dip-coating PVC tubing with membrane cocktail, is inserted onto the end of a 1 mL Eppendorf pipette tip. 47
- Figure 3.3:** Experimental set-up. All measurements were made using three heparin sensors to obtain a mean voltage change  $\pm$  standard deviations for all samples tested. The larger circle contains an enlarged view of the experimental cell. Heparin sensors were approximately 1.5 cm in length extending from the narrow end of a 1 mL Eppendorf pipette tip. 48
- Figure 3.4:** EMF changes of two contaminated samples (A and B) and two clean samples (C and D) with amounts of OSCS determined by NMR data provided by Baxter Inc. Each sample was measured with three sensors to obtain standard deviations. Average potential and standard deviations are as follows: (A) Avg = -78.3 mV, s.d. = 2.11 mV; (B) Avg. = 79.9 mV, s.d.= 2.32 mV, (C) Avg. = -52.8 mV, s.d. = 1.59 mV; (D) Avg. = -55.3 mV, s.d = 1.24 mV. 50
- Figure 4.1:** Schematic diagram of the flow-injection system coupled with polyion selective polymeric membrane-based pulstrode used for the experiments reported. 58
- Figure 4.2:** Movement of salt and ions within membrane and at interfaces during pulse sequence employed for detection of polyanions using anodic current pulse in FIA arrangement. The polyion is represented by  $P^{z-}$ , the interfering ions by  $I^{+}$  and  $A^{-}$ , and  $R^{+}$  and  $R^{-}$  are the  $TMDA^{+}$  and  $DNNS^{-}$  ions of the lipophilic ion-exchanger salt within the membrane phase. It should be noted that smaller anions ( $A^{-}$ ) also enter outer surface of sensing membrane during pulse 1 period, but are eventually outcompeted for serving as the counteranions to  $R^{+}$  sites by the polyanions ( $P^{z-}$ ). 61
- Figure 4.3:** Dynamic potentiometric response of polyion pulstrode to (A) protamine; duplicate sequential injections of standards in range from 10  $\mu\text{g/mL}$  - 100  $\mu\text{g/mL}$ ; and (B) heparin; duplicate sequential injections of standards in range from 40  $\mu\text{g/mL}$  - 200  $\mu\text{g/mL}$  in 10 mM phosphate buffer, pH 7.4, with 10 mM NaCl present. The diluent stream was the same buffer solution and flow rates were set at 0.6 mL/min. Numbers above and below peaks represent concentrations in  $\mu\text{g/mL}$ . Every 100 pulses is  $\sim$ 30 min. 62
- Figure 4.4:** Open circuit potentiometric response of polymeric membrane electrode to  $10^{-3}$  M KBr (A) before pulstrode measurements; (B) 64

after 500 pulse sequences in flow mode, anodic current applied during galvanostatic pulse; (C) after 3 d in flow system with no galvanostatic pulsing, and (D) after 500 pulse sequences in flow mode with cathodic current applied during galvanostatic pulse. All measurements were conducted in 10 mM phosphate buffer, pH 7.4, containing 10 mM NaCl.

- Figure 4.5:** (A) Calibration of DEMF response (peak voltage – baseline voltage) to protamine in flow-injection mode in 10 mM phosphate buffer, pH 7.4, containing 100 mM NaCl. It should be noted that standard deviation for n=3 injections at each concentration is so small that it cannot be observed for some data points; (B) Response to increasing concentrations of heparin with a constant concentration of 60  $\mu\text{g/mL}$  protamine present in test sample in 10 mM phosphate buffer, pH 7.4, containing 100 mM NaCl. Data in (B) represents testing with three different sensors with the same membrane composition in the FIA system, where standard deviation was calculated using data from all three sensors. Flow rates for both A and B were set at 0.6 mL/min. 67
- Figure 4.6:** Dynamic potentiometric response to repeated injections (n=20) of 60- $\mu\text{g/mL}$  protamine in 10 mM phosphate buffer, pH 7.4 containing 100 mM NaCl. A sampling rate of approximately 20 samples per hour has been achieved. For data shown, the average DEMF = 33.7 mV  $\pm$  1.42 mV (n=20). Flow rate was set at 0.93 mL/min. 69
- Figure 5.1:** Schematic of polyanion substrate degradation by enzyme. (A) Separate measurement sensor responses to intact polyanion and digested polyanion. Scales for the potentiograms are the same. (B) Sensor response during an enzymatic reaction where the polyanion is added to a background solution and the enzyme is injected once the signal to the polyion is stable. A reversal in signal is observed due to the digestion of the substrate. 78
- Figure 5.2:** (A) Dynamic response and (B) calibration curve for hexametaphosphate in 1 mM NaCl, 10 mM MES buffer. For substrate digestion to be observed using pulstrode, a large concentration within the linear must be selected to monitor the enzymatic activity. The concentration used in all experiments was 40  $\mu\text{g/mL}$  hexametaphosphate. 79
- Figure 5.3:** (A) Potentiometric data for enzyme activities of 0.15, 0.25, 0.35, 0.5, and 0.75 U/mL in 40  $\mu\text{g/mL}$  hexametaphosphate, 1 mM NaCl, 10 mM MES buffer. (B) Enlarged graph of the first ~2 min of EMF vs. time curves after injection of 0.35 U/mL acid phosphatase activity. 81

- Figure 5.4:** Rate of potential change vs. acid phosphatase activity, where  $n=6$ . 81  
All measurements were made in 40  $\mu\text{g/mL}$  hexametaphosphate, 1 mM NaCl, 10 mM MES buffer, pH 5.2.
- Figure 5.5:** Discontinuity in reversal in signal induced by 1 U/mL acid 82  
phosphatase in 40  $\mu\text{g/mL}$  hexametaphosphate, 1mM NaCl, and 10 mM MES buffer, pH 5.2.
- Figure 5.6:** Effect of inhibitor concentration on acid phosphatase activity at 83  
0.75 U/mL. The inset shows the linearity of data points between 0 and 0.00025% inhibitor solution.
- Figure 6.1:** Potentiometric data for 5 (black asterisk), 4 (red asterisk), 3 (blue 90  
asterisk), 2 (green asterisk), and 1 wt% (purple asterisk) PPS in 400  $\mu\text{g/mL}$  heparin, 1 mM NaCl, 10 mM phosphate buffer. A 1 s, 10  $\mu\text{A}$  current pulse, 0.5 s open-circuit pulse, and 15 s potentiostatic pulse was applied.
- Figure 6.2:** Detection limits for 1, 2, 3, 4 and 5 wt% PPS in heparin 91  
preparations. A 1 s, 10  $\mu\text{A}$  current pulse, 0.5 s open-circuit pulse, and 15 s potentiostatic pulse was applied. At 5 wt% PPS, the detection limits are half of what has been calculated for 1 wt%. No linearity is observed.
- Figure 6.3:** Response to heparin and heparin spiked with PPS. Measurements 92  
for 400  $\mu\text{g/mL}$  heparin followed by heparin spiked with 10 wt% PPS (annotated with \*), where pulse sequence was a 1 s, 20  $\mu\text{A}$  current pulse, a 0.5 s open-circuit pulse, and a 15 s, 0 V potentiostatic pulse. Averages and standard deviations of measurements for heparin and 10 wt% PPS are -97.0 and  $\pm 0.693$  mV, and -106 and  $\pm 0.873$  mV, respectively. The average difference between pure heparin and PPS spiked heparin is -8.67 mV with standard deviation of  $\pm 0.473$  mV.
- Figure 6.4:** Potential changes associated with different time lengths of open- 93  
circuit measurements. Each point represents the average potential change for a given time length. For the above points, standard deviations are as follows: (0.5 s) 0.515 mV, (1 s) 6.15 mV, (2 s) 2.62 mV, (5 s) 9.62 mV, and (10 s) 6.02 mV. A 1 s, 15  $\mu\text{A}$  current pulse and a 15 s potentiostatic pulse were applied.
- Figure 6.5:** Membrane concentration profile scheme. As current polarizes the 95  
membrane, the concentration of salt components increase at opposite interfaces of the membrane. The purple and green traces represent TDMA<sup>+</sup> and DNNS<sup>-</sup>, respectively, migrating towards the opposite interfaces. The red and blue lines represent TDMA<sup>+</sup>

and DNNS- at their final concentrations, just before the open-circuit zero-current pulse is applied.

**Figure 6.6:** The dynamic response for 1 s 10  $\mu$ A current measurements for heparin and heparin samples spiked with 5 wt% PPS. Measurements of heparin spiked with 5% PPS are noted with asterisks (\*). 97

**Figure 7.1:** Examples of structures of linear and branched fucoidans found in brown seaweed. (A) Linear fucoidan harvested from *fucus evanescens* (species of brown seaweed) and (B) branched fucoidan harvested from *chorda filum* (species of brown seaweed). 104

## LIST OF TABLES

<b>Table 3.1:</b>	Potentiometric responses and standard deviations for sensors used to measure Baxter samples. <sup>a</sup>	51
<b>Table 6.1:</b>	Average potential change for heparin (0% PPS), 10 wt% PPS in heparin, and the average potential difference between the two measurements. For all measurements, n=3, except for 10 and 20 $\mu\text{A}$ , where n=7. The blue highlighted data represents the ideal current magnitude for detection of high charge density species (PPS) in heparin preparations with polymeric membrane compositions.	97

## ABSTRACT

### **Fundamental and Applied Studies of Electrochemical Methods for the Detection of Polyanion and Polycation Species**

by

Andrea K. Bell-Vlasov

**Chair:** Mark E. Meyerhoff

Potentiometric polyion sensors have many advantages and potentially important applications in the clinical/biomedical field. Although conventional polyion sensors have been applied for detecting a wide range of polyionic analytes and enzymes that can depolymerize these species, they are essentially single-use devices, which limit broader applications, especially in automated flow-through analytical methods. Within the last ten years, reversible chronopotentiometric polyion sensors (pulstrode) have been developed to overcome the limitations of the single-use devices. In this thesis, further mechanistic studies and a quality control application of the single-use polyion sensors are examined, and additional development and novel applications of the newer pulstrode type polyion sensor systems are reported. First, the mechanism of potentiometric response of the single-use polyanion sensor is re-examined. Using fractionated heparin void of low molecular weight heparins, the extraction and transport of macromolecular heparin into

the polymer membrane of the sensor as a complex with tridodecylmethylammonium ion is reconfirmed, and diffusion coefficients of  $2.7 \times 10^{-9} \text{ cm}^2 \text{ s}^{-1} \pm 0.27$  for the complex are found. Such polyanion sensors are then employed in detecting the presence of oversulfated chondroitin sulfate (OSCS) contaminant/adulterant in commercially available lots of heparin from Baxter, Inc. Results using the polyanion sensor are found to correlate 100% with NMR data.

In the second portion of this research, a reversible pulstrode type polyanion sensor is applied to study three different systems. The pulstrode is utilized for the first time as a detector in flow-injection analysis (FIA). The system is capable of measuring both polycations and polyanions in the 10-100  $\mu\text{g/mL}$  and 40-200  $\mu\text{g/mL}$  range, respectively, using the same sensor/membrane formulation with a sample throughput of up to 20 samples/h. The pulstrode is also employed in monitoring enzymatic reactions, where hexametaphosphate/acid phosphatase is used as a model substrate/enzyme system. The rate of reversal in potentiometric polyanion signal indicates the rate of digestion of the polyanionic substrate, hexametaphosphate, and hence the amount of enzyme activity present. Lastly, the pulstrode's parameters (current pulse magnitude, etc.) are optimized to improve the detection limits in the application of this sensor to detect high charge density contaminants in heparin preparations, achieving an LOD of 2 wt% for pentosan polysulfate in heparin.

## CHAPTER 1

### INTRODUCTION

#### **1.1 Ion-selective Electrodes**

Polymeric membrane-based ion-selective electrodes (ISE) are commonly used to monitor the activities/concentrations of biologically important ions, such as  $\text{Na}^+$  and  $\text{K}^+$ , and are also now used to measure pH. Such devices are based on incorporating lipophilic ion-exchangers and/or ionophores within the organic membranes that are capable of selectively interacting with target anions or cations within the sample phase. The predictable and reproducible responses of ISEs, along with their ability to make measurements in turbid solutions (e.g., whole blood) make these sensors ideal for rapidly determining concentrations of biologically important analyte ions.<sup>1-4</sup>

ISEs monitor ion activity by measuring the potential difference between two membrane interfaces: the inner solution/membrane interface and the sample/membrane interface. The ISE membrane potential of the inner solution/membrane interface is considered constant since the ion activity within the inner filling solution of the electrode does not change. Therefore, the overall membrane potential is a function of the phase boundary potential developed at the sample/membrane interface that is dependent on the equilibrium of the analyte ion across that interface with components in the membrane

(e.g., ionophore) (Figure 1.1). This membrane potential is added with the other potentials that occur in series for the measurement cell, including the potential of the inner reference electrode (e.g., Ag/AgCl) and the external reference electrode. The overall cell potential that is measured is mathematically described by the Nernst equation:

$$E = K + \frac{RT}{zF} \ln a$$

where  $E$  is the membrane potential,  $K$  is the sum of all constant components of the overall cell potential,  $a$  is the target analyte activity in the sample phase,  $R$  is the gas constant,  $T$  is temperature,  $F$  is Faraday's constant, and  $z$  is the charge of the target analyte ion. Data outputs from ISEs are voltage per activity/concentration, and should exhibit a Nernstian slope equal to  $RT/zF = 59.2 \text{ mV}/z.^2$  Therefore, as the analyte charge increases, the system's sensitivity to small concentration changes diminishes (i.e., the Nernstian slope decreases).

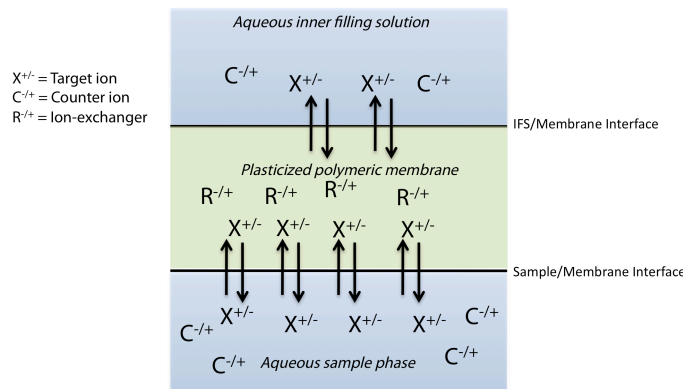


**Figure 1.1. Scheme of ion-selective membrane. Target ion activity is constant within the aqueous inner filling solution phase: therefore, the membrane potential changes in response to change of the target ion concentration in the aqueous sample phase. Note that  $R^{+/-}$  may also be an ionophore.**

Based on the general ISE response mechanism, which requires the target ion to participate in an equilibrium reaction across the membrane/sample interface, it was once thought that larger multi-valent polyion analytes could not be measured because the observed signal would be too small to be analytically useful, and the chances that such larger ionic species could actually be extracted and interact via an equilibrium process with lipophilic species (ion-exchangers and/or ionophores) within the polymeric organic phase was considered unlikely. However, optimization and development of ISE membrane compositions in the early 90's led to the development of the first polyion sensors, a breakthrough that yielded unexpectedly large EMF signal changes to low concentrations (e.g.,  $\mu\text{g/ml}$ ) of higher molecular weight polyionic analytes (e.g., heparin, pentosan polysulfate, protamine, etc.).

## **1.2 Potentiometric Polyion Selective Electrodes**

Polyion selective sensors were pioneered by the Meyerhoff group in the early 90's and have been employed in variety of applications including heparin detection in whole blood (its first application),<sup>5-8</sup> monitoring enzymatic activity,<sup>9</sup> monitoring protamine assays,<sup>10</sup> determining carrageenan in food products,<sup>11</sup> and its most recent application, detection of toxic, high charge density polyanionic contaminants (i.e., oversulfated chondroitin sulfate) in commercially available heparins.<sup>12</sup>

Heparin is a polydisperse glycosaminoglycan (GAG) with a charge density of  $\sim -70$ .<sup>13</sup> It is an anticoagulant which is administered during procedures such as open-heart surgery<sup>14</sup> or used therapeutically for conditions like deep vein thrombosis.<sup>15</sup> It is important to monitor polyanionic heparin due to its association with dangerous side

effects such as hemorrhaging/bleeding.<sup>16</sup> The most common method used to monitor heparin activity is the Active Clotting Time (ACT) assay. The ACT assay measures the time it takes for whole blood to clot before, during, and after surgeries like cardiopulmonary bypass (CPB).<sup>17</sup> Although ACT is commonly used in clinical settings, it has slow response times, lacks specificity and yields results which are easily perturbed by many variables (e.g., patients with lupus, hypothermia, factor deficiencies, and diseases that impact platelet count and function like thrombocytopenia).<sup>18-20</sup> However, polyion sensors can monitor heparin in whole blood and provide rapid measurements with good selectivity, avoiding the shortcomings of ACT.<sup>5-8</sup> In addition, protamine, the antidote for heparin (when it forms a strong, neutral complex with heparin), can also be monitored indirectly with the heparin sensor<sup>10</sup> via heparin titration or monitored directly with a protamine sensor (+20/molecule charge), where the polymeric membrane is modified (in comparison to the heparin sensor) to give the sensor protamine selectivity.<sup>21</sup>

During the development of this sensor, efforts were made to determine the optimal membrane composition for the detection of heparin, which has a charge density of  $\sim -70$ . Various ion-exchangers were doped into plasticized polymeric membranes, and the resulting EMF response to heparin was examined.<sup>6</sup> It was determined that 1.5 wt% tridodecylmethylammonium chloride (TDMACl) doped into a poly(vinyl chloride) (PVC) membrane plasticized with dioctyl sebecate (DOS) provided the optimal heparin response. Heparin and other polyanions make strong cooperative ion-pairs with TDMA<sup>+</sup> species, displacing chloride, and therefore enhance membrane polyion selectivity over other simple anionic species such as Cl<sup>-</sup>. Although sensors doped with ion-exchangers (in the absence of ionophores) should exhibit responses to anions predicted by the

Hofmeister series<sup>2</sup> (e.g., based on lipophilicity of anions), large super-Nernstian responses were observed in the presence of very hydrophilic heparin when the sensor was not conditioned in the target analyte (e.g., heparin) prior to measurements.

Efforts were also made to improve detection limits by optimizing the polymer:plasticizer ratio.<sup>7</sup> Changing the ratio to 2:1 polymer to plasticizer improved the detection limits (unlike classical ISEs, which typically have a polymer:plasticizer ratio of 1:2). This more rigid membrane composition limits diffusion of heparin into the membrane, causing a large EMF change at the membrane/sample interface at even lower concentrations of heparin in the sample. Two mechanisms were found to fully describe the response behavior of this sensor: (1) the equilibrium response and (2) the quasi-steady state response.<sup>7</sup>

### *1.2.1 Equilibrium Response*

In the presence of large concentrations of polyanion (assuming the membrane has not been conditioned in the target polyion and only in physiological phosphate buffer) or for very long conditioning/equilibration times in buffer containing the polyanion, Cl<sup>-</sup> ions in the membrane phase will be fully displaced at the sample/membrane interface by the target polyion analyte. A large decrease in the phase boundary potential of the sample/membrane interface occurs due to the association of the polyanion with the TDMA<sup>+</sup> sites within membrane. This initial potential change saturates immediately in the presence of such high concentrations of the polyion to the so-called equilibrium response, which is not analytically useful (e.g., for heparin, <-1 mV/decade). However, the overall potential change is calculated by subtracting the baseline potential from the

equilibrium potential, and this value distinguishes polyions based on their difference in charge density since the overall potential change increases proportional to the charge density.<sup>8</sup> This is due to the thermodynamics of extraction of the different polyanions to form ion-pairs with the TDMA<sup>+</sup> species. Figure 1.1 demonstrates the different responses observed to chondroitin sulfate (CS), heparin, and dextran sulfate (DS), where the charge densities increase in the order of CS < heparin < DS.

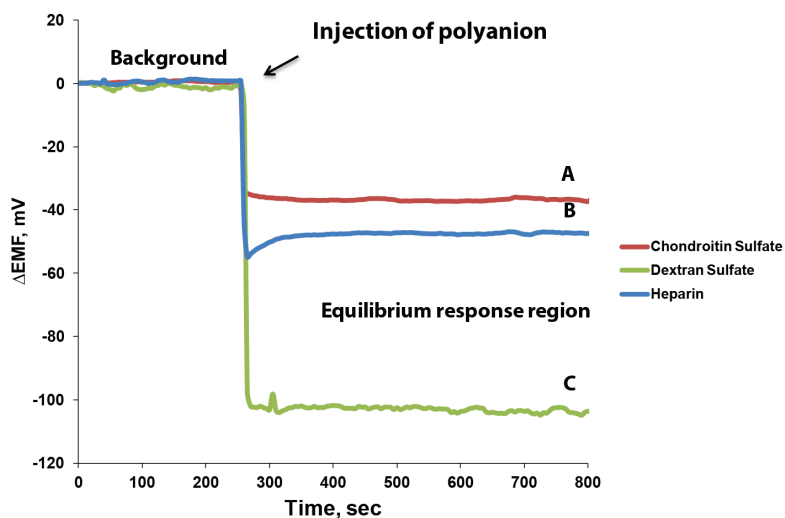


**Figure 1.2. Overall potentiometric responses to (A) chondroitin sulfate, (B) heparin, and (C) dextran sulfate at 1 mg/ml. Approximate  $\Delta$ EMF for each polyion are as follows; (A)  $\sim$ 35 mV, (B)  $\sim$ 50 mV, and (C)  $\sim$ 100 mV. Measurements were made in separate solutions in a background of 120 mM NaCl in phosphate buffer, pH 7.4.**

This phenomenon allowed Wang et al. to demonstrate the feasibility of detecting oversulfated chondroitin sulfate (OSCS),<sup>12,22</sup> a lethal and high charge density contaminant that was found in commercially available heparins in 2008 (by NMR and capillary electrophoresis), and caused many deaths. Indeed, in the simultaneous presence of two polyanions with different charge densities, the sensor response is governed by the

larger charge density analyte because the cooperative ion-pair formation thermodynamically favors analytes with higher charge densities.

Although the heparin sensor is an accurate, robust, and reproducible method of detecting heparin and other high charge density polyanions, it is a single-use device. Due to the strong cooperative ion-pairing between the polyanions and the TDMA anion-exchanger, polyanion dissociation is extraordinarily slow, and thus the sensor is rendered incapable of repeated use. However, within the last ten years, reversible polyion sensor technology has been developed to address these issues.<sup>24-27</sup> Additional discussion of this topic can be found in Section 1.3, below.

### *1.2.2 Quasi-Steady-State Response*

The useful analytical working range of the polyion sensor is limited over a relatively narrow concentration and is dictated by a non-equilibrium response mechanism, which is best described as a quasi-steady-state EMF response.<sup>7</sup> At very low concentrations, the polyion is pulled into the membrane to form a complex, or cooperative ion-pair, with the ion-exchanger. The target polyions diffuse from the sample phase into the polymer membrane surface, thermodynamically driven by polyion/ion-exchanger complex formation. While extraction of polyion from the sample phase is occurring, the cooperative ion-pair simultaneously diffuses into the bulk of the membrane at a slower rate (i.e., the rate limiting step) owing to the small diffusion coefficient of such complexes within the highly viscous polymeric phase. A steady-state phase boundary potential at the membrane/sample interface can be observed when the rate of polyion mass transport to the surface of the polymer membrane is equal to the rate

of the polyion-TDMA complex moving into the bulk of the polymer membrane phase. Such steady-state response is analytically useful to determine concentrations of the polyion. However, with extended time, no matter what concentration of polyion is present in the sample, a gradual drift down in the EMF values to the equilibrium response (i.e., over a ~24 h period after sample introduction) is observed (Figure 1.2). As the polyion/ion-exchanger complex migrates across the membrane, it will eventually break through to the backside interface, and a reversal of EMF signal is observed (changes the phase boundary potential at the inner solution/membrane interface). Recent studies, however, have questioned whether a large heparin/TDMA complex is capable of this membrane bulk-diffusion.<sup>28-32</sup>

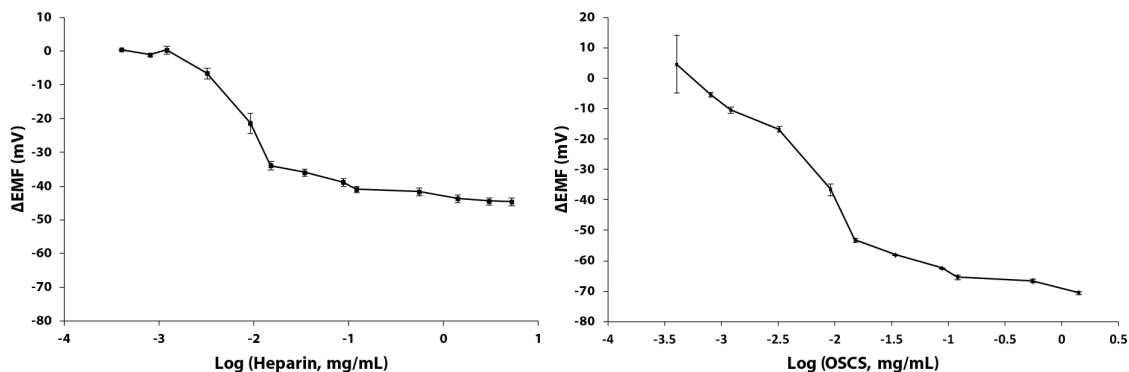


**Figure 1.3. Sensor response to concentrations of heparin and OSCS within the analytical working range of the polyion sensor.**

### 1.2.3 Transport Studies

Since the quasi-steady-state model is highly dependent on the polyanion extraction into the membrane, heparin transport studies were conducted during its early development to confirm this mechanism. Transport studies involved equilibrating

membranes for long time periods while monitoring the membrane potential response to heparin as it was extracted into the membrane (Figure 1.3) as well as spectrophotometrically monitoring fluorescein-labeled heparin with multiple layers of polyion sensing membranes.<sup>7</sup>

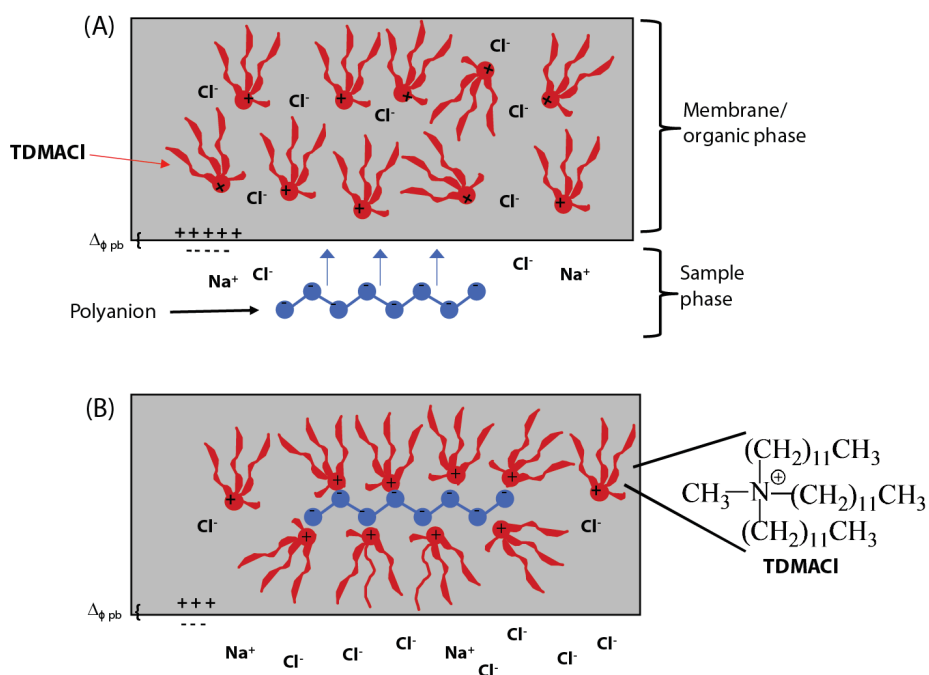


**Figure 1.4. Polyion extraction from the sample phase into the membrane phase. (A) Polyion added to the sample phase and (B) Polyion extraction into the membrane phase to make a cooperative ion-pair with TDMA<sup>+</sup>, where the phase boundary potential,  $\Delta\phi_{pb}$ , at the sample/membrane interface decreases.**

Recent literature, on the other hand, suggested that the response mechanism used to describe the sensor was not completely valid, as heparin may not be capable of penetrating the membrane in this fashion.<sup>28-32</sup> In these recent studies, voltammetry and amperometry were employed to measure unfractionated heparin. It was suggested that high molecular weight (HMW) heparin might only adsorb to the surface of the membrane with limited extraction into the membrane phase. Amemiya and co-workers studied

heparin transport across a liquid/liquid interface of two immiscible electrolyte solutions (ITIES) via voltammetry.<sup>28-30</sup> Since heparin is very polydispersed, this study concluded that only low molecular weight (LMW) heparin could penetrate the organic phase. Similar conclusions were made by Samec and co-workers, who reported amperometric studies that employed glassy carbon electrodes coated in plasticized membranes doped with different ion-exchangers.<sup>31,32</sup> These recent studies suggest that the reversal in potentiometric signal reported by Meyerhoff and co-workers might have been a result of LMW heparins being extracted into the membrane, while HMW heparins were only adsorbed to the surface. These reports prompted a re-evaluation of the heparin sensor mechanism,<sup>33</sup> as described extensively in Chapter 2 of this thesis.

### **1.3 Chronopotentiometry and Polyion Sensitive Pulstrodes**

A chronopotentiometric method for *reversible* detection of polyions was pioneered by the Bakker group in the early 2000's.<sup>23-26</sup> In the early stages of its development, this reversible method was used to determine concentrations of Na<sup>+</sup> and K<sup>+</sup>.<sup>27</sup> The experimental set-up consisted of three conventional electrodes: working, counter, and reference (Figure 1.4).

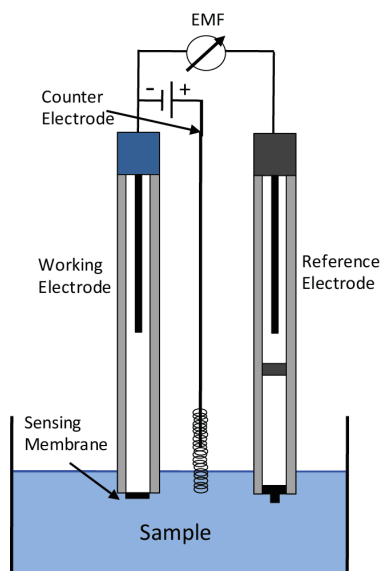


**Figure 1.5. Conventional three-electrode set-up for pulstrode: the working electrode houses the sensing membrane and the platinum counter electrode and a double-junction reference electrode complete the electrochemical cell.**

The working electrode functioned as the sensing membrane, which was doped with a  $\text{Na}^+$  ionophore and a lipophilic supporting electrolyte. The sensing membrane had no intrinsic ion-exchange properties. A typical measurement consisted of a two-pulse sequence: a galvanostatic (current) pulse, employed to polarize the membrane and induce an ion-flux towards the sample/membrane interface, and a potentiostatic pulse, designed to depolarize the membrane and regenerate the original phase boundary at the sample/membrane interface by expelling ions pulled in during the current pulse. Potentiometric data was collected during the current pulse. The galvanostatically-controlled system is tunable and allows for adjustment of several parameters that cannot be controlled in conventional potentiometric experiments. The current magnitude regulates the concentrations of extracted ions and the observed selectivity. For example, in these early experiments, potential response to  $\text{Na}^+$  is observed over  $\text{K}^+$  since the sensor

is doped with a sodium-selective ionophore. This experiment is carried out using lower current magnitudes (-1 to -15  $\mu\text{A}$ ) where the uptake of  $\text{Na}^+$  is assisted by the ionophore as well as the current. In contrast, if the current magnitude exceeds -25  $\mu\text{A}$ , the sensor response is no longer assisted by the ionophore, and the potential response to  $\text{K}^+$  is observed due to the greater lipophilicity of  $\text{K}^+$  over  $\text{Na}^+$ . In addition to controlling selectivity, the type of ion (cation vs. anion) that is extracted is also controlled by the direction of current so that cations and anions can be measured with the same membrane formulation (though not necessarily the formulation mentioned above). Therefore, the magnitude and direction of ion fluxes (induced by the current pulse) across the ion-selective membrane is another factor that can be controlled.

The innovation of implementing a galvanostatic pulse allows for greater flexibility in experimental conditions without reformulating the sensor membrane, as is required in classical potentiometry and the non-classical polyion sensors. Most significantly, the development of this chronopotentiometric method directly addresses the problems associated with irreversible single-use potentiometric polyion sensors, and is a springboard towards future advances in polyion sensing (see below).

### *1.3.1 Pulstrode for Polycation Sensing*

In 2004, modifications were made to the previous system reported by Bakker and co-workers for the detection of the polycation protamine.<sup>24</sup> An additional third pulse was added to the original two-pulse sequence, providing a sequence order as follows: a 1.0 s galvanostatic pulse, a zero-current open-circuit pulse of 0.5 s, and a 15 s potentiostatic pulse.<sup>25</sup> The additional open-circuit pulse measurement can be directly compared to open

circuit potentiometry. The data is sampled at the end of the open circuit pulse in contrast to the original method and provides measurements without the undesirable  $iR$  drop observed in potential data collected during the current pulse. It should be noted that during a typical measurement, raw data is collected for both current and potential during all three pulses (Figure 1.5A and 1.5B).

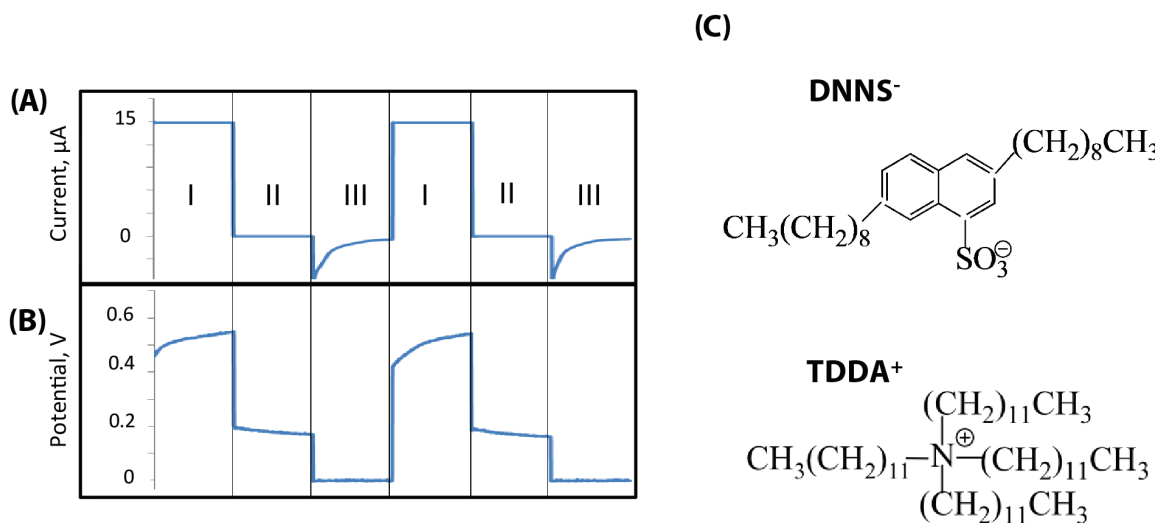


**Figure 1.6. (A) Current-time behavior and (B) potential-time behavior, where I is the galvanostatic pulse, II is the open circuit zero current pulse where data is sampled and averaged over the last 10% of the pulse period, and III is the potentiostatic pulse. (C) Structures of lipophilic salt species used to prepare polyion sensing pulstrode membrane.**

Another major sensor modification pioneered by Bakker and co-workers was replacing the sodium selective ionophore and lipophilic supporting electrolyte with a dinonylnaphthalene sulfonate (DNNS<sup>-</sup>): tetradodecylammonium (TDDA<sup>+</sup>) salt (Figure 1.5C). Protamine (an arginine rich low molecular weight polycationic protein that neutralizes heparin activity) makes a strong cooperative ion-pair with DNNS<sup>-</sup>, and when a cathodic current is pulsed, the sensor displays protamine selectivity. This cathodic current pulse applied to the sensor polarizes the ion-exchanger salt so that the DNNS<sup>-</sup>

migrates to the sample/membrane interface, causing the interface to become a cation-exchanging interface. During the zero current pulse, DNNS<sup>-</sup> can then exchange small inorganic ions, such as Na<sup>+</sup>, for protamine, since protamine is the more preferred ion for the cooperative ion-pairing reaction with the DNNS<sup>-</sup> species. Potentiometric data obtained using this method, termed ‘pulstrode’, is collected as an average of the last 10% of the open circuit EMF measurement data, in contrast to the original set-up, where potentiometric data was collected during the current pulse (Figure 1.6). These differences distinguish the two methods that use the same instrument: the former is called chronopotentiometry and the latter method is termed ‘pulstrode’ by Bakker and co-workers. Chronopotentiometry is useful for monitoring changes at concentrations in the millimolar range, whereas the pulstrode configuration allows for measurements in systems where the membrane resistance is large (no *iR* drop observed during open-circuit measurement period) and/or for measurements in lower concentration ranges (in respect to cations/polycations).<sup>24</sup>

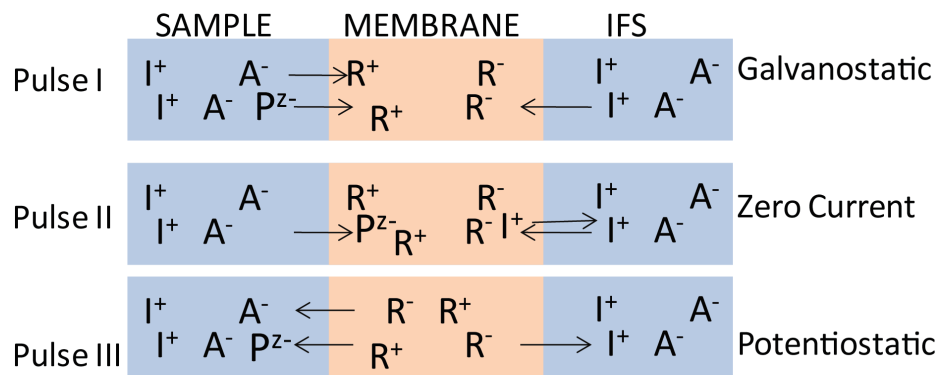


**Figure 1.7. Membrane configurations during each pulse of pulstrode system; Pulse I denotes the direction of the ion-flux under an anodic current pulse, Pulse II shows the membrane during open circuit measurement where the ion-exchanger forms a complex with the target analyte, and Pulse III demonstrates the voltage pulse where ions that were pulled in during Pulse I are expelled. Ion notations are as follows: P<sup>z-</sup> is polyanion, A<sup>-</sup> is the interfering ion (Cl<sup>-</sup>), and I<sup>+</sup> is the counterion (Na<sup>+</sup>), R<sup>+</sup> is the anion of the lipophilic ion-exchanger salt (TDMA<sup>+</sup>) and R<sup>-</sup> is the cation of the lipophilic ion-exchanger salt.**

### 1.3.2 Pulstrode for Polyanion Sensing

The pulstrode system is also capable of measuring polyanions in addition to polycations such as protamine, if a directional reversal of applied current during the galvanostatic pulse is implemented. The ion-exchanger salt used in the pulstrode is effective since protamine can form a strong cooperative ion-pair with  $\text{DNNS}^-$  when cathodic current is applied. However, although the  $\text{DNNS}^-$  contained within the pulstrode membrane can form a cooperative ion-pair with polycations such as protamine when cathodic current is pulsed, for polyanion sensing with the same membrane, the cation of the partner ion-exchanger salt must be able to make a strong cooperative ion-pair with the target polyanion when anodic current is pulsed. In 2010, Gemene et al. reported successful detection of glycosaminoglycans (GAGs) (e.g., CS, heparin, OSCS, pentosan polysulfate (PPS)) with a pulstrode type sensor. The ion-exchanger salt had been changed to a  $\text{DNNS}^-/\text{TDMA}^+$  salt (see Figure 1.3 for structure of  $\text{TDMA}^+$ ) in order to improve the observed response when measuring these specific GAGs.<sup>34</sup> During the development of the single-use heparin sensor in the 90's, many quaternary ammonium species were examined and their ion-exchange/ion-pairing properties assessed with respect to heparin detection. Very little response to heparin was observed for  $\text{TDDA}^+$  doped membranes, due to the quaternary- $\text{N}^+$  being sterically hindered by the four long alkyl chains of the molecule. On the other hand,  $\text{TDMA}^+$  has only three long alkyl chains and one methyl group; consequently, the quaternary- $\text{N}^+$  is more easily accessible for heparin to form a strong cooperative ion-pair. The use of  $\text{TDMA}^+$  as a partner to  $\text{DNNS}^-$  has led to the development of other pulstrode applications.<sup>35</sup>

### *1.3.3 Chronopotentiometric Detection of Protamine: Improving Detection Limits*

Protamine detection limits in physiological NaCl have recently been improved by reformulating the sensing membrane and monitoring the voltage during the current pulse instead of the zero-current open-circuit measurement period.<sup>35</sup> In the developing stages of the pulstrode, the 1:1 molar ratio of the ion-exchanger salt was essential to obtain stable and reproducible measurements. Great care must be taken in synthesizing the salt so that the 1:1 molar ratio is achieved. Recently, a new ion-exchanger salt with a 2:1 molar ratio of DNNS<sup>-</sup>: TDDA<sup>+</sup> was reported. In addition to modifying the ion-exchanger salt composition, a porous polypropylene membrane was utilized as a scaffold to hold the new ion-exchanger salt dissolved into a plasticizer. This differs from the original formula, which incorporated the ion-exchanger salt into a plasticized polymeric membrane. Essentially, the porous polypropylene allows for a much thinner membrane with very low resistance. The original 1:1 TDDA/DNNS sensing membrane also had no intrinsic ion-exchange properties, as mentioned above, in contrast to the 100% molar excess of DNNS<sup>-</sup> in the 2:1 ratio of DNNS<sup>-</sup>: TDDA<sup>+</sup>, which is ion-exchanging, without the assistance of the pulse sequence. The excess DNNS<sup>-</sup> forms a complex with protamine and the extra protamine inside the membrane now prevents interfering ions like Na<sup>+</sup> from being extracted into the membrane during the current pulse by the law of mass action, and consequently decreases the detection limits in the presence of physiological NaCl.<sup>35</sup>

Another major difference between this method and the polyion sensing pulstrode method is the data acquisition. The potentiometric data is collected during the current pulse, and the length of this pulse is also extended beyond 1 s to ensure depletion of the target analyte. In addition, the sequence of pulses is re-arranged: (1) open-circuit pulse,

(2) current pulse, and (3) potentiostatic pulse. During the current pulse, the voltage is monitored and an inflection in signal is observed when the diffusion layer is depleted of the target analyte. The time it takes for the inflection in signal to appear (transition time) increases as the target analyte concentration increases. The magnitude of the current pulse can also be manipulated to alter the linear response of the sensor. As the magnitude of the current increases, the linear range is shifted to larger concentrations. Smaller current magnitudes are incapable of depleting the diffusion layer of the target analyte at high concentrations; an inflection point in the potentiometric data cannot be distinguished. By increasing the magnitude of the current, larger concentrations of target analyte can be depleted, and a shift in linear range is observed. This method has applications in monitoring protamine in whole blood and heparin indirectly by observing a decrease in concentration of protamine due to the neutral complex formed between heparin and protamine.<sup>36</sup>

#### **1.4 Statement of Research**

In this dissertation, applications of existing and newer electrochemical detection methods of polyions are explored. In Chapter 2, the mechanism of the previously developed single-use heparin sensor, based on heparin diffusion through the membrane, is re-examined in response to recent reports that suggest that heparin is only adsorbed to the surface of the membrane. Electrochemical impedance spectroscopy is employed to monitor heparin diffusion into polyion sensing membranes. Further, purified heparin is employed for these experiments to remove low molecular weight components. Gel electrophoresis is utilized to visually confirm the molecular weight differences of fractionated, unfractionated, and low molecular weight heparins. In addition to those

experiments, transport cells are used to monitor the EMF of membrane over a 72 h period as heparin is extracted into the membrane. To validate the established mechanism, an equation, derived from Fick's II law and the Nernst equation, is used to calculate the diffusion coefficients of heparin through membranes of various thicknesses. The work in Chapter 2 was published in *Electroanalysis* (2012, 24, 53-59).

In Chapter 3, the biomedically relevant application of heparin sensors for the detection of high charge density species (i.e., OSCS) in real heparin samples is described. Heparin samples provided by Baxter, Inc. are analyzed and compared to NMR data (also provided by Baxter). A 100% correlation between results from the heparin sensor method and the reported NMR data is found.

Chapter 4 focuses on the use of the reversible pulstrode sensor as a detector in a flow-injection analysis (FIA) system. The newer ion-exchanger salt (DNNS/TDMA) has the advantageous potential ability to measure both polycations and polyanions with the same sensor and the *same* membrane formulation simply by changing the direction of current. A cathodic current is applied to measure polycations and anodic current is applied for polyanion detection. In contrast to the single-use sensors, the ability of the pulstrode system to regenerate the initial state of the membrane allows for system automation. These two advantages permit pulstrode functionality as a detector in FIA. This method has applications in monitoring enzymatic activity and has higher throughput capabilities, compared to the static mode (absence of flowing solution). Both protamine and heparin are measured and used to demonstrate this new concept. Experiments are carried out to determine the stability and sensor reproducibility in the flow-injection mode. Based on protamine/heparin titration measurements in physiological NaCl

concentrations, a possible application for monitoring heparin in whole blood is suggested, although such blood experiments have not yet been optimized for this system. This subject is discussed in more detail within Chapter 7. The research in Chapter 4 was published in *Analytical Chemistry* (**2014**, *86*, 4041-4046).

Chapter 5 demonstrates the application of the pulstrode device in monitoring enzymatic reactions. The degradation of the substrate hexametaphosphate by acid phosphatase is used as a model system. The potential induced by the substrate is monitored and the addition of the enzyme induces a reversal in the signal indicative of the degradation of the substrate. The enzymatic reaction rate is calculated from the slopes in the EMF reversal during the first two min after injection of the enzyme while the rates of reaction increase as the activity of the enzyme increases. The effects of adding enzyme inhibitor are also examined. A decrease in enzyme activity, as the concentration of enzyme inhibitor increases, is observed and represented by a slower reversal in EMF signal for one given enzyme activity level.

It should be noted that single-use polyion sensors have been successfully employed for enzyme assays previously.<sup>9,10</sup> Polyion digestion in enzymatic reactions is easily observed upon measurement with potentiometric polyion sensors. The main limitation of single-use polyion sensors is their irreversible nature. When these sensors are employed in monitoring enzymatic reactions, a change in potential towards the baseline *is* observed, but the signal never fully reaches the baseline. This may be due to the polyion-TDMA<sup>+</sup> pair diffusing further into the membrane, where a small proportion of these pairs may not be accessible for enzymatic cleavage. Consequently, as the dissociation of the cooperative ion-pair is slow, the sensor cannot be used twice.

Therefore, the pulstrode addresses the problem of irreversibility of the single-use sensor in this application.

In Chapter 6, the use of the pulstrode for the detection of higher charge density species as contaminants in heparin is investigated. Although the detection of high charge density species in heparin with detection limits as low as those reported for single-use polyion sensors<sup>12</sup> (0.5 wt% OSCS in heparin) have yet to be achieved due to the pulstrode system's kinetics (explained in more detail in Chapter 6), optimization of system parameters including length of current pulse, length of open-circuit pulse, and magnitude of current pulse, are explored. Pentosan polysulfate (PPS) is used as a model for high charge density species doped into heparin preparations and detection limits of this species in a heparin background are determined.

In Chapter 7, conclusions, along with plans for future work, are presented. Moreover, applications for a reformulated membrane for reversible polyion sensors and a different data acquisition method, as well as further applications for the pulstrode system coupled with FIA are discussed.

## 1.5 References

- [1] Bard, A. J; Faulkner, L. R., *Electrochemical Methods: Fundamentals and Applications* 2<sup>nd</sup> ed.; Harris, D., Ed.; Wiley: New York, 2001; p 110.
- [2] Morf, W. E., *The Principles of Ion-Selective Electrodes and of Membrane Transport*; Elsevier Scientific: New York, 1981.
- [3] Fraticelli, Y. M.; Meyerhoff, M. E., *Anal. Chem.* **1982**, *54*, 27R-44R.
- [4] Buck, R. P., *Sensors and Actuators* **1981**, *1*, 197-260.
- [5] Ma, S.; Yang, V.; Meyerhoff, M., *Anal. Chem.* **1992**, *64*, 694-697.
- [6] Ma, S.; Yang, V.; Fu, B.; et. al., *Anal. Chem.* **1993**, *65*, 2078-2084.
- [7] Fu, B.; Bakker, E.; Yun, J.; et. al., *Anal. Chem.* **1994**, *66*, 2250-2259.
- [8] Fu, B.; Bakker, E.; Yang, V.; et. al., *Macromolecules* **1995**, *28*, 5834-5840.
- [9] Esson, J.; Meyerhoff, M., *Electroanalysis* **1997**, *9*, 1325-1330.
- [10] Yun, J. H.; Meyerhoff, M. E.; Yang, V. C., *Anal. Biochem.* **1995**, *224*, 212-220.
- [11] Hassan, S.; Meyerhoff, M.; Badr, I., *Electroanalysis* **2002**, *14*, 439-444.
- [12] Wang, L.; Buchanan, S.; Meyerhoff, M., *Anal. Chem.* **2008**, *80*, 9845-9847.
- [13] Linhardt, R. J., *J. Med. Chem.* **2003**, *46*, 2551-2564.
- [14] Hunt, B. J.; Segal, H. C.; Yacoub, M., *J. Thorac. Carciovasc. Surg.* **1992**, *104*, 211-212.
- [15] Wakefield, T. W., *J. Vasc. Surg.* **2004**, *31*, 613-620.
- [16] Walenga, J. M.; Frenkel, E. P.; Bick, R. L., *Hematol. Oncol. Clin. N.* **2003**, *17*, 259-282.
- [17] Hattersley, P. G., *Am. J. Clin. Pathol.* **1976**, *66*, 899-904.
- [18] Despotis, G. J.; Hogue, C. W.; Saleem, R.; et. al., *Anesth. Analg.* **2001**, *93*, 28-32.
- [19] Feindt, P.; Volkmer, I.; Seyfert, U.; et. al., *Thorac. Cardiov. Surg.* **1993**, *41*, 9-15.
- [20] De Jong, M. A., *J. Extra. Corpor. Technol.* **1999**, *31*, 76-79.
- [21] Yun, J. H.; Meyerhoff, M. E.; Yang, V. C., *Anal. Biochem.* **1995**, *224*, 212-220.
- [22] Wang, L.; Meyerhoff, M. E., *Electroanalysis* **2010**, *22*, 26-30.
- [23] Shvarev, A.; Bakker, E., *J. Am. Chem. Soc.* **2003**, *125*, 11192-11193.
- [24] Makarychev-Mikhailov, S.; Shvarev, A.; Bakker, E., *J. Am. Chem. Soc.* **2004**, *126*, 10548-10549.
- [25] Shvarev, A.; Bakker, E., *Anal. Chem.* **2005**, *77*, 5221-5228.
- [26] Xu, Y.; Shvarev, A.; Makarychev-Mikhailov, S.; Bakker, E., *Anal. Biochem.* **2008**, *374*, 366-370.

- [27] Shvarev, A.; Bakker, E., *Anal. Chem.* **2003**, *75*, 4541-4550.
- [28] Guo, J.; Yuan, Y.; Amemiya, S., *Anal. Chem.* **2005**, *77*, 5711-5719.
- [29] Rodgers, P.J.; Jing, P.; Kim, Y.; Amemiya, S., *J. Am. Chem. Soc.* **2008**, *130*, 7436-7442.
- [30] Jing, P.; Kim, Y.; Amemiya, S., *Langmuir* **2009**, *25*, 13653-13660.
- [31] Langmaier, J.; Olsak, J.; Samcova, E.; et. al., *Electroanalysis* **2006**, *2*, 115-120.
- [32] Langmaier, J.; Olsak, J.; Samcova, E.; et. al., *Electroanalysis* **2006**, *13-14*, 1329-1338.
- [33] Bell, A. K.; Höfler, L.; Meyerhoff, M. E., *Electroanalysis* **2012**, *24*, 53-59.
- [34] Gemene, K.; Meyerhoff, M. E., *Anal. Chem.* **2010**, *82*, 1612-1615.
- [35] Crespo, G. A.; Afshar, M. G.; Bakker, E., *Angewandte* **2012**, *51*, 12575-1257.
- [36] Bakker, E.; Crespo, G. A.; Afshar, et. al., *Chimica*, **2013**, *67*, 350-350.

## CHAPTER 2

### REVISITING THE RESPONSE MECHANISM OF POLYMERIC MEMBRANE BASED HEPARIN ELECTRODES

#### 2.1 Introduction

A series of studies carried out by this research group nearly 2 decades ago focused on developing a simple potentiometric sensor to monitor levels of the anticoagulant heparin in whole blood.<sup>1-4</sup> It was found that a plasticized polymer (PVC) membrane doped with tridodecylmethylammonium chloride (TDMACl) could yield significant and analytically useful *EMF* response to heparin. The heparin response was attributed to the ability of the TDMA<sup>+</sup> cationic sites in the membrane to form a strong cooperative ion-pair with heparin, and extract heparin species into the membrane phase.<sup>4</sup> The overall theory for the observed potentiometric response was developed based on two different response regimes to heparin: 1) the equilibrium potentiometric response at high concentrations of heparin; and 2) the quasi non-equilibrium steady-state response that occurs only at low concentrations of the polyanion. The equilibrium response is induced using high concentrations of heparin (e.g., >1 mg/mL) and a rapid anion exchange takes place at the sample/membrane interface (Cl<sup>-</sup> is exchanged for heparin). The surface of the membrane reaches equilibrium with the sample quickly and the response can be predicted by the Nernst equation as applied for a polyionic species with a large negative charge, e.g. -70 (slope of < 1 mV/decade). A large change in potentiometric signal (ca. -

50 mV) is observed initially to any added heparin in this higher concentration region and is due to a voltage difference in phase boundary potential between the front and backside of the membrane. This voltage difference is caused by a change in charge separation that is induced when the highly negative charge of heparin (ca. -70) interacts with the positively charged TDMA<sup>+</sup> in the membrane phase with a very favorable free energy change of  $11.42 \text{ kJ}\cdot\text{mol}^{-1}z^{-1}$  (where  $z$  is the charge on the polyanion).<sup>4</sup>

The sensor can also detect heparin via a significant *EMF* vs. concentration dose-response at lower, clinically relevant levels of  $\sim 10^{-7} \text{ M}^{1,3}$  (e.g.,  $\mu\text{g}/\text{mL}$  range). At these low concentrations, the membrane response is described by a quasi-steady state non-equilibrium mechanism.<sup>3</sup> Here, the flux of polyanion toward the surface of the membrane must be equal to the rate of heparin diffusing (as a complex with TDMA<sup>+</sup>) into the bulk of the membrane away from the sample/membrane interface. This response cannot be explained by the Nernst equation, since it only occurs under non-equilibrium conditions. Indeed, changes in stirring rate<sup>3</sup> or preparing rotating electrode type devices<sup>5</sup> can be used to alter the concentration range of heparin that can be detected. However, no matter what experimental conditions are employed, after long equilibration times ( $\sim 24 \text{ h}$ ), the expected full equilibrium response to heparin of ca.  $-1 \text{ mV}/\text{decade}$  is observed even at these lower concentrations.

The quasi-steady state model is highly dependent on the extraction of heparin into the organic membrane phase. Therefore, experiments were conducted to determine if extraction of heparin into the membrane does indeed take place via fluorophore labeled heparin as well as long-term potentiometric measurements.<sup>3</sup> In one set of experiments, after the addition of high concentrations of heparin and the initial large negative *EMF*

response toward heparin is observed, after several hours, a reversal in the potentiometric signal occurs.<sup>3</sup> At the time of these experiments, this reversal in the signal provided evidence of heparin extraction into the polymer films, since such a result should only occur if heparin reaches the backside of the membrane and changes the phase boundary potential at that interface, canceling the voltage change on the front-side of the membrane. Further, using fluorescein labeled heparin and multi-layers of TDMACl doped plasticized PVC membranes that can be peeled apart after long-term equilibration with solutions containing heparin, the fluorophore labeled species were found to be present in the middle layers. Together, the results of these experiments suggested that heparin is likely extracted into the bulk of the organic polymer membrane phase.

Recently, there have been other electrochemical studies that suggest that heparin does not diffuse into the bulk of organic phases containing lipophilic anion exchangers like TDMA<sup>+</sup>, but is only adsorbed at the aqueous/organic interface.<sup>6-10</sup> These studies employ voltammetry/amperometry and examine a liquid/liquid interface of two immiscible electrolyte solutions (ITIES)<sup>8-10</sup>, or use glassy carbon electrodes coated with a plasticized PVC membrane.<sup>6,7</sup> Samec and co-workers employed amperometry with a rotating glassy carbon electrode coated with an *o*-nitrophenyl octyl ether (*o*-NPOE) plasticized membrane doped with different anion-exchangers, including TDMA<sup>+</sup>, and a negligible response to heparin was observed.<sup>6</sup> However, another study compared the response mechanism of membranes doped with hexadecyltrimethylammonium (HTMA<sup>+</sup>) and TDMA<sup>+</sup> and reported that the amperometric response of the electrode coated with the membrane doped with TDMA<sup>+</sup> was governed by the transport of the heparin complex with the TDMA<sup>+</sup> inside the organic membrane phase, unlike the response of the

membrane doped with HTMA<sup>+</sup>, which was governed by adsorption of the heparin at the sample-membrane interface.<sup>7</sup> Amemiya and co-workers employed voltammetric methods utilizing ITIES to analyze the response to heparin.<sup>10</sup> It was concluded that unfractionated heparin could only be adsorbed to the surface of the organic phase at the sample/organic phase interface owing to the large and narrow current peak observed on the reverse sweep seen on the cyclic voltammograms. This was hypothesized to represent heparin being desorbed quickly at the liquid (aqueous)/liquid (organic) interface as the voltage was decreased. In another study conducted by Amemiya and co-workers, Arixtra, a heparin mimetic with a molecular weight of only 1.5 kDa, was examined using the same techniques.<sup>9</sup> Cyclic voltammograms showed a much smaller and broader current peak on the reverse sweep, which indicated that Arixtra was indeed extracted into the organic phase doped with TDMACl.<sup>9</sup> The authors further concluded that if any heparin were to be extracted and diffuse into organic phases, it would likely be the low-molecular weight species.

It is possible that the data reported by Amemyia et al.<sup>8-10</sup> as well as that originally reported by our group<sup>1-4</sup> may have been a result of only low MW components of unfractionated heparin being extracted and transported. In fact, unfractionated heparin is a heterogeneous mixture of sulfonated/carboxylated polysaccharides, with an average MW of 15 kDa, but with some fraction of species < 10 kDa.<sup>13,14</sup> Therefore, in this paper, results of experiments to determine whether extraction/diffusion into/through plasticized PVC membranes containing TDMACl occurs when using a fractionated heparin preparation that contains predominantly high MW fractions are reported. The extraction/diffusion of the fractionated heparin is determined by two independent

methods; *EMF* reversal of the polymer membrane response and impedance spectroscopy of the heparin sensitive polymeric membrane used to prepare heparin/polyanion sensors.

## **2.2 Experimental Section**

### *2.2.1 Membrane Preparation*

Membranes were made using 32.5% by weight poly(vinyl chloride) (PVC) (high molecular weight, Fluka), 66% by weight dioctyl sebecate (DOS) (Fluka), and 1.5% by weight TDMACl (26.2 mM) (Fluka). This mixture was dissolved in distilled tetrahydrofuran (THF) (Fisher) to yield 100 mg/mL mixture, at volumes of 750 mL or 1500 mL (yielding membranes of ca. 100 and 200 mm thick, respectively) that were cast into glass rings (25 mm diameter) and left to dry overnight. Once the films were dry, they were conditioned in 50 mM NaCl for 24 to 48 h.

### *2.2.2 Transport Cell Setup*

A single membrane was placed between two glass cells as part of the transport cell set-up (see Figure 1). The donor solution contained 5 mg/mL heparin sodium salt ( $8.3 \times 10^{-5}$  M using 15 kDa as average MW) in 50 mM NaCl background solution and the recipient cell also contained 50 mM NaCl. Both cells contained a stir bar and a total volume of 6 mL. A Ag/AgCl wire was placed inside each cell to monitor the transmembrane potential and connected to a Lawson Labs high impedance 8-channel voltmeter (Pennsylvania, USA). Each cell was stirred continuously throughout a 68 to 72 h data acquisition period. The thicknesses of the membranes were measured using a gravimetric method<sup>11</sup> and these values were used in the final calculation of the heparin diffusion coefficients within the membrane phase.

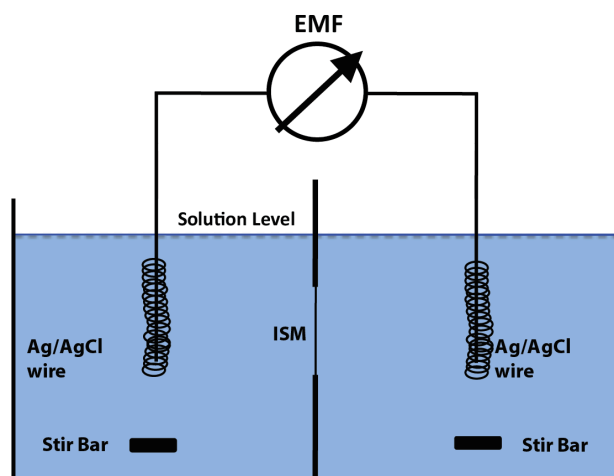


**Figure 2.1. Sketch of transport cell set-up. Ag/AgCl wires were used for reference and working electrodes and cells were stirred throughout the data acquisition period. The ISM is the ion-selective polymer membrane containing TDMACl that is sensitive to heparin.**

### *2.2.3 Impedance Measurements*

For impedance measurements, the same membrane formulation and transport cell setup was used. The impedance spectra were recorded (EG&G instruments, model 6310) (Tennessee, USA) in the frequency range of 100 kHz to 1 Hz using a sinusoidal excitation signal with amplitude of 5 mV and DC potential used was the open circuit potential of the system.

### *2.2.4 Sample Preparation*

Fractionated heparin samples were prepared using 10 000 molecular weight cut-off tubes, centrifuged 3 times at 4000 rpm in a background solution of 50 mM NaCl, and re-diluted to a final concentration of 30 mg/mL. The fractionation was confirmed by gel electrophoresis. Fifty mL of 20% polyacrylamide gel (Fisher) was prepared with 300 mL of a 10% filtered ammonium persulfate (Fisher) solution and 30  $\mu$ L of tetramethylethylenediamine (TEMED) (BioRad). The gel was pre-run at 16 W for 30

min using a 1x Tris/Borate/EDTA (TBE) (Fisher) as the running buffer (pH 8.0). Heparin and enoxaparin (LMW heparin preparation) samples for gel were prepared as above at concentrations of 5 mg/mL. A volume of 10  $\mu$ L per lane for each sample was loaded onto the gel and was run at 16 W for 1.5 h. The gel was stained for 30 min with a 10x dilution of a mixture containing 0.1% (w/v) toluidine blue-o, 50% (v/v) methanol (Fisher), 10% (w/v) acetic acid (Fisher), 0.25% glycerol (Fisher), 4 mM Tris base (Fisher), and 0.1 mM EDTA (Fisher). All appropriate preparations were prepared using Milli-Q grade deionized water (18.2 MW, Millipore Corp., Billerica, MA).

## **2.3 Results and Discussion**

### *2.3.1 Theory*

The diffusion coefficient of ions in the polymer membrane can be assessed in a single ion-breakthrough experiment. The *EMF* of a primary ion-free membrane (Note: in this case heparin is considered as primary ion, but the theory is also valid for any ionic species) is measured in a symmetrical electrochemical cell. Initially there is a constant concentration of interfering ions on both sides of the membrane (i.e., chloride in the case of the TDMACl-based membrane). After a stable membrane potential is reached, a high concentration of heparin or primary ion is injected into the sample solution side of the membrane. By the application of the phase boundary potential model<sup>15</sup> it can be proven that the slope of the reverse potential response curve only depends on the diffusion coefficient in the membrane and the thickness of the membrane.

The  $EMF$  value for a symmetrical electrochemical cell with negligible diffusion potential according to the phase-boundary potential model<sup>16,17</sup> is given by the following expression:

$$EMF = E_f - E_b \quad (1)$$

where  $EMF$  is the electromotive force,  $E_f$  and  $E_b$  are the phase boundary potentials at the front and the backside of the membrane. Once the high concentration of heparin is added, the aqueous and outer (sample side) membrane phases equilibrate with the heparin via favorable anion-exchange, with heparin displacing chloride in the outer region of the organic membrane phase. The phase boundary potential at the backside of the membrane is governed by the interfering ion (chloride) concentration until significant amounts of heparin reach the interface. The aqueous phase boundary concentration of chloride within the internal solution is assumed to be constant for the entire course of the experiment due to the high concentration of chloride. During the initial period of the experiment (first 1–2 h) the membrane phase boundary concentration of heparin on the backside is 0 until the first molecules of heparin reach that backside interface (when voltage starts reversal in Figure 2.2a). Of course, the time required for the backside of the organic membrane phase to reach full equilibrium (with all chloride replaced by heparin) and the cell potential to level off (long time period), depends on the thickness of the membrane employed. Further, given the favorable equilibrium constant for heparin ion-pairing with  $TDMA^+$  in the membrane phase, even after long periods of time (i.e., 30 h) there is little or no heparin within the inner aqueous phase boundary layer ( $c_J(aq) = 0$ ).

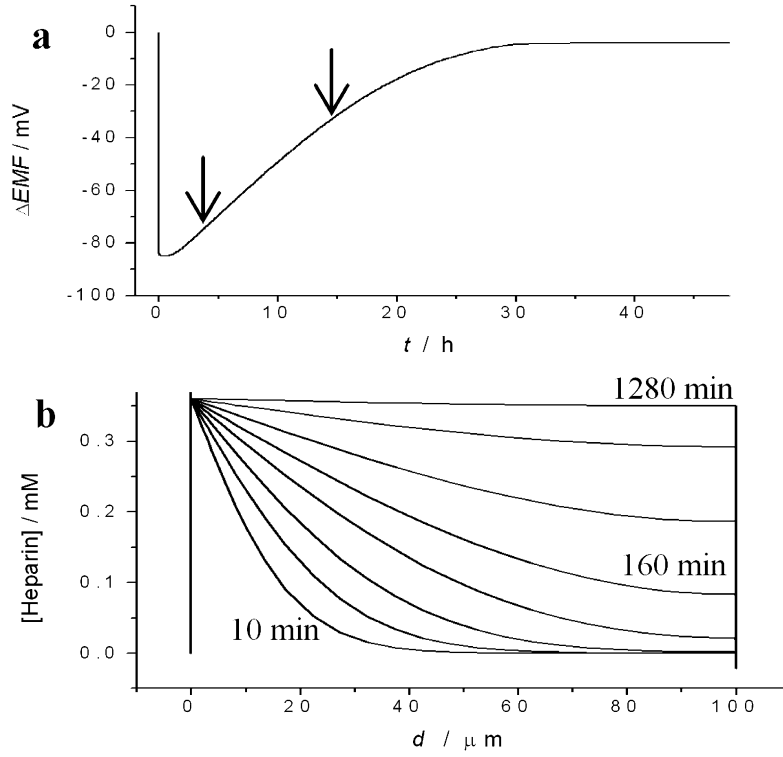


**Figure 2.2.** a) Finite-element simulation of the potential response curve of a 100  $\mu\text{m}$  membrane. The membrane is conditioned in 50 mM interfering ion (chloride) solution. At 0 h the primary ion (heparin) concentration is set to 5 mg/mL in the sample solution. Arrows show the range used for the linear regression. b) Concentration profiles of heparin in the membrane at 10, 20, 40, 80, 160, 320, 640, and 1280 min after the addition of 5 mg/mL in the sample solution.

Applying these considerations, an equation where the only time dependent term is the interfering ion concentration ( $\text{Cl}^-$  in this case) at the inner membrane boundary (backside) can be obtained,  $c_J(\text{org})$ .

$$EMF = E_f - \frac{RT}{z_J F} \ln \frac{k_J c_J(\text{aq})}{c_J(\text{org})} = E^0 - \frac{RT}{z_J F} \ln \frac{1}{c_J(\text{org})} \quad (2)$$

where,  $k_J$  is a direct function of free energy of transfer of the interfering ion,  $c_J(\text{aq})$ ,  $c_J(\text{org})$  are the concentration of interfering ion in aqueous solution and the membrane, respectively. The  $z_J$  is the valence of the interfering ion.  $F$ ,  $R$ , and  $T$  are the Faraday

constant, the gas constant and the temperature, respectively. It is important to note that the Equation 2 is also valid when an ionophore is present in the ion-selective membrane (ISM), and the introduction of an equilibrium constant changes the  $E^\circ$  but the only time dependent term remains the  $c_J(\text{org})$  term.

Due to the diffusion of heparin through the membrane, when it arrives to the backside of the membrane it replaces the chloride. The total concentration of negatively charged polyanions in the membrane is determined by the concentration of the lipophilic cationic sites, TDMA<sup>+</sup> ( $R_T$ ), in the membrane phase ( $RT=z_I c_I(\text{org})+z_J c_J(\text{org})$ ). By applying the classical solution of Ficks second law<sup>18</sup> to the ISMs,  $c_J(\text{org})$  can be expressed by

$$c_J(\text{org}) = \frac{4R_T}{\pi z_J} \exp\left(\frac{-\pi^2 D_{org} t}{(2d_{org})^2}\right) \quad (3)$$

where  $D_{org}$  is the diffusion coefficient of the primary ion (heparin) in the membrane;  $d_{org}$  and  $t$  are the membrane thickness, and the time elapsed from the injection of the primary ion, respectively. Thus, by plugging Equation 3 into Equation 2, the  $EMF$  can be described by a first order equation as a function of time:

$$EMF = A + B \cdot t = \left[ E^0 + \frac{RT}{z_J F} \ln\left(\frac{4R_T}{\pi z_J}\right) \right] + \frac{RT}{z_J F} \ln\left(\frac{-\pi^2 D_{org}}{(2d_{org})^2}\right) t \quad (4)$$

The diffusion coefficient of the primary ion in the membrane ( $D_{org}$ ) can be calculated from the slope of the line, B.

$$D_{org} = -\frac{4 \cdot B \cdot d_{org}^2 \cdot F \cdot z_J}{\pi^2 \cdot R \cdot T} \quad (5)$$

To validate this approach, we utilized a 1D finite-element method to solve a coupled Nernst–Planck–Poisson (NPP) differential equation system.<sup>19</sup> With this simulation technique, it is possible to assess the time-dependent behavior of ion-selective membranes in contact with aqueous sample solutions containing heparin in a background of chloride anions. The simulated system consisted of two aqueous diffusion layers and the ion-selective membrane. The simulation grid consisted of 600 elements. These elements were closely placed near the phase boundaries. The thicknesses of the diffusion layers and the membranes were considered to be 100  $\mu\text{m}$ . Relative permittivities of water and the ISM were considered to be 80.1 and 10, respectively. The diffusion coefficient in the aqueous phase and the membrane were  $10^{-5} \text{ cm}^2\text{s}^{-1}$  and  $2 \times 10^{-9} \text{ cm}^2\text{s}^{-1}$  (Note: the diffusion coefficient for heparin was an estimate made based on the experimental data shown in Figure 2.5a). The TDMA<sup>+</sup> concentration was 26.2 mM, and the charges of heparin and chloride were considered as -70 and -1, respectively. The forward heterogeneous rate constants across the interface for heparin and chloride were considered as  $10^{-7} \text{ ms}^{-1}$  and  $2 \times 10^{-5} \text{ ms}^{-1}$ ; the backward heterogeneous rate constants across the membrane/solution interface for heparin and chloride were  $10^{-9} \text{ ms}^{-1}$  and  $10^{-3} \text{ ms}^{-1}$ .

The NPP simulations confirmed that the assumptions used in the derivation of the Equation 5 were correct. The backside phase boundary concentration of heparin in the membrane is zero during the initial portion ( $t=0-2 \text{ h}$ ) of the potentiometric curve (Figure 2.2a). Note that reversal in signal is observed after this initial time period since the

diffusion layer inside the membrane continues to decrease in thickness and eventually heparin finally completely replaces chloride on the backside of the membrane phase, where the horizontal portion of the *EMF* response vs. time curve is observed ( $t > 30$  h). The  $E_f$  was constant during the entire course of the simulation. The slope of the linear range is marked in Figure 2.2a and that range was used to calculate the diffusivity of ions through the membrane. The slope obtained by linear regression was within 5% relative error of the value calculated with Equation 4.

### 2.3.2 Impedance Spectroscopy

The bulk resistance of an ion-selective membrane can be measured with electrochemical impedance spectroscopy experiments.<sup>20</sup> The potentiometric technique provides useful information on the backside phase boundary concentrations, and therefore the arrival of heparin to the backside can be observed with the reversal of the potentiometric signal. As a complementary method, impedance spectroscopy gives valuable information on the total concentration of heparin in the membrane.

Initially, the membrane is filled with chloride anion as the counter ion of TDMA<sup>+</sup>. During the experiment, the negatively charged heparin replaces the chloride due to its higher preference by the ISM (formation of ion-pair with TDMA<sup>+</sup>). The total bulk resistance of the membrane under steady-state conditions is given by the following formula:<sup>21</sup>

$$R_m = \frac{d_{org} RT}{AF^2} \sum_i \frac{1}{z_i D_i c_i(org)} \quad (6)$$

where A is the membrane area. From the classical solution of Ficks Law<sup>18</sup> it can be shown that the total resistance of the membrane changes in time according to the Equation 7:

$$\frac{R_m(t) - R_{\min}}{R_{\max} - R_{\min}} = 1 - \sum_{n=0}^{\infty} \frac{8}{(2n+1)^2 \pi^2} \exp\left[\frac{-D_{org}(2n+1)^2 \pi^2 t}{4d_{org}^2}\right] \quad (7)$$

where  $R_{\min}$  is the initial resistance when the membrane only contains chloride as counteranions and  $R_{\max}$  is the steady-state resistance when heparin exchanged the chloride in the entire membrane.

### 2.3.3 Fractionation of Heparin

Heparin was fractionated and gel electrophoresis was used to assess the success of the fractionation. Lanes of fractionated heparin were compared to lanes of enoxaparin and the original unfractionated heparin, which were used as the standards. It was hypothesized that the fractionated heparin should look similar to the unfractionated heparin on the gel based on the molecular weight distribution found in the literature<sup>12</sup> and the enoxaparin should represent a molecular weight distribution not contained in either the fractionated or unfractionated heparin samples. Gel electrophoresis (see Figure 2.3) demonstrated that the fractionated heparin preparation did not extend quite as far down in MW as the unfractionated sample but was more similar to the unfractionated heparin because it is known that the molecular weight distribution of unfractionated heparin does not extend much below 7 kDa and that which does is a very small percentage.<sup>12</sup> In contrast, the band for enoxaparin extended to a MW range far below that seen for the

other two samples (Figure 2.3). These data suggest that heparin was successfully fractionated, and contained little or no low MW fragments.

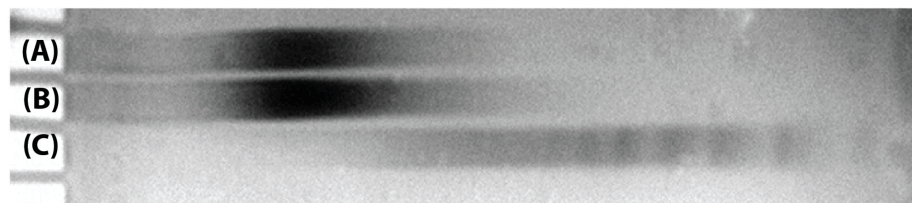


**Figure 2.3. Results of gel electrophoresis of various heparin preparations; (A) contains fractionated heparin, (B) contains unfractionated heparin, and (C) contains enoxaparin (low molecular weight heparin). Heparins were introduced onto the gel at the left of the figure (left side negative(-), right side positive(+)). Gel was run at 16 W for 1.5 h.**

#### *2.3.4 Electrochemical Characterization and Determination of Diffusion Coefficients for Fractionated Heparin in Plasticized PVC Films Doped with TDMACl Using Classic Potentiometry and Impedance Spectroscopy*

In this study, the fractionated heparin was used to study the extraction and diffusion of higher MW heparin species through polymeric plasticized membranes doped with TDMACl. The fractionated heparin sample prepared in this work was used to rule out diffusion of low molecular weight heparins present in the unfractionated sample (i.e., species  $< 8$  kDa), unlike earlier studies that used unfractionated heparin. The potentiometric study was carried out using diffusion (transport) cells (see Figure 2.1) containing two solutions (50 mM NaCl and 5 mg/mL fractionated heparin in 50 mM NaCl) separated by the ion-selective polymer membrane. Membrane thicknesses of between 100 and 250  $\mu\text{m}$  were used to study the diffusion of the fractionated heparin. Like earlier studies carried out during the development of the sensor, an initial drop in the potentiometric signal characteristic of heparin is observed and after several hours, the

reversal in the potentiometric signal is also observed (see Figure 2.4) for every thickness of the membranes. However, the thinner membranes exhibit a much faster reversal in signal when compared to the thicker membranes, which is predicted by the theoretical model. Diffusion coefficients were calculated and an average value of  $ca. 2.7 \times 10^{-9} \text{ cm}^2 \text{ s}^{-1} \pm 0.27$  (*SD* for  $n=15$  measurements) was determined from all of the membranes tested. The clear reversal in *EMF* signal and relatively consistent diffusion coefficient values for the heparin-TDMA complex moving within the membrane, no matter what the thickness of the membrane, strongly supports the heparin extraction model and cannot be predicted to occur if only interfacial adsorption occurs.

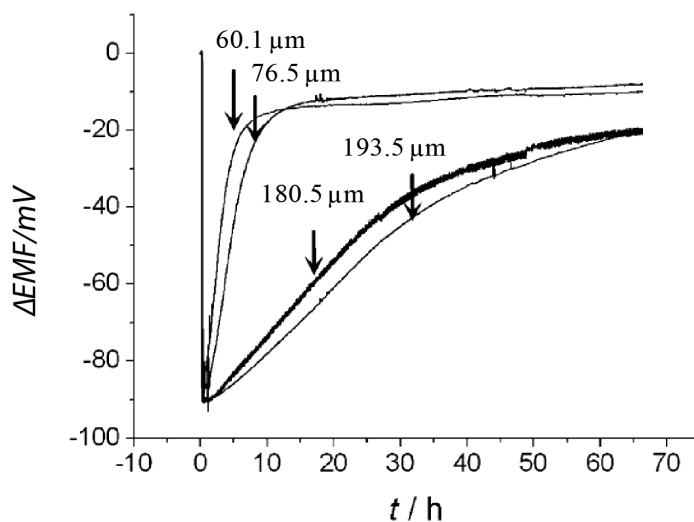


**Figure 2.4. Dynamic potentiometric response curves of ion-selective membranes containing TDMACl with thicknesses of 60.1  $\mu\text{m}$ , 76.5  $\mu\text{m}$ , 180.5  $\mu\text{m}$ , and 193.5  $\mu\text{m}$ , from left to right, respectively, after addition of 5 mg/mL of heparin to the frontside of the membrane.**

Enoxaparin (average MW = 4500 Da) was also studied using the diffusion cell setup. The diffusion coefficient calculated for enoxaparin is expected to be larger than the fractionated heparin samples, and indeed, a diffusion coefficient of  $3.2 \times 10^{-9} \pm 0.60$

$\text{cm}^2\text{s}^{-1}$  (for  $n=9$  measurements) is found based on the rate in EMF reversal. Using a 95% confidence level, the diffusion coefficients calculated for heparin and enoxaparin are significantly different. The same initial potential change and reversal in signal is observed as the fractionated heparin samples. This may be further evidence that the fractionated heparin did not contain LMW heparin and that it is possible for larger molecular weight fragments of heparin to be extracted into the bulk of the organic membrane phase.

The diffusion coefficients determined here were calculated using the given membrane thickness (for an experiment with that membrane) and the slope of the linear region (Figure 2.4) in the reversal in EMF signal, B, by Equation 5. The experimental slopes for the thinner membranes are much steeper than the thicker membranes because heparin reached the backside of the membrane sooner, and hence the flux of heparin to the back-side is greater for the thinner membranes. The calculated diffusion coefficients are very similar for all of the membrane thicknesses.

Electrochemical impedance spectroscopy was also employed to examine whether heparin is extracted and diffuses through the membrane as an ion-pair with  $\text{TDMA}^+$ . Impedance spectroscopy is a useful technique to determine the total bulk resistance of the membrane. This total resistance depends on the concentrations of the mobile ionic species in the membrane. It can be seen in Figure 2.5b that the theoretical curve (solid line) calculated with the diffusion coefficient from the slope of the reversed potentiometric signal (Figure 2.5a), fits the measured impedance data quite well. The bulk resistance was measured every 2 h over a ca. 80 h period using the same diffusion cell set-up as employed for the potentiometric experiments. As heparin diffuses into the

membrane, the resistance of the membrane increases, due to the lower mobility of the heparin-TDMA<sup>+</sup> ion pair compared to the chloride ion.

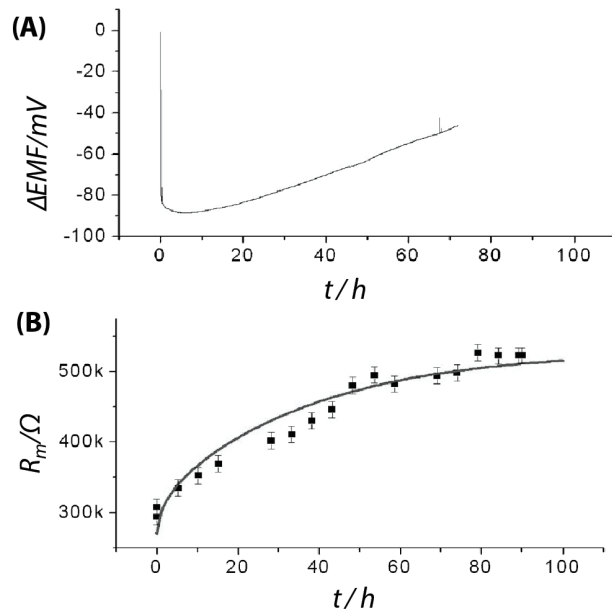


**Figure 2.5. (A) Potentiometric response curve of a 300  $\mu\text{m}$  ion-selective membrane. (B) Bulk resistance of the ion-selective membrane, the dots are the experimental results, the solid line is the theoretical response curve based on Equation 7. Note: The potentiometric curve in Figure 2.5A was generated from the same membrane used to map resistance as function of time in Figure 2.5B. Potentiometric curves in Figure 2.4 were generated from different membranes.**

## 2.4 Conclusions

We have provided new experimental results and corresponding theory concerning the extraction and diffusion of high charge density polyanionic heparin into and through plasticized PVC membranes doped with TDMA<sup>+</sup>Cl<sup>-</sup>, the same membranes used to prepare potentiometric heparin sensors. These results reaffirm earlier experiments<sup>3,4</sup> regarding the mechanism of potentiometric polyanion response, with fractionated heparin possessing only higher MW components still exhibiting the reversal in  $EMF$  response expected as it reaches the backside of the membrane. This reversal of potentiometric

signal after several hours cannot be explained by a surface adsorption only process. Theory predicts this reversal, since, as heparin arrives to the backside of the membrane, the backside phase boundary potential starts to approach the phase boundary potential of the front-side, resulting in a smaller membrane potential (eventually approaching zero). It is important to emphasize that the  $\Delta EMF$  depends almost entirely on the ion concentrations at the backside and the front-side of the membrane. Hence it is important that the extraction and diffusion of heparin is further verified independently via impedance spectroscopy, that provides information about the total concentration of heparin within the bulk of the membrane phase. Clearly, the impedance data presented here also supports the presence of the high MW fractionated heparin species within the polymeric membrane phase.

## 2.5 References

- [1] Ma, S.; Meyerhoff, M. E. ; Yang, V. C., *Anal. Chem.* **1992**, *64*, 694-697.
- [2] Ma, S.; Yang, V.C.; Fu, B.; Meyerhoff, M.E., *Anal. Chem.* **1993**, *65*, 2078-2084.
- [3] Fu, B.; Bakker, E.; Yun, J.H.; Yang, V.C.; Meyerhoff, M.E., *Anal. Chem.* **1994**, *66*, 2250-2259.
- [4] Fu, B.; Bakker, E.; Yang, V.C.; Meyerhoff, M.E., *Macromolecules*, **1995**, *28*, 5834-5840.
- [5] Ye, Q.; Meyerhoff, M. E., *Anal. Chem.*, **2001**, *73*, 332-336.
- [6] Langmaier, J.; Olsak, J.; Samcova, E.; Samec, Z.; Trojanek, A., *Electroanalysis*, **2005**, *2*, 115-120.
- [7] Langmaier, J.; Olsak, J.; Samcova, E.; Samec, Z.; Trojanek, A., *Electroanalysis*, **2006**, *13-14*, 1329-1338.
- [8] Jing, P.; Kim, Y.; Amemiya, S., *Langmuir*, **2009**, *25*, 13653-13660.
- [9] Rodgers, P.J.; Jing, P.; Kim, Y.; Amemiya, S., *J. Am. Chem. Soc.*, **2008**, *130*, 7436-7442.
- [10] Guo, J.; Yuan, Y.; Amemiya, S., *Anal. Chem.*, **2005**, *77*, 5711-5719.
- [11] Oesch, U.; Simon, W., *Anal. Chem.*, **1980**, *52*, 692-700.
- [12] Bertini, S.; Bisio, A.; Torri, G.; Bensi, D.; Terbojevich, M., *Biomacromolecules*, **2005**, *6*, 168-173.
- [13] *Carbohydrates as Drugs-Heparin Oligosaccharides-New Analogs Development and Applications* (Eds: R. J. Linhardt, T.Toida, Z. B. Witczak, K. A. Neiforth,) Marcel Dekker, New York **1997**, pp. 277-341.
- [14] Linhardt, R.J., *J. Med. Chem.*, **2003**, *46*, 2551-2564.
- [15] Bakker, E.; Buhlmann, P.; Pretsch, E., *Talanta*, **2004**, *63*, 3-20.
- [16] Nagele, M.; Bakker, E.; Pretsch, E., *Anal. Chem.*, **1999**, *71*, 1041-1048.
- [17] Ceresa, A.; Radu, A.; Peper, S.; Bakker, E.; Pretsch, E., *Anal. Chem.*, **2002**, *74*, 4027-4036.
- [18] Linossier, I.; Gaillard, F.; Romand, M.; Feller, J.R., *J. Appl. Polym. Sci.*, **1997**, *66*, 2465-2473.
- [19] Sokalski, T.; Lingenfelter, P.; Lewenstam, A., *J. Phys. Chem. B*, **2003**, *107*, 2443-2452.
- [20] Lindfors, T.; Höfler, L.; Jgerszki, G.; Gyurcsanyi, R.E., *Anal. Chem.*, **2011**, *83*, 4902-4908.
- [21] Sandifer, J.R.; Iglehart, M.L.; Buck, R.P., *Anal. Chem.*, **1989**, *61*, 1624-1630.

## CHAPTER 3

### DETECTION OF OVERSULFATED CHONDROITIN SULFATE CONTAMINANT/ADULTERANT IN COMMERCIALY AVAILABLE HEPARINS: A PRACTICAL APPLICATION OF POTENTIOMETRIC POLYANION SENSITIVE POLYMERIC MEMBRANE ELECTRODES

#### **3.1 Introduction**

Large doses of heparin are administered every day in hospitals both during surgery and therapeutically for conditions like deep vein thrombosis.<sup>1</sup> In 2008, several lots of pharmaceutical grade heparin were recalled due to adverse side effects that included allergic type reactions and, in more severe cases, death. It was later found that crude heparin from China, which Baxter Inc. (Deerfield, IL) had purchased and used in their heparin preparations, had been adulterated with a synthetic contaminant, oversulfated chondroitin sulfate (OSCS). The presence of OSCS was directly linked to the adverse reactions associated with particular heparin lots.

Over one million multi-dose vials of heparin are purchased every month, half of which are manufactured by Baxter Inc.<sup>2</sup> Before the 2008 outbreak of adverse side effects, the only screening method required for commercially available heparin was the Factor Xa/IIa ratio test, which is used to determine heparin efficacy and purity. The

Factor Xa/IIa ratio test, with respect to OSCS detection, was determined to have detection limits of 15 wt % OSCS in heparin, far above the toxicity levels of OSCS, which are  $\geq 5$  wt %.<sup>3</sup> Since OSCS has strong anti-factor IIa activity and only one half of the activity of heparin toward anti-factor Xa, samples containing 5-25 wt% OSCS in heparin went undetected because measurements still fell within the United States Pharmacopeial standards (Xa activity)/IIa activity = 0.9-1.1).<sup>4</sup>

A detailed investigation into the contaminated heparin episode was executed by the FDA. They utilized capillary electrophoresis (CE) and determined which commercial lots were suspected to have the contaminant/adulterant, and with further isolation, proton nuclear magnetic resonance (H-NMR) was used to elucidate the structure of the contaminant/adulterant. Later, CE and H-NMR became required screening methods within the Heparin Sodium USP Monograph.<sup>3</sup> Although these screening methods are reliable and were effective in discovering the OSCS species present in the samples that caused patient deaths, they can be time consuming, expensive, require extensive training and knowledge to use the instruments, and are not easily applicable in clinical settings.

Potentiometric plasticized polymeric membrane-based polyion sensors for the determination of heparin were pioneered by the Meyerhoff group in the early 1990's.<sup>5-8</sup> These sensors have many applications, including monitoring heparin in whole blood,<sup>6</sup> monitoring enzymatic reactions,<sup>9</sup> and measuring carrageenan in food products.<sup>10</sup> The sensor mechanism is based on a non-classical non-equilibrium response and is described in Chapter 2. It is easy to differentiate between glycosaminoglycans (GAGs) when measuring them with this polyion sensor. Generally, since the charge density of these GAGs largely contributes to the EMF response that is observed during measurements, the

variations of charge density amongst GAGs can be easily observed. Specific GAGs (Figure 3.1), measured by this sensor in 120 mM NaCl in 10 mM phosphate buffer, have characteristic EMF changes associated with them. When a concentration of target analyte is measured that is large enough to induce the equilibrium response of the sensor, a large EMF drop in sensor signal is observed, and the overall potential change is associated directly to the charge density of the polyion analyte present; the larger the charge density of the polyion, the larger the potential change that is observed (see Figure 1.2 chapter 1).<sup>6,11</sup> For example, when measuring heparin, which has a charge density of  $\sim -4$  per disaccharide unit, in 120 mM NaCl/10 mM PBS, an approximately  $-50$  mV change in EMF of the measurement cell occurs. In contrast, chondroitin sulfate, which has a much smaller charge density,  $-2$  per disaccharide unit, only yields  $\sim -35$  mV change in signal.

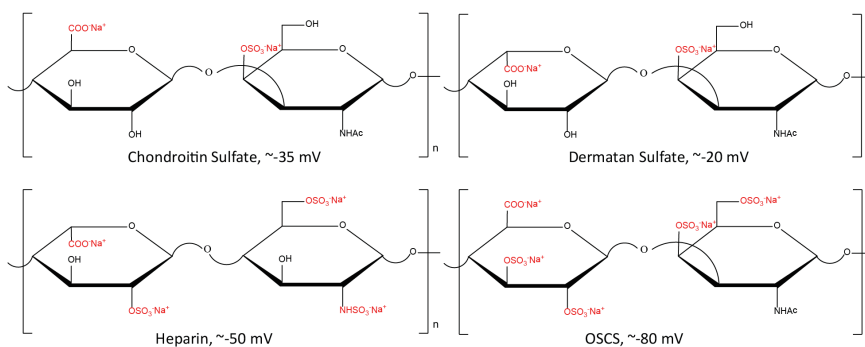


**Figure 3.1. Different glycosaminoglycans and their respective potential changes in a background solution of 120 mM NaCl/10 mM phosphate buffered saline.**

When two different GAGs are present in the same sample, the potential change that is observed is governed by the higher charge density species because the thermodynamics of the cooperative ion-pair formed between  $\text{TDMA}^+$  and polyanion are in favor of the larger charge density species.<sup>11</sup> This phenomenon allows for the detection

of OSCS in commercially available heparins simply because the charge density of OSCS is much larger than heparin itself.

In 2008, Wang, et al. reported that the heparin sensor could be used to determine levels of OSCS down to 0.5 wt% within heparin preparations.<sup>11</sup> In that work, a slow drift of the potential, which eventually stabilized at approximately -80 mV (the overall potential change associated with OSCS), was observed when the OSCS levels were < 5 wt% of the heparin sample. Levels of OSCS above this 5 wt% threshold immediately induced a rapid equilibrium phase boundary potential change at the outer membrane/sample interface of the sensor resulting in an ca. -80 mV change in cell potential.

Although this sensor had been successful in determining OSCS in adulterated heparin samples prepared in the research laboratory, it had not been used to measure the OSCS in any commercial samples known to be contaminated with this agent. Herein, the ability to detect the presence of OSCS in commercial lots of Baxter heparin is demonstrated and shown to correlate perfectly with the NMR data provided by Baxter for these lots.

## **3.2 Experimental Section**

### *3.2.1 Polyion Sensor Preparation*

The membrane cocktail was made using 66 wt% poly(vinyl chloride) (PVC) (high molecular weight, Fluka), 32.5 wt% dioctyl sebecate (DOS) (Fluka), and 1.5 wt% TDMACl (26.2 mM) (Fluka). This mixture was dissolved in distilled tetrahydrofuran (THF) (Fisher) to yield a 100 mg/mL mixture at a volume of 15 mL. To assemble the

polyion-selective disposable sensors, Tygon tubing (i.d. 1/16 in., o.d. 1/8 in.,  $\frac{3}{4}$  in length) was placed onto the distal tip of a closed-end glass capillary tube (o.d. 0.8-1.1 mm) with the closed end of the capillary protruding out from the tubing  $\sim 4$  mm. This end was then dip-coated with the membrane cocktail 12 times, allowing 10 min in between each dip-coat for the THF to evaporate. Once the tubing/capillaries were completely dip-coated, they were left to dry over night. Before measurements, tubing/capillaries were conditioned in 120 mM NaCl in 10 mM PBS, pH 7.4, for approximately 15 min before the glass capillaries were carefully removed from the Tygon tubing, leaving a sensing membrane at the distal end. The Tygon tubing was then filled with the same buffer and placed back into the conditioning solution over night. Conditioned sensors were fitted onto the narrow end of 1 mL disposable pipette tips with a thin Ag/AgCl wire (0.5 mm) inserted inside the pipette tip and into the inner buffer solution. Parafilm was used to seal the wider end of the pipette tip with the Ag/AgCl wire extending out from the top and parafilm (Figure 3.2).

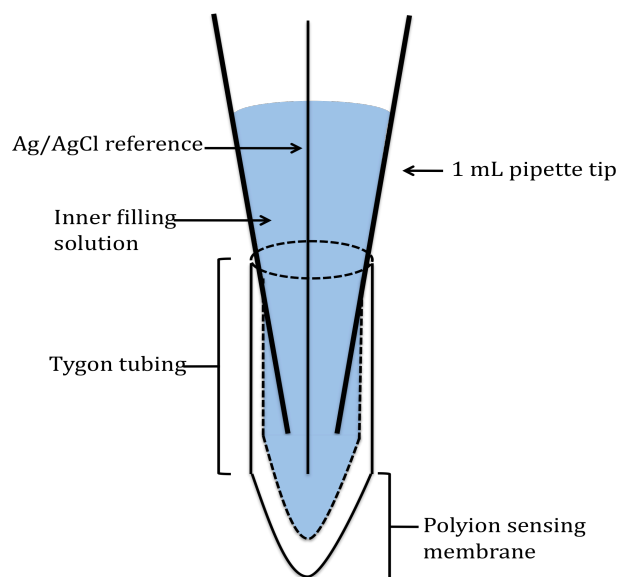


**Figure 3.2. Polyion sensor arrangement where the conditioned polyion selective sensor, made from dip-coating PVC tubing with membrane cocktail, is inserted onto the end of a 1 mL Eppendorf pipette tip.**

### *3.2.2 Measurements in Commercial Lots of Heparin*

Multi-dose injection vials of heparin concentrations in 1000, 5000, and 10,000 USP units/mL were supplied by Baxter Healthcare Corporation, Inc. (Deerfield, Ill.). All samples were diluted to 1 mg/mL (182 units/mL) concentrations with a total volume of 4 mL for sensor measurements. Sensors were immersed into sample solutions with continuous stirring and measured against a commercial miniaturized Ag/AgCl reference electrode (BASi, West Lafayette, IN) filled with 3 M KCL. Three membrane electrode sensors were used per sample to obtain a mean and standard deviation for each sample. All sensors were connected to a Lawson Labs 8 channel high impedance interface (Pennsylvania, USA) during the ~20 min data acquisition period. See Figure 3.3 for the experimental set-up.

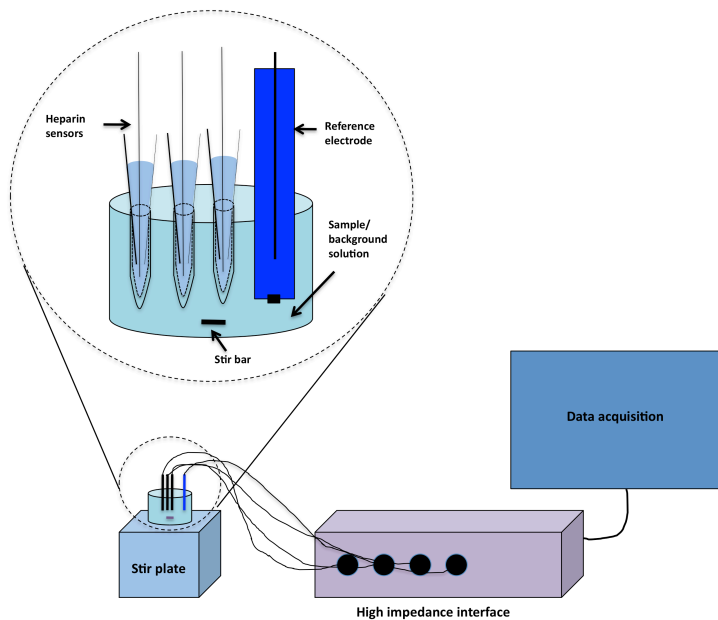


**Figure 3.3. Experimental set-up.** All measurements were made using three heparin sensors to obtain a mean voltage change  $\pm$  standard deviations for all samples tested. The larger circle contains an enlarged view of the experimental cell. Heparin sensors were approximately 1.5 cm in length extending from the narrow end of a 1 mL Eppendorf pipette tip.

Three to six sensors from each batch of polyion sensors were used to measure a standard heparin solution of 1 mg/mL concentrations under constant stirring to ensure the overall potential change of a known uncontaminated heparin sample measured with sensors from a given batch was  $\sim -50$  mV. Overall potential changes were determined by subtracting the stable starting baseline EMF value recorded in 120 mM NaCl/10 mM PBS, pH 7.4, from potentials generated 10 min after the injection of the heparin samples.

### 3.3 Results and Discussion

Twelve commercial heparin samples were analyzed for the presence of OSCS using the homemade potentiometric polyion sensitive membrane electrodes. When concentrations of OSCS in heparin preparations do not exceed 5 wt% (as determined by

Baxter using H-NMR), the equilibrium response to OSCS is not immediately induced; rather the equilibrium EMF response to heparin, or responses somewhat larger than heparin but not equal to -80 mV (as concentrations of OSCS increases from 0.5-< 5 wt%) are initially observed, and then a drift more negative to the equilibrium EMF response of OSCS, as reported in Wang, et. al.<sup>11</sup> A different trend is observed when contaminated samples have concentrations of OSCS that are high enough to induce the equilibrium response toward OSCS ( $\geq 5$  wt% in heparin), as previously mentioned, where sensors exhibit immediate potential changes of  $\sim -80$  mV. The concentrations of OSCS in the heparin samples provided by Baxter were high enough to impose the rapid equilibrium phase boundary potential change at the membrane/sample interface associated with their charge densities. Therefore, it appeared that none of the contaminated samples that were screened with the potentiometric polyion sensors contained concentrations of OSCS less than the 5 wt% threshold, suggesting that all samples were contaminated/adulterated with amounts that exceeded the toxicity level of OSCS.

Samples were monitored for  $\sim 10$  min after injection and determined to contain OSCS or not contain this species based on the total change in EMF from baseline values. Samples were considered void of OSCS if the sensors used to make the measurement exhibited equilibrium EMF shifts of approximately -50 mV in respect to background potentials. Potential changes that reached  $\sim -80$  mV with respect to the initial background potential indicated that the sample was contaminated with OSCS (see Figure 3.4 for EMF data obtained for four representative lots of Baxter heparin). NMR data was provided by Baxter and used to correlate the potentiometric data with known amounts of OSCS present. Exactly 100% of the 12 lots of heparin screened via the heparin sensor

were determined to be in agreement with the NMR data for each sample regarded as contaminated or uncontaminated (see Table 3.1).

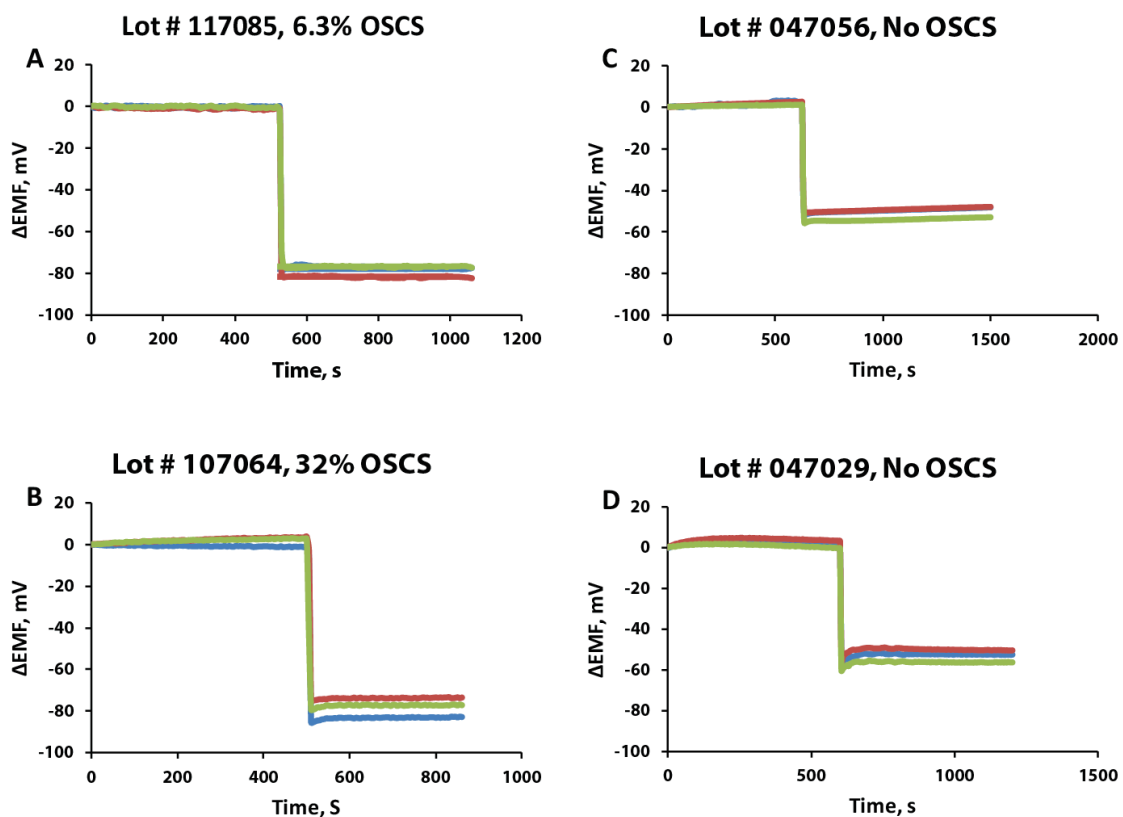


**Figure 3.4. EMF changes of two contaminated samples (A and B) and two clean samples (C and D) with amounts of OSCS determined by NMR data provided by Baxter Inc. Each sample was measured with three sensors to obtain standard deviations. Average potential and standard deviations are as follows: (A) Avg = -78.3 mV, s.d. = 2.11 mV; (B) Avg. = 79.9 mV, s.d.= 2.32 mV, (C) Avg. = -52.8 mV, s.d. = 1.59 mV; (D) Avg. = -55.3 mV, s.d = 1.24 mV.**

**Table 3.1. Potentiometric responses and standard deviations for sensors used to measure Baxter heparin samples.<sup>a</sup>**

Lot Number	Avg $\Delta$ EMF, mV	Stdev, mV	% OSCS in Sample
37057	-49.0	4.72	ND
47029	-54.7	2.30	ND
47056	-52.8	1.59	ND
67069	-51.5	2.03	ND
97079	-73.4	2.00	4.7
97081	-81.4	1.70	4.0
106082	-54.9	2.99	ND
107064	-79.6	2.34	32
107111	-74.3	5.80	13.4
116041	-48.4	1.57	ND
117085	-78.3	2.11	6.3
1060-07-0002	-48.1	0.330	ND

<sup>a</sup> Values reported in the “% OSCS in Sample” column represent wt% of OSCS determined by NMR in each lot. All values reported in red are considered to be contaminated/adulterated samples. ND is short for ‘none detected’. All NMR data were provided by Baxter.

### 3.4 Conclusions

The data provided in this chapter suggests that simple potentiometric polyanion sensors can accurately screen commercially available heparin for the presence of high charge density species like OSCS. It should be noted that this method is not meant to replace CE or H-NMR. However, it could compliment the screening process by pre-inspecting samples to determine if further screening is necessary, lowering the total cost of screening and concomitantly lowering the cost of heparin products. Furthermore, this method could readily be used in clinical or other commercial settings (including facilities where heparin is extracted from pig tissue, etc.) that don’t have access to high cost H-NMR and CE instruments.

Overall, in this work, potentiometric polyanion sensors have been proven to provide a simple method for screening commercially available heparin preparations that is accurate, robust, easy to use, and also inexpensive.

### 3.5 References

- [1] Linhardt, R.J., *J. Med. Chem.*, **2003**, *46*, 2551-2564.
- [2] U.S. Food and Drug Administration,  
<http://www.fda.gov/drugs/drugsafety/postmarketdrugsafetyinformationforpatientsandproviders/ucm112597.htm>, (December 2012).
- [3] McKee, J.; Bairstow, S.; Szabo, C.; et. al., *J. Clin. Pharm.*, **2010**, *50*, 1159-1170.
- [4] Keire, D.; Mans, D.; Ye, H.; et. al., *J. Pharm. Biomed. Anal.*, **2010**, *52*, 656-664.
- [5] Ma, S.; Yang, V.; Meyerhoff, M., *Anal. Chem.*, **1992**, *64*, 694-697.
- [6] Ma, S.; Yang, V.; Fu, B.; et. al., *Anal. Chem.*, **1993**, *65*, 2078-2084.
- [7] Fu, B.; Bakker, E.; Yun, J.; et. al., *Anal. Chem.*, **1994**, *66*, 2250-2259.
- [8] Fu, B.; Bakker, E.; Yang, V.; et. al., *Macromolecules*, **1995**, *28*, 5834-5840.
- [9] Esson, J.; Meyerhoff, M., *Electroanalysis*, **1997**, *9*, 1325-1330.
- [10] Hassan, S.; Meyerhoff, M.; Badr, I., *Electroanalysis*, **2002**, *14*, 439-444.
- [11] Wang, L.; Buchanan, S.; Meyerhoff, M., *Anal. Chem.*, **2008**, *80*, 9845-9847.

## CHAPTER 4

### POLYION SELECTIVE POLYMERIC MEMBRANE BASED PULSTRODE AS A DETECTOR IN FLOW-INJECTION ANALYSIS

#### 4.1 Introduction

Polyanions such as glycosaminoglycans (GAGs) (e.g., the anticoagulant heparin and the anti-inflammatory agent chondroitin sulfate), sulfated polysaccharides (e.g., fucoidan, pentosan polysulfate, carageenans), and polyphosphates, as well as many important polycationic species (e.g., arginine-rich polypeptides including protamine (the antidote of heparin), polymers of quaternary ammonium species, etc.) are difficult analytical targets for direct detection owing to their lack of strong absorbance at wavelengths  $> 260$  nm and no presence of electrochemically active domains. To address this problem, non-equilibrium polyion selective polymeric membrane electrodes for heparin and protamine (as representative biomedically important polyions) were first introduced by our group in the early 90's.<sup>1-6</sup> Such devices have been demonstrated to have many potential practical applications including the measurement of heparin in whole blood,<sup>2</sup> the quantitation of carrageen in food products,<sup>7</sup> and the detection of enzyme activities that cleave polyions into smaller fragments not sensed by the electrodes and the detection of high-charge density contaminants in commercially available heparins.<sup>8,9</sup> These sensors are prepared by doping polymeric membranes (e.g., plasticized PVC) with lipophilic anion-exchangers (tridodecylmethylammonium chloride

(TDMACl)) for polyanions or lipophilic cation exchangers (e.g., dinonylnaphthalene sulfonic acid (DNNSH)) for polycations that can form strong cooperative ion pairs with the target polyion, causing polyion extraction into the organic membrane phase and hence a change in the phase boundary potential of the membrane.<sup>3</sup> Although such sensors are inexpensive and robust, they are irreversible, and hence they are usually employed as single-use devices and are not adaptable to higher throughput flow-through analysis methods (e.g., flow-injection analysis (FIA)), where fully reversible potentiometric responses is required.

The Bakker group first pioneered a reversible polyion-selective sensor in the early 2000s and termed the device a pulstrode.<sup>10,11</sup> Since then, these pulstrodes have been used to detect both polyanions and polycations.<sup>11,12</sup> The pulstrode is a three-electrode system involving working, counter, and reference electrodes, where the polymeric membrane within the working electrode is doped with a lipophilic ion-exchanger salt with no intrinsic ion-exchange properties. Although the membrane does not have ion-exchange properties initially, a galvanostatic pulse between the working and counter electrode for a short time period (1 s) can polarize the lipophilic salt species in the membrane phase and induce localized ion-exchange at the membrane/sample interface. This provides the basis for subsequent potentiometric measurement during a period when no current pulse is applied. A typical measurement consists of a three-pulse sequence: the galvanostatic pulse, an open-circuit period, and then a potentiostatic pulse at a given applied potential. The principles of this method and the function of each of these steps have been provided in prior work reported by Bakker and coworkers<sup>10,11</sup> with respect to polycation sensing, as well as Gemene et al.<sup>12</sup> for polyanion sensing.

In principle, the pulstrode sensor, unlike the earlier single-use polyion selective membrane electrodes, should be useful as a detector in flow-through analytical systems. Herein, we explore for the first time this avenue by demonstrating the utility of a plasticized PVC membrane-based electrode containing the lipophilic salt of (TDMA/DNNS) as both a polycation and polyanion sensitive detector in a simple flow-injection analysis (FIA) arrangement. Both protamine and heparin are used as model analytes, and it is shown that the pulse sequence for detection can be optimized to achieve sample throughputs of up to 20 samples/h with detection limits of 10  $\mu\text{g/mL}$  protamine and 40  $\mu\text{g/mL}$  heparin, respectively, when a 200  $\mu\text{L}$  injection loop is employed.

## **4.2 Experimental Section**

### *4.2.1 Reagents*

High molecular weight poly(vinyl chloride) (PVC), 2-nitrophenyloctyl ether (o-NPOE), tridodecylmethylammonium chloride (TDMACl), tetrahydrofuran (THF), heparin sodium salt, protamine sulfate salt from salmon, and all buffer salts were purchased from Sigma Aldrich (St. Louis, MO). Dinonylnaphthalene sulfonic acid (DNNSH) as a 49% solution in xylenes was a gift from King Industries (Norwalk, CT).

### *4.2.2 Preparation of Ion-exchanger Salt*

The lipophilic ion-exchanger salt was prepared by metathesis in benzene in a 1:1 molar ratio of DNNSH and TDMACl. The benzene-salt solution was washed several times with deionized water until the aqueous solution was neutral. The benzene phase

was then dried, and the residual salt was re-dissolved in THF and then dried again for use in preparation of the polyion selective membranes.

#### *4.2.3 Membrane Preparation*

All polyion selective membrane films contained 10 wt% of TDMA/DNNS salt and were ~200  $\mu\text{m}$  thick. The sensing membranes were all formulated to contain a 1:2 by weight ratio of PVC and o-NPOE plasticizer. All membrane components were dissolved in THF and the membrane was prepared by solvent casting this solution into glass rings on glass plates and letting the solutions dry overnight (in fume hood).

#### *4.2.4 Electrodes*

Membranes were cut with a cork borer (8 mm diam.) from the parent membrane and placed into an electrode body (Oesch Sensor Technology, Sargans, Switzerland). The actual membrane area was 20  $\text{mm}^2$ . All sensors were conditioned overnight in 10 mM phosphate buffer, pH 7.4, with 10 mM NaCl added, and the inner-filling solution in contact with the inner Ag/AgCl reference was the same as the outer conditioning solution. The external reference electrode was a double-junction Ag/AgCl electrode with 3 M KCl as the inner filling solution and 1 M LiOAc as a bridge electrolyte. A coiled Pt-wire was used as a counter electrode for all pulsed chronopotentiometric measurements (see Figure 4.1).

#### *4.2.5 Measurements*

A conventional three-electrode set-up was used for the pulstrode measurements with the TDMA/DNNS-based polymeric membrane electrode serving as the working

electrode with the flowing sample passing over the outer surface of the membrane in a wall-jet configuration (see Figure 4.1). The solution outlet holes of the plastic syringe that provided the housing for the wall-jet assembly entered into a small beaker into which the reference and counter electrodes were placed.

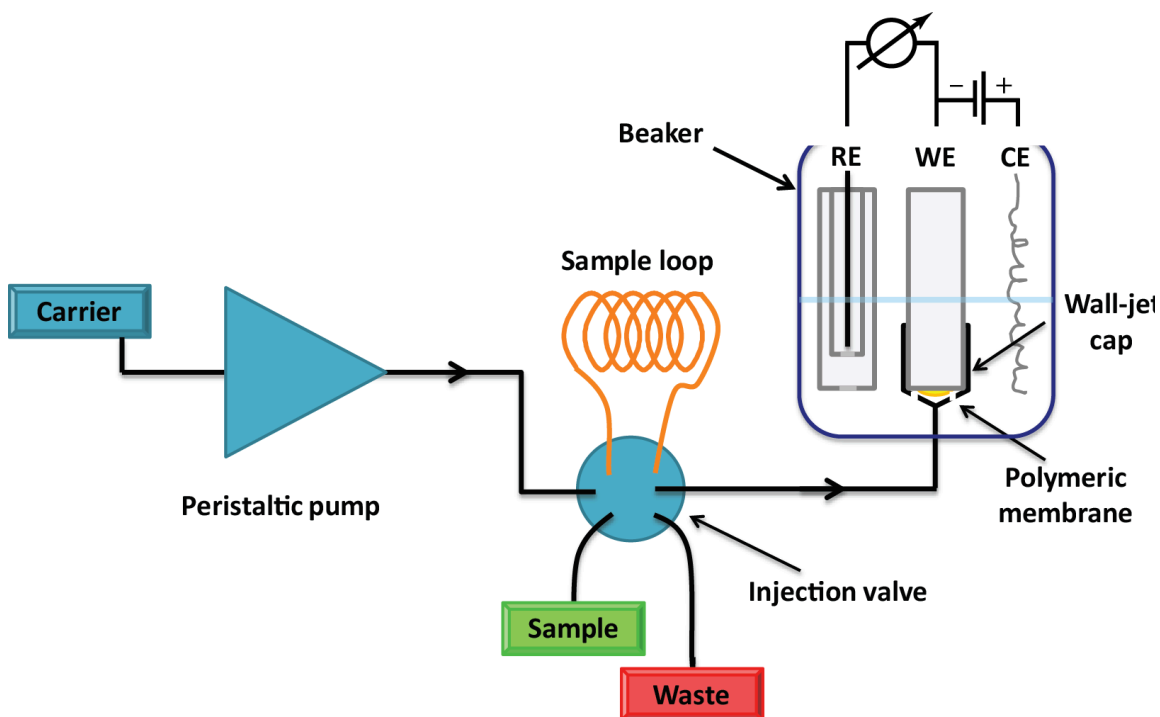


**Figure 4.1.** Schematic diagram of the flow-injection system coupled with polyion selective polymeric membrane-based pulstrode used for the experiments reported.

The electrochemical measurements were conducted with an AFCBI bipotentiostat (Pine Instruments, Grove City, PA) controlled by a NI-DAQPad 6015 interface board and LabVIEW 8.6 data acquisition software (National Instruments, Austin, TX) on a PC computer. Initially, an uptake (galvanostatic pulse) time of 1 s (magnitude and direction changed depending on the target analyte), a zero-current pulse of 0.5 s, and a potentiostatic pulse of 0 V vs. Ag/AgCl (stripping potential) of 15 s were used. Eventually, to enhance throughput, the potentiostatic pulse period was varied to examine

the shortest period that still provide a full return to baseline potential. For measurements involving heparin, a 20  $\mu\text{A}$  current was employed during the galvanostatic pulse, and for protamine a -12  $\mu\text{A}$  current pulse was applied. These current magnitudes have been previously optimized for largest EMF responses during the zero current pulse period under static conditions (in absence of flow) for heparin<sup>12</sup> and protamine.<sup>11</sup> The potentials were sampled as the averaged data during the last 10% time period of the 0.5 s zero current pulse. To assess the composition changes in the membranes of the working electrode as a function of use time in the FIA system, classical potentiometric measurements were conducted with the working electrodes using a 16-channel, high-impedance interface (Lawson Laboratories Inc., Malvern, PA) vs. the same double junction reference electrode used in the pulsed chronopotentiometric FIA measurements. All experiments were carried out at room temperature (21-23 °C).

#### *4.2.6 FIA System*

A schematic representation of the flow injection analysis system used throughout the experiments reported here is shown in Figure 4.1. A peristaltic pump (MINIPULS3, Gilson, Middleton, WI) was used to induce carrier stream (buffer) flow and a 6-port manual injection valve (VICI, Houston, TX), equipped with a 750  $\mu\text{L}$  sample loop (or 200  $\mu\text{L}$  sample loop for higher throughput rate only), was employed to introduce samples into the system. A polyion selective membrane electrode, serving as detector, was mounted in a wall-jet mode using custom made adapter (plastic syringe housing). The entire flow-through system was assembled using Teflon tubing (0.8 mm i.d.).

### 4.3 Results and Discussion

In this work, a polyion selective pulstrode is employed as a universal polyion detector in an FIA system to detect both polycations and polyanions with the same membrane composition. Initial preliminary experiments were conducted using a carrier stream of 10 mM phosphate buffer, pH 7.4, with 10 mM NaCl at a flow rate of 0.6 mL/min and a 750  $\mu$ L sample loop. The large sample volume employed was to ensure that an adequate number of data points (EMF measurements) could be obtained in the presence of the sample to define a full sample peak, given that a voltage signal is only recorded every 16.5 s. (see parameters for pulses in Experimental Section). The polymer membrane of the working electrode is doped with a 1:1 molar ratio of tridodecylmethylammonium (TDMA<sup>+</sup>) and dinonylnaphthalene sulfonate (DNNS<sup>-</sup>), where TDMA<sup>+</sup> provides selectivity to polyanions (heparin)<sup>12</sup> and DNNS<sup>-</sup> to polycations (protamine)<sup>11</sup> when the membrane is polarized. During a typical pulse sequence, the galvanostatic pulse is applied through the working sensor and counter electrode, during which the membrane is polarized, with a concomitant ion-flux of complementarily charged ions migrating from the sample towards the polymeric membrane (see Figure 4.2). Under an anodic current pulse, the lipophilic ion-exchanger salt ions are redistributed in the membrane, with TDMA<sup>+</sup> migrating toward the sample/membrane interface, and DNNS<sup>-</sup> moving toward the inner interface in contact with the fixed internal electrolyte solution. Thus, the outer interface becomes an anion exchange interface and the inner solution/membrane a cation exchange interface (see Figure 4.2). An analogous process occurs when an initial cathodic current pulse is applied, with DNNS<sup>-</sup> moving toward the sample/membrane interface for selective detection of polycations. During the subsequent open circuit portion of the sequence, the previously extracted background

ions are exchanged with the target polyions from the sample to provide a phase boundary potential change that relates to the concentration of polyions present. The measured EMF during this period is void of undesired  $iR$  drop, making it analogous to classical zero current potentiometric measurements. During the potentiostatic pulse, the membrane is depolarized, and all ions that are initially extracted are stripped out to restore the membrane to its original composition, making the sensor fully reversible and suitable for FIA measurements.

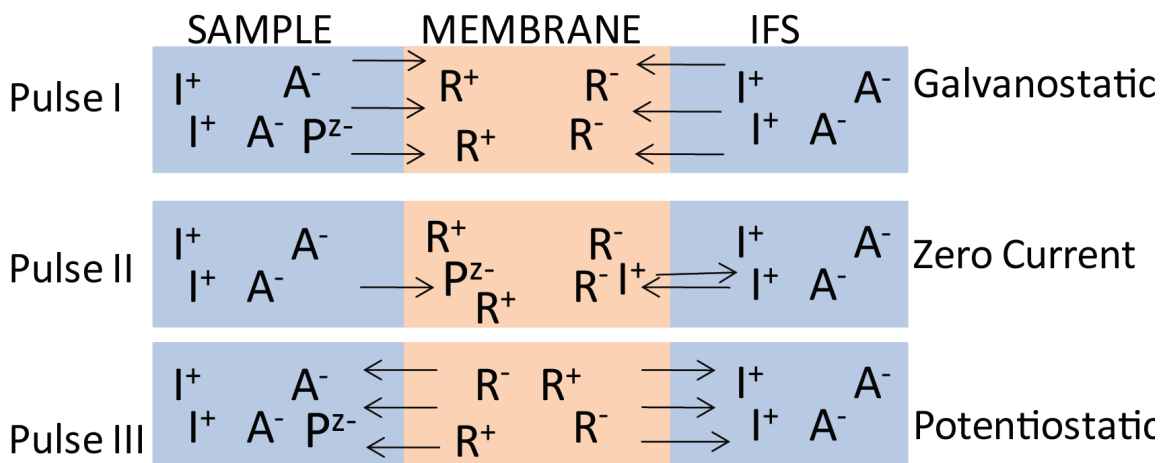


**Figure 4.2.** Movement of salt and ions within membrane and at interfaces during pulse sequence employed for detection of polyanions using anodic current pulse in FIA arrangement. The polyion is represented by  $P^{z-}$ , the interfering ions by  $I^+$  and  $A^-$ , and  $R^+$  and  $R^-$  are the  $TMDA^+$  and  $DNNS^-$  ions of the lipophilic ion-exchanger salt within the membrane phase. It should be noted that smaller anions ( $A^-$ ) also enter outer surface of sensing membrane during pulse 1 period, but are eventually outcompeted for serving as the counteranions to  $R^+$  sites by the polyanions ( $P^{z-}$ ).

The typical dynamic potentiometric responses of the pulstrode detector in the FIA mode (using preliminary pulse parameters) toward injected samples of protamine and heparin samples are shown in Figure 4.3. All signals, obtained for differing concentrations of both protamine and heparin, exhibit good reproducibility for duplicate injections and reversibility. However, it should be noted that these measurements are only used to demonstrate the detectable concentration range and not employed to

demonstrate true precision and stability of the sensors (see Figures 4.5 and 4.6, below, for precision data). In the polyanion sensing mode that employs an anodic current pulse (i.e., heparin as the target analyte), a slight negative baseline shift is observed, which may be due to very small amounts of higher MW heparin remaining inside the membrane during the potentiostatic pulse due to the very strong cooperative ion pair it makes with TDMA<sup>+</sup>.<sup>4</sup> However, the overall potential changes from baseline for a given concentration of heparin remained relatively constant and reproducible. The linear response range for protamine injections is 10 - 100  $\mu\text{g/mL}$ , whereas for heparin the range is from 40 to 200  $\mu\text{g/mL}$  (equivalent to 7 -36 Units/mL).

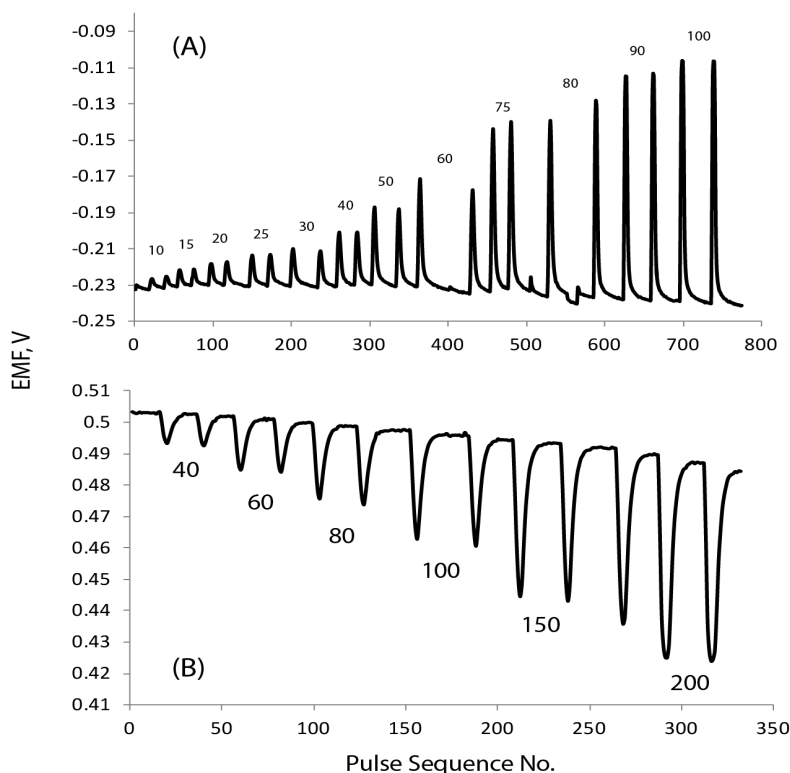


**Figure 4.3. Dynamic potentiometric response of polyion pulstrode to (A) protamine; duplicate sequential injections of standards in range from 10  $\mu\text{g/mL}$  - 100  $\mu\text{g/mL}$ ; and (B) heparin; duplicate sequential injections of standards in range from 40  $\mu\text{g/mL}$  - 200  $\mu\text{g/mL}$  in 10 mM phosphate buffer, pH 7.4, with 10 mM NaCl present. The diluent stream was the same buffer solution and flow rates were set at 0.6 mL/min. Numbers above and below peaks represent concentrations in  $\mu\text{g/mL}$ . Every 100 pulses is  $\sim 30$  min.**

Since the measurements are conducted under flowing conditions, it is essential to determine the stability of the sensors. Two different pulstrode sensors with the same membrane composition were used for calibrations toward protamine and heparin, respectively. Each sensor was calibrated twice a day and placed in stagnant conditioning buffer solution between measurements. The FIA response toward protamine was found to be stable for 3 d, while responses towards heparin were stable over a 5 d period, with stability defined as potential change values of less than 5% in peak heights when compared to those on day 1 of operation for a particular sensor. After these times, the overall EMF responses decreased significantly. The reason for the longer stability towards heparin may be related to the lipophilicities of each portion of the ion-exchanger salt within the membrane phase. Values of organic-aqueous phase partition coefficients for  $\text{DNNS}^-$  and  $\text{TDMA}^+$  were determined using Virtual Computational Chemistry Laboratory.<sup>14</sup> The results show that  $\text{DNNS}^-$  has a ca. two orders of magnitude smaller partition coefficient compared to that of  $\text{TDMA}^+$  ( $\log K^{\text{part}} = 7.71$  vs.  $9.75$ ).

To confirm that  $\text{DNNS}^-$  was more quickly washed out from the membrane phase, studies were conducted using classical potentiometry using KBr as the analyte species. For freshly prepared membranes, the ion-exchanger salt in the membrane has no intrinsic ion-exchange properties and, therefore, does not respond to any ions present in the sample solution in classical zero-current potentiometry (see Figure 4.4A). However, when sensors are placed in a continuous flow arrangement (exposed to flowing 10 mM phosphate buffer, pH 7.4. with 10 mM NaCl) without pulsing for 3 days and then tested on the bench using conventional potentiometry, they exhibit a more significant negative voltage response towards additions of standard 1 mM KBr compared to freshly made

working electrodes that were not exposed to flowing conditions for 3 d (see Figure 4.4C). This anionic response to bromide ion suggests that some excess TDMA<sup>+</sup> was present in the polymeric membrane phase following the extended exposure to flowing buffer.

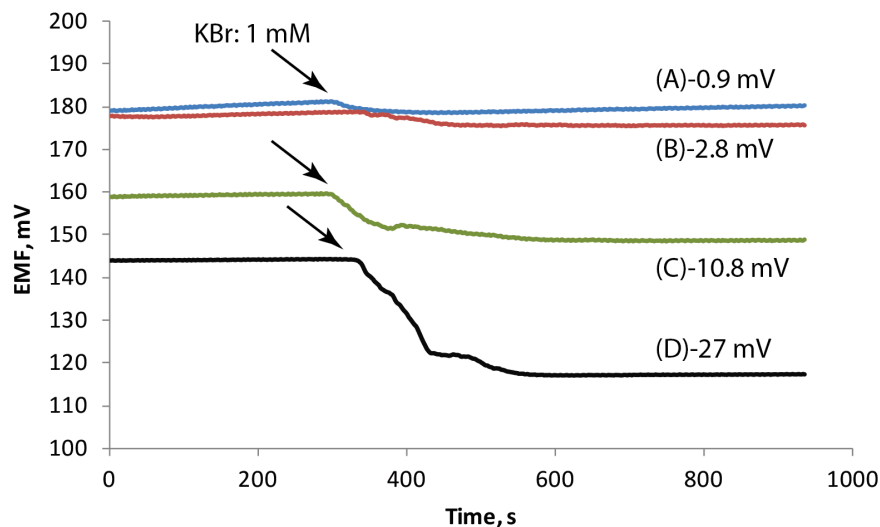


**Figure 4.4.** Open circuit potentiometric response of polymeric membrane electrode to  $10^{-3}$  M KBr (A) before pulstrode measurements; (B) after 500 pulse sequences in flow mode, anodic current applied during galvanostatic pulse; (C) after 3 d in flow system with no galvanostatic pulsing, and (D) after 500 pulse sequences in flow mode with cathodic current applied during galvanostatic pulse. All measurements were conducted in 10 mM phosphate buffer, pH 7.4, containing 10 mM NaCl.

When a fresh sensor is placed under flowing conditions with the polyanion pulse sequence but only for 500 pulses (during 1<sup>st</sup> day), only a very small negative potential change is observed in the presence of KBr, similar to the sensor that has not been exposed to flowing conditions. However, when the sensor is polarized in the flow mode for 3 d using a cathodic current pulse (as would be employed for polycation detection) it exhibits a much larger negative potential change of  $\sim -30$  mV in response to 1 mM KBr in the static potentiometric beaker experiment (see Figure 4.4D). This is likely because as the cathodic current is applied during the galvanostatic pulse, DNNS<sup>-</sup> moves towards

the sample/membrane interface and concentrates in this region, allowing it to be more efficiently washed out from the membrane phase owing to its decreased lipophilicity. In contrast, when the anodic current pulse is applied for polyanion sensing, the  $\text{DNNS}^-$  moves towards the membrane/inner filling solution interface, where the solution is stagnant and  $\text{DNNS}^-$  can partition back into the membrane, while  $\text{TDMA}^+$  ions move to the front side of the membrane. Since  $\text{TDMA}^+$  is more lipophilic than  $\text{DNNS}^-$ , much less  $\text{DNNS}^-$  is washed out from the membrane by the flowing conditions and hence the 1:1 molar ratio of  $\text{DNNS}^-$  to  $\text{TDMA}^+$  within the sensing membrane remains constant for a longer period of time when using the polyanion sensing mode of operation. As expected, this ‘extraction’ effect is much less pronounced in static measurements with polyanion sensors, and likely also with pulstrodes used in similar non-flowing conditions.

The most widely used polyions in pharmaceutical applications are heparin and protamine.<sup>15-20</sup> Protamine is an arginine rich polypeptide used as an antidote to the anticoagulant heparin in medical procedures where it binds strongly to heparin forming a neutral complex.<sup>17</sup> Since large heparin doses can lead to bleeding complications, and protamine overdose is known to cause complement activation and other toxic effects in patients, monitoring of their concentration in blood is potentially quite useful.<sup>16-20</sup> Considering that the pulstrode response is also governed by the presence of sodium or chloride ions, experiments were carried out to determine both heparin and protamine in a FIA mode in which a physiological level of NaCl background is present. Experiments using samples made in a 10 mM phosphate buffer, pH 7.4, with 100 mM NaCl and using this same buffer as the carrier stream were therefore performed. Significant potentiometric response to protamine is still observed (Figure 4.5A) when sensing

polycations, while indiscernible FIA signals for different heparin concentrations are observed in the polyanion sensing mode (data not shown). This is consistent with the low responses toward heparin obtained in static (no flow) measurements using the pulstrode method under similar high NaCl conditions,<sup>12</sup> and may relate to much slower kinetics of ion-exchange at the membrane/sample interface for heparin compared to protamine, given that the average MW of heparin is in the range of 15,000 daltons (compared to protamine MW = 5,100).<sup>21</sup> Since the period where heparin can be effectively extracted into the membrane is only during the galvanostatic and open circuit periods (1.5 s), it is likely that significantly more protamine can be extracted during this short period than heparin, and thus the ability to outcompete the smaller counterions in the sample and membrane phases during and after the polarization period ( $\text{Na}^+$  in polycation sensing mode and  $\text{Cl}^-$  in the polyanion sensing mode) is greater in the case of protamine sensing.

To detect heparin under physiological conditions in the FIA mode, a constant concentration of protamine (60  $\mu\text{g}/\text{mL}$ ) was then mixed with standard amounts of heparin and the resulting mixture was injected into the FIA system operated in the polycation-sensing mode. As shown in Figure 4.5B, as the concentration of heparin increases, a decrease in the EMF response to protamine is observed. The linear range of heparin concentrations that can be detected is from 10 - 35  $\mu\text{g}/\text{mL}$ , which corresponds to 2 - 6 U/mL, lying within the range of heparin concentrations used in certain clinical procedures, like open-heart surgery, extracorporeal membrane oxygenation, etc.<sup>16-19</sup>

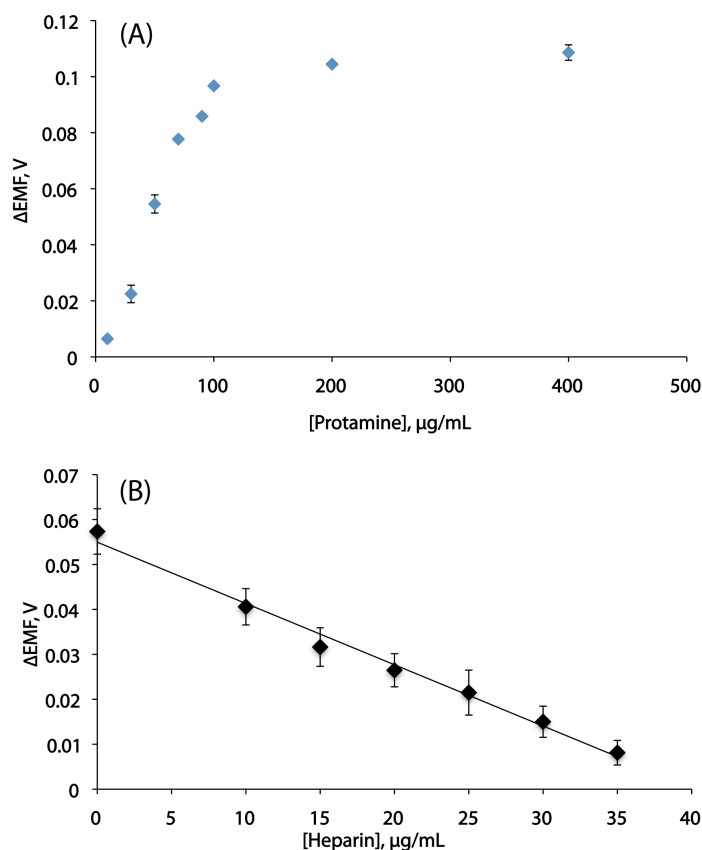


**Figure 4.5. (A) Calibration of DEMF response (peak voltage – baseline voltage) to protamine in flow-injection mode in 10 mM phosphate buffer, pH 7.4, containing 100 mM NaCl. It should be noted that standard deviation for  $n=3$  injections at each concentration is so small that it cannot be observed for some data points; (B) Response to increasing concentrations of heparin with a constant concentration of 60  $\mu\text{g/mL}$  protamine present in test sample in 10 mM phosphate buffer, pH 7.4, containing 100 mM NaCl. Data in (B) represents testing with three different sensors with the same membrane composition in the FIA system, where standard deviation was calculated using data from all three sensors. Flow rates for both A and B were set at 0.6 mL/min.**

It should also be noted that preliminary experiments using protamine spiked into blood plasma were also attempted with the new FIA arrangement. Such experiments showed much larger positive EMF responses than for the same concentration of protamine alone in buffer. This data is at odds with what was previously reported by Bakker and co-workers,<sup>11</sup> using pulstrode type protamine sensors in the static mode,

where the presence of blood components did not perturb the ability to detect protamine. The only difference in the sensor employed in that earlier work vs. the present device was the anion exchanger species of the lipophilic salt used within the membrane, which was a tetradodecylammonium species, compared to tridodecylmethylammonium employed in this work. However, the cationic species is moved toward the inner interface during the cathodic current pulse for polycation detection, and hence more research is needed to understand why some components in the blood that was tested in this work led to such a larger positive interference in detection of protamine.

Flow-injection analysis normally allows for high sample throughput, and therefore flow rate and potentiostatic pulse duration times were further optimized to increase the number of samples analyzed per hour via the arrangement shown in Figure 4.1. To achieve higher throughput, we examined shortening the potentiostatic pulse segment of the sequence. Experiments were carried out to determine how short the potentiostatic pulse could be without compromising reproducibility and maintaining a stable baseline. In prior studies with pulstrodes, it was recommended to apply a 10-30 times longer potentiostatic pulse than galvanostatic one to restore the membrane to its initial state.<sup>11</sup> However, in the optimized polyion sensing FIA system it was found that decreasing the pulse to 6 s and thereby collecting data points every 8 s could be implemented without decreasing reproducibility. In order to further improve the number of samples measured per hour, experiments were carried out to optimize sample loop size and flow rate. Ultimately, a much smaller sample loop volume of 200  $\mu\text{L}$  (vs. 750  $\mu\text{L}$  originally) and increased flow rate up to 0.93 mL/min were employed. Under these conditions, a sampling rate of 20 samples/h can be achieved with a relative standard

deviation of  $\pm 4.2\%$  for the DEMF peak values when monitoring  $60 \mu\text{g/mL}$  protamine (see Figure 4.6).

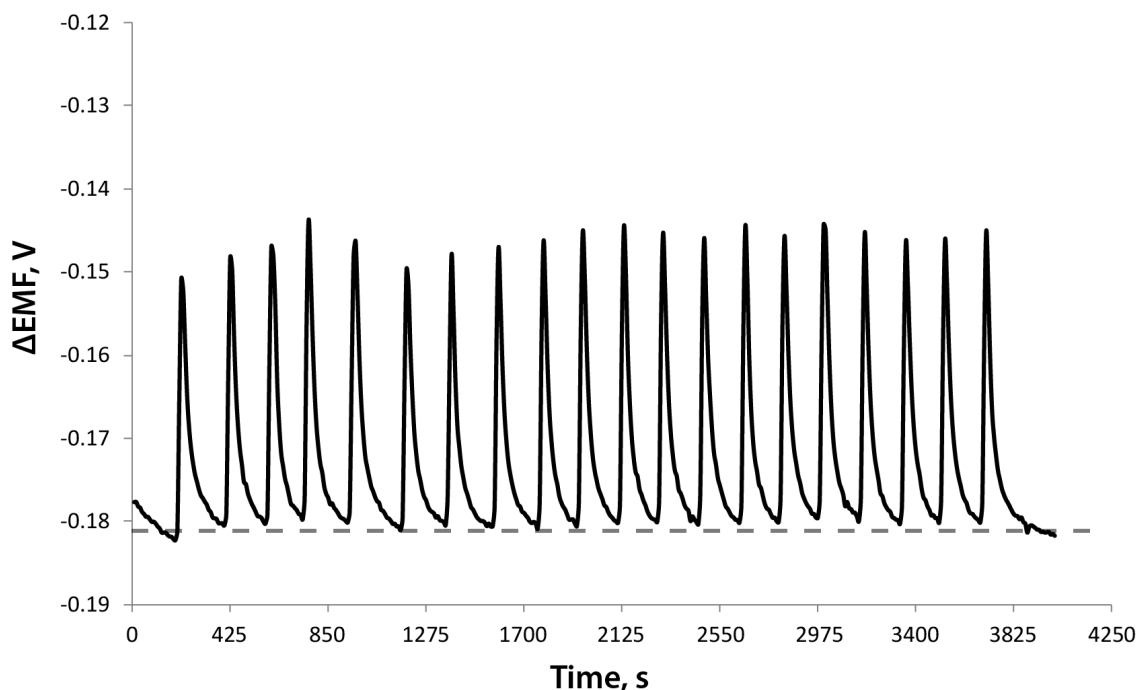


**Figure 4.6. Dynamic potentiometric response to repeated injections ( $n=20$ ) of  $60\text{-}\mu\text{g/mL}$  protamine in  $10 \text{ mM}$  phosphate buffer,  $\text{pH } 7.4$  containing  $100 \text{ mM NaCl}$ . A sampling rate of approximately  $20$  samples per hour has been achieved. For data shown, the average  $\text{DEMF} = 33.7 \text{ mV} \pm 1.42 \text{ mV}$  ( $n=20$ ). Flow rate was set at  $0.93 \text{ mL/min}$ .**

Typically,  $30\text{-}300$  samples per hour can be handled in modern FIA systems, and even up to  $1000$  have been reported in specially designed microsystems with optical detection.<sup>13</sup> Thus, the obtained sample throughput in this work may not appear to be significant. However, given the high molecular weights of the species detected and considering that use of the traditional pulstrode method in a static mode requires manually changing sample and background solutions as well as further manually rinsing of all the electrodes between samples, detecting polyions at low levels with a throughput of  $20$  samples per hour is still a step forward. By using more highly plasticized

membranes in the working electrode, or even fully organic liquid membranes, it may be possible to increase the rate of polyion extraction during and after the galvanic pulse. This might also lead to faster membrane recovery times during the potentiostatic pulse. Taken together, this approach might enable use of smaller sample volumes and shorter pulse sequences that may lead to even higher throughputs.

#### **4.4 Conclusions**

We have demonstrated, for the first time, that polyion selective pulstrodes can be used as detectors in an FIA measurement configuration. Within such a flow-through system, this sensing mode provides relatively stable and reproducible signals that are proportional to both polycation and polyanion concentrations using a single working membrane electrode. While demonstrated here for use in detecting heparin and protamine as model analytes, it is envisioned that this method could prove useful for quality control monitoring of a wide range of products/supplements that utilize polyions as active ingredients. Further, the methodology described here should also be applicable in developing flow-through methods to detect specific enzyme activities that cleave polyions into smaller fragments that are not sensed by the pulstrode. Finally, the use of polyion selective pulstrodes as universal detectors in preparative LC separation methods employed to isolate or fractionate polyion species, as well as their use as detectors in modern microfluidic devices, should also be possible.

## 4.5 References

- [1] Ma, S.; Meyerhoff, M. E.; Yang, V. C., *Anal. Chem.*, **1992**, *64*, 694-697.
- [2] Ma, S.; Yang, V. C.; Fu, B.; Meyerhoff, M. E., *Anal. Chem.*, **1993**, *65*, 2078-2084.
- [3] Fu, B.; Bakker, E.; Yun, J. H.; Yang, V. C.; Meyerhoff, M. E., *Anal. Chem.* **1994**, *66*, 2250-2259.
- [4] Fu, B.; Bakker, E.; Yang, V. C.; Meyerhoff, M. E., *Macromolecules*, **1995**, *28*, 5834-5840.
- [5] Ye, Q.; Meyerhoff, M. E., *Anal. Chem.*, **2001**, *73*, 332-336.
- [6] Yun, J. H.; Meyerhoff, M. E.; Yang, V.C., *Anal. Biochem.*, **1995**, *224*, 212-220.
- [7] Hassan, S. S. M.; Meyerhoff, M.E.; Badr, I.H.A.; Abd-Rabboh, H.S.M., *Electroanalysis*, **2002**, *14*, 439-444.
- [8] Wang, L.; Buchanan, S.; Meyerhoff, M. E., *Anal. Chem.*, **2008**, *24*, 9845-9847.
- [9] Wang, L.; Meyerhoff, M. E., *Electroanalysis*, **2010**, *22*, 26-30.
- [10] Shvarev, A.; Bakker, E., *JACS*, **2003**, *125*, 11192-11193.
- [11] Shvarev, A.; Bakker, E., *Anal. Chem.*, **2005**, *77*, 5221-5228.
- [12] Gemene, K.; Meyerhoff, M. E., *Anal. Chem.*, **2010**, *82*, 1612-1615.
- [13] Du, W.; Fang, Q.; He, Q.H.; Fang, Z.L., *Anal. Chem.*, **2005**, *77*, 1330-1337.
- [14] VCCLAB, Virtual Computational Chemistry Laboratory, <http://www.vcclab.org>, 2005.
- [15] Despotis, G. J.; Joist, J. H.; Goodnough, L. T., *Clin. Chem.*, **1997**, *43*, 1684-1696.
- [16] FitzGerald, D. J.; Patel, A.; Body, S.C.; Garvin, S., *Perfusion*, **2009**, *24*, 93-96.
- [17] Gautam, N. K.; Schmitz, M.L.; Harrison, D.; Zabala, L.M.; Killebrew, P.; et. al., *Pediatric Anesthesia*, **2013**, *23*, 233-241.
- [18] Koster, A.; Fischer, T.; Praus, M.; Haberzetti, H.; et. al., *Anesthesiology*, **2002**, *97*, 837-841.
- [19] Despotis, G. J.; Joist, J. H.; Hogue, C.W.; Alsoufiev, A.; et. al., *J. Thorac. Cardiovasc. Surg.*, **1995**, *110*, 46-54.
- [20] Bhaskar, U.; Sterner, E.; Hickey, A. M.; Onishi, A.; et. al., *Appl. Microbiol. Biotechnol.*, **2012**, *93*, 1-16.
- [21] Ando, T.; Watanabe, S., *Int. J. Protein Res.*, **1969**, *3*, 221-224.

## CHAPTER 5

### MONITORING ENZYMATIC REACTIONS USING POLYMERIC MEMBRANE-BASED POLYION SELECTIVE PULSTRODES

#### 5.1 Introduction

The ability to study enzymatic reactions facilitates the understanding of biological processes. Therefore, there are many techniques that have been developed to investigate substrate specificity, reaction rates, and other important biological characteristics of enzyme systems. Commonly used methods for monitoring enzymatic activity include: spectrophotometry (UV-Vis), fluorometry, and chemiluminescence. Although effective, these methods require significant sample preparations, can have selectivity issues, and cannot measure in turbid solutions (e.g., whole blood).<sup>1-3</sup>

Ion-selective electrodes (ISEs) for polyanion detection were developed in the early 1990's by the Meyerhoff group and have since been utilized for many applications including detection of the highly sulphated glycosaminoglycan heparin<sup>4-7</sup> and monitoring enzymatic reactions (e.g., protamine/trypsin, and polyphosphates/acid phosphatase).<sup>8-10</sup> These sensors are easy to operate, are cost-effective, robust, and take measurements in complex and turbid media, such as whole blood.<sup>5</sup> These sensors are unlike classical ISEs in the sense that their response is based on a non-equilibrium mechanism.<sup>7</sup> For polyanion sensing, the membrane is doped with an anion-exchanging lipophilic quaternary

ammonium species that makes a strong cooperative ion pair with the target polyanion. This action yields a non-equilibrium steady-state phase boundary potential change ( $\Delta$ EMF) at the membrane/sample interface. When enzymatic activity is monitored with this sensor, the continuous change in substrate size (i.e., the digestion of the substrate) is evident in the degree of EMF response. The smaller digested substrate fragments form much weaker cooperative ion-pairs with the ion-exchanger in the membrane, and therefore, the absolute value of the potential change decreases, which can be observed in real time.

Although polyion sensors for both polyanions and polycations have been successfully used to monitor enzymatic activities,<sup>9,10</sup> many of these studies have employed sensors that are considered single-use devices because the strong cooperative ion-pairs made between the ion-exchanger and target polyions are so strong that the dissociation of the ion-pair in the membrane phase is extremely slow. Further, a small number of these ion-pairs can be extracted deep into the membrane<sup>8-10</sup> before the enzyme can digest the target analyte. Although a reversal in signal is observed during substrate digestion, the signal does not fully return to the baseline and therefore, the sensor cannot be re-used for a second measurement. This single-use characteristic impacts other applications of this method and has recently been addressed by a fully-reversible chronopotentiometric method called pulstrode.<sup>11-14</sup> The pulstrode configuration was pioneered by the Bakker group in the early 2000s, and within the last ten years has been developed for applications such as protamine detection in whole blood, protease activity monitoring,<sup>11-13</sup> and reversible detection of heparin and other glycosaminoglycans.<sup>14</sup> Although protease activities have been successfully monitored by the pulstrode

technology,<sup>15</sup> enzymatic reactions involving polyanions have not been previously reported in literature and are presented here for the first time. Indeed, in this paper it is demonstrated that the cleavage of polyphosphate anions via acid phosphatase can be monitored in real time using a polyanion sensitive pulstrode. Further, it is shown that inhibitors for such reactions can also be detected.

## **5.2 Experimental Section**

### *5.2.1 Reagents*

High molecular weight poly(vinyl chloride) (PVC), 2-nitrophenyloctyl ether (*o*-NPOE), tridodecylmethylammonium chloride (TDMACl), tetrahydrofuran (THF), hexametaphosphate, tripolyphosphate, acid phosphatase from potato, phosphatase inhibitor cocktail II, and all buffer salts were purchased from Sigma Aldrich (St. Louis, MO). Dinonylnaphthalene sulfonic acid (DNNSH) as a 49 wt% solution in xylenes was donated by King Industries.

### *5.2.2 Preparation of Ion-Exchanger Salt*

The lipophilic ion-exchanger salt was prepared by metathesis in benzene in a 1:1 molar ratio of DNNSH:TDMACl. The benzene-salt solution was washed several times with deionized water until the aqueous solution was neutral. The solvent of the organic phase was evaporated and the resulting salt was re-dissolved in THF and kept as a solution to be used in the membrane preparation.

### *5.2.3 Membrane Preparation*

All membranes contained 10 wt% TDMA<sup>+</sup>-DNNS<sup>-</sup>-ion-exchanger salt, 30 wt% PVC and 60 wt% *o*-NPOE. All membrane components were dissolved in THF and prepared by solvent casting into glass rings (30 mm diameter), which were left to dry overnight. A membrane cocktail containing 10 wt% inert lipophilic salt TDMA<sup>+</sup>-DNNS<sup>-</sup>, PVC and *o*-NPOE 1:2 by weight with approximate thickness of 200  $\mu\text{m}$  was employed for all experiments.

#### *5.2.4 Electrodes*

Membranes were cut with a cork borer from the parent membrane and placed into a Philips electrode body (Oesch Sensor Technology, Sargans, Switzerland). All sensors were conditioned overnight in 1 mM NaCl, and inner-filling solutions were the same as the conditioning solution, which were in contact with an internal Ag/AgCl reference electrode. The external reference electrode was a double-junction Ag/AgCl electrode (Accumet 13-620-658, Fisher Scientific) with 3 M KCl as the inner filling solution and 1 M LiOAc as a bridge electrolyte. A coiled Pt-wire was used as a counter electrode for all pulsed chronopotentiometric measurements.

#### *5.2.5 Measurements*

A three-electrode set-up was used for pulstrode measurements that employed a TDMA<sup>+</sup>-DNNS<sup>-</sup>-doped membrane working electrode, a commercial external double-junction reference (Accumet 13-620-658, Fisher Scientific), and a platinum counter electrode, which were all immersed into the sample solution/buffer of 2-(N-morpholino)ethanesulfonic acid at pH 5.2 (MES). Phosphatase inhibitor was used as 0.5 and 1 v% stock solutions in MES buffer, pH 5.2 of the original proprietary blend. Both

the substrate and enzyme were dissolved in MES buffer, pH 5.2, immediately before use. Before measurements, varying concentrations of inhibitor and the substrate were mixed into the background solution. After 3 pulse sequences, the enzyme was injected into the solution. The final concentrations of the substrate and enzyme were 40  $\mu\text{g/mL}$  and 0.75 U/mL, respectively. The measurements were conducted with an AFCBI biopotentiostat (Pine Instruments, Grove City, PA) controlled by a NI-DAQPad 6015 interface board and LabVIEW 8.6 data acquisition software (National Instruments, Austin, TX) on a PC computer. Measurements were based on a three-pulse sequence involving a 1 s, 20  $\mu\text{A}$  galvanostatic (uptake) pulse, a 0.5 s open circuit measurement period, and a 15 s, 0 V potentiostatic (stripping) pulse. The potentials were sampled as the averaged EMF values of the last 10% of data collected during the zero current pulse. All experiments were conducted at room temperature (25°C) inside a Faraday cage.

## **5.3 Results and Discussion**

### *5.3.1 Mechanistic Response*

Polyion selective pulstrodes were employed to monitor enzymatic activity using acid phosphatase and hexametaphosphate as a model system. Measurements were made using a conventional three-electrode system (working, counter, reference) based on a three-pulse sequence: (1) the galvanostatic pulse, (2) an open-circuit period, and (3) the potentiostatic pulse. The polymeric membrane within the working electrode is doped with a lipophilic ion-exchanger salt with no intrinsic ion-exchange properties. However, during pulse 1, a 20  $\mu\text{A}$  current is applied to the membrane for 1 s. The current induces a flux of anionic species from the sample towards the membrane, and concomitantly

polarizes the lipophilic salt species in the membrane phase. During this pulse, the TDMA<sup>+</sup> inside the membrane migrates to the sample/membrane interface. Subsequently, the sample/membrane interface now has anion-exchange properties, and TDMA<sup>+</sup> can exchange less preferred anionic background ions, such as Cl<sup>-</sup>, for the target analyte (hexametaphosphate) during the 0.5 s open circuit pulse (pulse 2). Potentiometric data is acquired during pulse 2, where the last 10% of the cell EMF data is averaged and used as a single data point, which represents a single pulse sequence. The reversibility of this sensor is dependent on pulse 3, where a 15 s, 0 V pulse depolarizes the membrane and expels target polyanion (hexametaphosphate) and background ions that were forced into the membrane during pulse 1. The principles of this method have been reported by Bakker and co-workers<sup>11,12</sup> and the functions of each of these steps have been described in prior work reported by Gemene et al.<sup>14</sup> for polyanion sensing.

The same principles for monitoring enzymatic activity with single-use polyion sensors can be used to understand the response observed in the pulstrode measurements. As the intact hexametaphosphate is digested, the smaller fragments that are produced make weaker cooperative ion-pairs with the ion-exchanger, which is observed in the reversal in signal towards baseline potentials. A schematic of this process is shown in Figure 5.1.

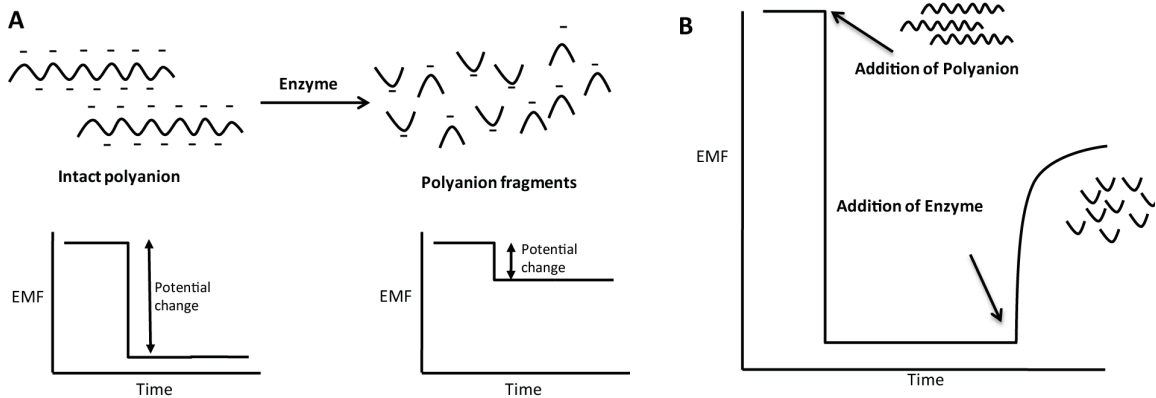


**Figure 5.1. Schematic of polyanion substrate degradation by enzyme. (A) Separate measurement sensor responses to intact polyanion and digested polyanion. Scales for the potentiograms are the same. (B) Sensor response during an enzymatic reaction where the polyanion is added to a background solution and the enzyme is injected once the signal to the polyanion is stable. A reversal in signal is observed due to the digestion of the substrate.**

### 5.3.2 Hexametaphosphate Measurements

Measurements were carried out using polyanion selective pulstrodes to measure activity of acid phosphatase when hexametaphosphate was present as the substrate. All measurements were subtracted from background solution potentials (1 mM NaCl in 10 mM MES buffer, pH 5.2). The linear response range of the sensor towards hexametaphosphate was determined, and a concentration of 40  $\mu\text{g/mL}$ , near the end of the linear response region (see Figure 5.2), was used throughout all experiments. It is necessary to use a substrate concentration within this region so that enzyme activity could be easily observed. For example, if the initial substrate concentration fell beyond the higher end of the linear range, the reversal in signal could not be seen immediately, and only when the enzyme digested enough of the substrate to decrease the concentration to one which fell within the linear range boundaries would a significant signal change be observed. Since acid phosphatase loses significant activity at room temperature within

24 h,<sup>17</sup> it is important that the reversal in signal is observed immediately so that the enzyme's initial activity can be calculated accurately. However, it is also important to choose a concentration within the linear range high enough to create a fairly large overall potential change when the pure substrate is measured, so that a significant reversal in signal can be observed when the enzyme is added and the rate of change can be easily calculated. Therefore, subsequent enzyme activity measurements were made using 40  $\mu\text{g}/\text{mL}$  hexametaphosphate to ensure that the potential change to this concentration was stable and reproducible with an average potential change of  $-85.3$  mV and standard deviation of  $2.50$  mV ( $n=3$ ).

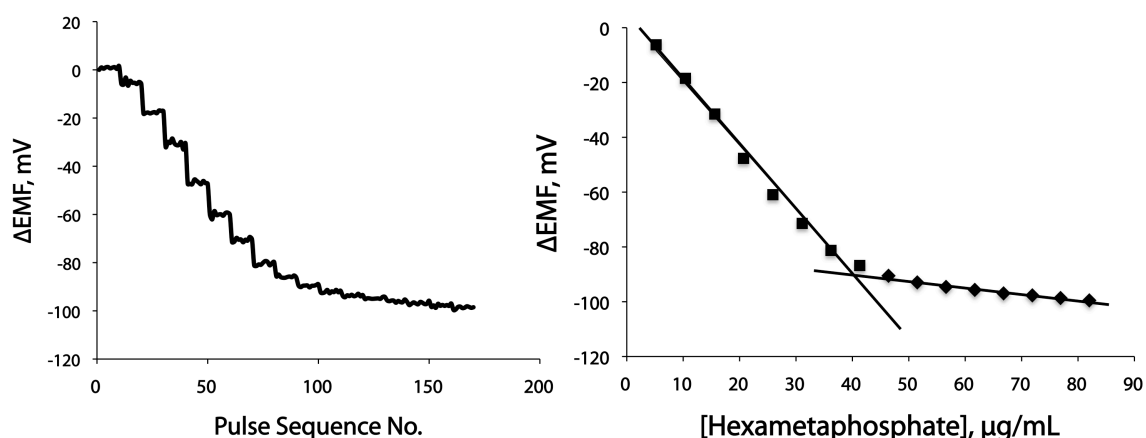


**Figure 5.2.** (A) Dynamic response and (B) calibration curve for hexametaphosphate in 1 mM NaCl, 10 mM MES buffer. For substrate digestion to be observed using pulstrode, a large concentration within the linear must be selected to monitor the enzymatic activity. The concentration used in all experiments was 40  $\mu\text{g}/\text{mL}$  hexametaphosphate.

### 5.3.3 Digestion of Hexametaphosphate by Acid Phosphatase

Different acid phosphatase concentrations were monitored using the polyion selective pulstrode. During a typical measurement, background solution potentials were

measured first, for 10 pulse sequences, to establish a baseline potential. Then background containing 40  $\mu\text{g/mL}$  hexametaphosphate was recorded for 10 pulse sequences and the potential was subtracted from the baseline measurement to determine potential response to the substrate followed by a second background measurement to ensure the same baseline potential can be obtained before monitoring the substrate in the presence of enzyme. For enzyme activity measurements, the substrate was added to solution and measured for three pulse sequences before enzyme was injected. The total pulse sequence number was extended to 40 for these measurements, which were approximately 12 min from the point of enzyme injection (enzyme was injected after 3 pulses which is  $\sim 52$  s). Experiments were carried out to determine the initial rate of reaction by measuring the decrease in substrate response in the presence of the enzyme for the first 12 min. Once the enzyme was added to solution, a reversal in signal towards the baseline was immediately observed. As shown in Figure 5.3A, the signal reversal increases at a faster rate as the enzyme activity increases, indicating the faster digestion of hexametaphosphate as acid phosphatase activity increases. Enzyme activities of 0.15, 0.25, 0.35, 0.5, and 0.75 U/mL were measured and rates were determined by calculating the slope of potential response vs. time during the first two minutes after enzyme injection (Figure 5.3B).

Signal reversal rate vs. enzyme activity was plotted and a linear trend is observed for concentrations of 0.15 U/mL to 0.5 U/mL, as shown in Figure 5.4.

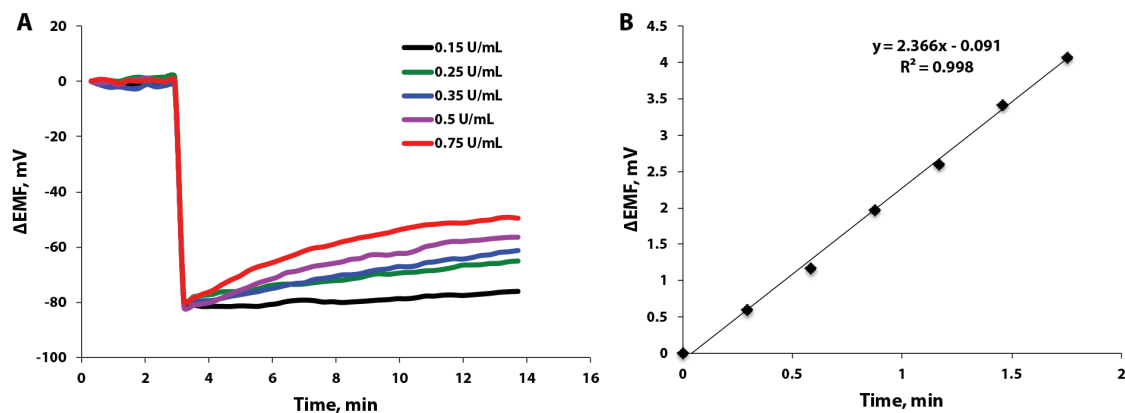


Figure 5.3. (A) Potentiometric data for enzyme activities of 0.15, 0.25, 0.35, 0.5, and 0.75 U/mL in 40  $\mu\text{g/mL}$  hexametaphosphate, 1 mM NaCl, 10 mM MES buffer. (B) Enlarged graph of the first ~2 min of EMF vs. time curves after injection of 0.35 U/mL acid phosphatase activity.

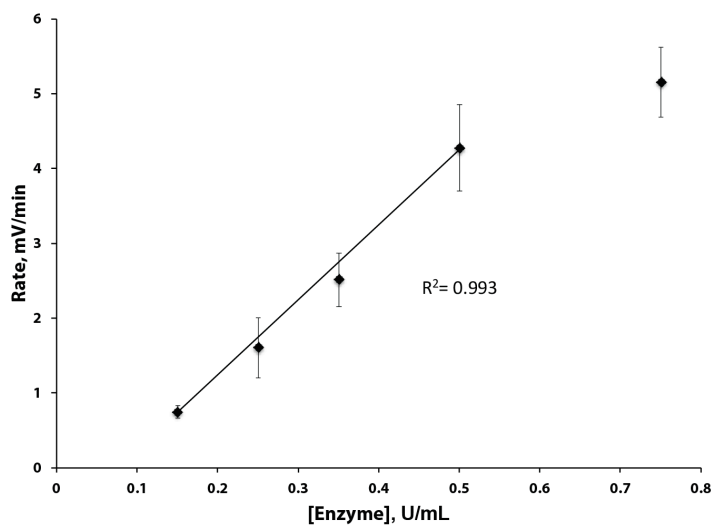
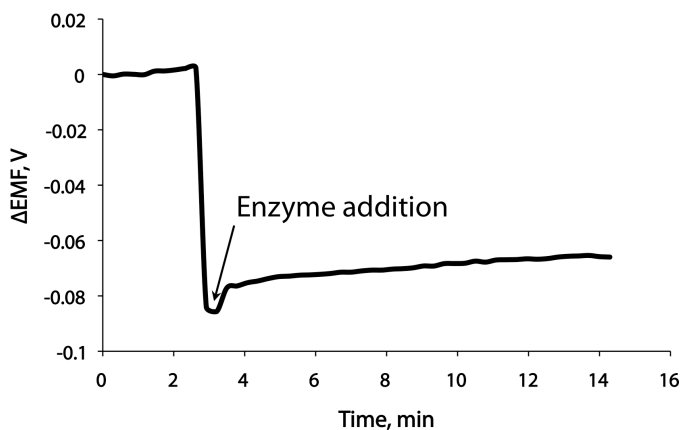


Figure 5.4. Rate of potential change vs. acid phosphatase activity, where  $n=6$ . All measurements were made in 40  $\mu\text{g/mL}$  hexametaphosphate, 1 mM NaCl, 10 mM MES buffer, pH 5.2.

Enzyme activity measurements for concentrations larger than 0.75 U/mL were conducted. However, an instant sharp increase in signal was observed immediately after enzyme injection, which then tapered off into a slower reversal in signal. This increase of the signal became larger as the enzyme concentrations increased and rates for these

concentrations could not be calculated due to the discontinuity in the data (see Figure 5.5 as example). Since data is only collected every 17.5 s, this may suggest that enzyme concentrations exceeding 0.75 U/mL are digesting the substrate too rapidly for the sensor to detect a continuous reversal in signal.



**Figure 5.5.** Discontinuity in reversal in signal induced by 1 U/mL acid phosphatase in 40  $\mu\text{g/mL}$  hexametaphosphate, 1 mM NaCl, and 10 mM MES buffer, pH 5.2.

Intuitively, shortening the pulse sequence length could assist in extending the linear range. Indeed, the potentiostatic pulse length has been reduced to 6 s without losing reproducibility in previous studies<sup>16</sup> but, unfortunately, this did not alleviate the sharp break in the data observed in this work. Obviously, diluting higher enzyme levels to achieve activities in the range where linear response to enzyme activity is observed is the simplest solution to this issue.

#### 5.3.4 Enzyme Inhibitors

The effect of an enzyme inhibitor on the hexametaphosphate/acid phosphatase system was also studied. A proprietary blend of enzyme inhibitors, which contains sodium tartrate, a well-known competitive inhibitor of acid phosphatase,<sup>18</sup> was diluted to a 1 v% solution and used for all measurements. One acid phosphatase concentration, 0.75 U/mL, was chosen to study enzyme inhibitor effects. As expected, a decrease in acid phosphatase activity was observed in the presence of the inhibitor. Solutions of 0.00005, 0.0001, 0.00025, 0.0005, 0.001, 0.002, 0.003, 0.004, 0.005 and 0.01 v% were examined to determine the effect on acid phosphatase activity and are presented in Figure 5.6. Fairly good linearity is observed between 0 and 0.00025 v% inhibitor solution before enzyme activity begins to level off at an extremely low level. Zero enzyme activity is finally reached when 0.1 v% solution of inhibitor is present.

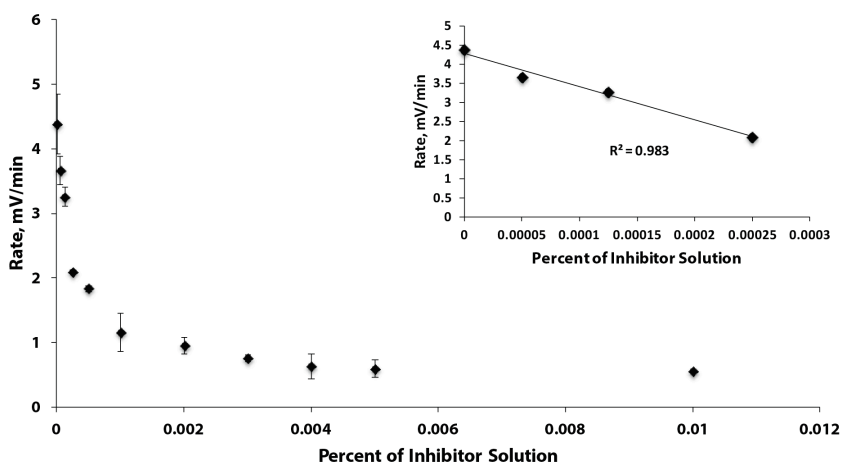


**Figure 5.6. Effect of inhibitor concentration on acid phosphatase activity at 0.75 U/mL. The inset shows the linearity of data points between 0 and 0.00025% inhibitor solution.**

## 5.4 Conclusions

A polyanion sensitive pulstrode has been successfully employed for monitoring acid phosphatase activity using hexametaphosphate as the substrate. ISEs, in general, provide a simple method for measuring enzyme activities in complex and turbid solutions that is stable and selective. Single-use polyion sensors have been utilized previously to determine enzyme activities, but their irreversible nature prevents multiple uses, which can be inconvenient when measuring many different samples. Thus, the pulstrode provides a stable and reproducible measurement system that can be employed for several assays without requiring many different sensors to determine enzyme activity in many samples. Although it may be necessary to optimize measurement conditions for different substrate/enzyme systems based on the given enzyme activity or sensor response to the polyion substrate, it is likely that the approach reported here could be utilized to detect the degradation of other substrates for acid phosphatase, such as diadenosine pentaphosphate and polyadenylic acid, or enzymes such as heparinase I, II, and III activity, which are known to cleave polyanionic heparin into small fragments.

## 5.5 References

- [1] Mountfort, D.; Kennedy, G.; Garthwaite, I.; Quilliam, M.; et. al., *Toxicon* **1999**, *37*, 909-922.
- [2] Kettling, U.; Koltermann, A.; Schwille., *Proc. Natl. Acad. Sci.* **1998**, *95*, 1416-1420.
- [3] Sergienko, E., Phosphatase Modulators. In *Methods in Molecular Biology*; Millán, J. L., Ed.; Humana Press: New Jersey, 2013; Vol. 1053 p. 7.
- [4] Ma, S.; Yang, V.; Meyerhoff, M., *Anal. Chem.* **1992**, *64*, 694-697.
- [5] Ma, S.; Yang, V.; Fu, B.; et. al., *Anal. Chem.* **1993**, *65*, 2078-2084.
- [6] Fu, B.; Bakker, E.; Yun, J.; et. al., *Anal. Chem.* **1994**, *66*, 2250-2259.
- [7] Fu, B.; Bakker, E.; Yang, V.; et. al., *Macromolecules* **1995**, *28*, 5834-5840.
- [8] Dai, S.; Meyerhoff, M. E., *Electroanalysis* **2001**, *13*, 276-283.
- [9] Yun, J. H.; Meyerhoff, M. E.; Yang, V. C., *Anal. Biochem.* **1995**, *224*, 212-220.
- [10] Esson, J.; Meyerhoff, M., *Electroanalysis* **1997**, *9*, 1325-1330.
- [11] Shvarev, A.; Bakker, E., *J. Am. Chem. Soc.* **2003**, *125*, 11192-11193
- [12] Makarychev-Mikhailov, S.; Shvarev, A.; Bakker, E., *J. Am. Chem. Soc.* **2004**, *126*, 10548-10549.
- [13] Shvarev, A.; Bakker, E., *Anal. Chem.* **2005**, *77*, 5221-5228.
- [14] Gemene, K.; Meyerhoff, M. E., *Anal. Chem.* **2010**, *82*, 1612-1615.
- [15] Xu, Y.; Shvarev, A.; Makarychev-Mikhailov, S.; Bakker, E., *Anal. Biochem.* **2008**, *374*, 366-370.
- [16] Bell-Vlasov, A.; Zajda, J.; Eldourghamy, A.; Malinowska, E.; Meyerhoff, M. E., *Anal. Chem.* **2014**, *86*, 4041-4046.
- [17] King, E. J.; Jegatheesan, K. A., *J. Clin. Path.* **1959**, *12*, 85-89.
- [18] Van Etten, R. L.; Saini, M. S., *Clin. Chem.* **1978**, *24*, 1525-1530.

## CHAPTER 6

# POLYION SELECTIVE POLYMERIC MEMBRANE-BASED PULSTRODE FOR THE DETECTION OF HIGH CHARGE DENSITY SPECIES IN HEPARIN PREPARATIONS

### 6.1 Introduction

The efficacy of single-use polymeric polyion sensors for the detection of high charge density contaminants (i.e., OSCS) was examined and demonstrated in Chapter 3. These sensors have viability for screening commercially available heparin preparations that is cost effective, easy to use, and reliable, with detection limits ( $\geq 0.5$  wt%),<sup>1</sup> well below the level of toxicity of OSCS in heparin (5 wt%).<sup>2</sup> A single use, hand held strip test device based on the principles of the single-use heparin sensor has recently been developed, and even lower detection limits of 0.005% OSCS in heparin preparations have been reported.<sup>3</sup> Although these qualities make these sensors desirable for heparin screening, their irreversible nature limits applications in clinical settings, such as in-line monitoring during heparin administration. In recent years, reversible non-equilibrium sensor applications have been pursued to improve and modify selectivity and to improve detection of large polyions like heparin and protamine.<sup>4-11</sup> Hence, a reversible detection method for high charge density (HCD) species in heparin should be pursued to extend the

applications in which polyion sensors can be useful to rule out contamination and/or tainting of commercial heparin products.

As discussed in Chapters 4 and 5, the polyion pulstrode device has addressed the irreversible quality of single-use polyion sensors by providing a system in which the membrane is renewed after each measurement of heparin or other polyions. Therefore, in this chapter, the optimization of this system for improving detection limits of HCD species in heparin preparations is pursued. The charge density of pentosan polysulfate (PPS) is much larger than heparin,<sup>12,13</sup> and this species is therefore useful as a model HCD species spiked into heparin preparations. Optimization of the current magnitude, length of the current pulse, and length of the zero-current, open-circuit pulse is carried out and the impact on detection limits of the PPS in heparin is demonstrated and discussed.

## **6.2 Experimental Section**

### *6.2.1 Reagents*

High molecular weight poly(vinyl chloride) (PVC), 2-nitrophenyloctyl ether (*o*-NPOE), tridodecylmethylammonium chloride (TDMACl), anhydrous tetrahydrofuran (THF), heparin sodium salt, and all buffer salts were purchased from Sigma Aldrich (St. Louis, MO). Pentosan polysulfate (PPS) was obtained from Bene Arzneimittel GmbH (Munich, Germany). Dinonylnaphthalene sulfonic acid (DNNSH) as a 49% solution in xylenes was a gift from King Industries (Norwalk, CT).

### 6.2.2 Preparation of Ion-Exchanger Salts

The lipophilic ion-exchanger salt used in the polymeric membrane was prepared by metathesis in benzene for a 1:1 molar ratio of DNNSH and TDMACl. The benzene-salt solution was washed several times with Milli-Q grade deionized water (18.2  $\Omega$ , Millipore Corp., Billerica, MA) until the aqueous solution was neutral. The benzene phase was then left to dry overnight (in open air in a fume hood), and the residual salt was re-dissolved in THF and then dried again overnight for use in preparation of the polyion selective membranes.

### 6.2.3 Polymeric Membrane Preparation

All polyion selective membrane films contained 10 wt% of TDMA/DNNS salt and were  $\sim 200$   $\mu\text{m}$  thick. The sensing membranes were all formulated to contain a 1:2 by weight ratio of PVC to *o*-NPOE plasticizer. All membrane components were dissolved in THF and membrane films were prepared by solvent casting solutions into glass rings on glass plates and letting the solutions dry overnight (in fume hood).

### 6.2.4 Electrodes

Sensor membranes were cut with a cork borer (8 mm diam.) from the parent membrane and placed into an electrode body (Oesch Sensor Technology, Sargans, Switzerland). The actual membrane area was 20 mm<sup>2</sup>. All sensors were conditioned overnight in 1 mM NaCl, 10 mM phosphate buffer, pH 7.4. The inner-filling solution in contact with the inner Ag/AgCl reference was the same as the outer conditioning solution. A double-junction Ag/AgCl electrode with 3 M KCl as the inner filling solution and 1 M LiOAc as a bridge electrolyte was used as the external reference electrode. A

coiled Pt-wire was used as a counter electrode for all pulsed chronopotentiometric measurements.

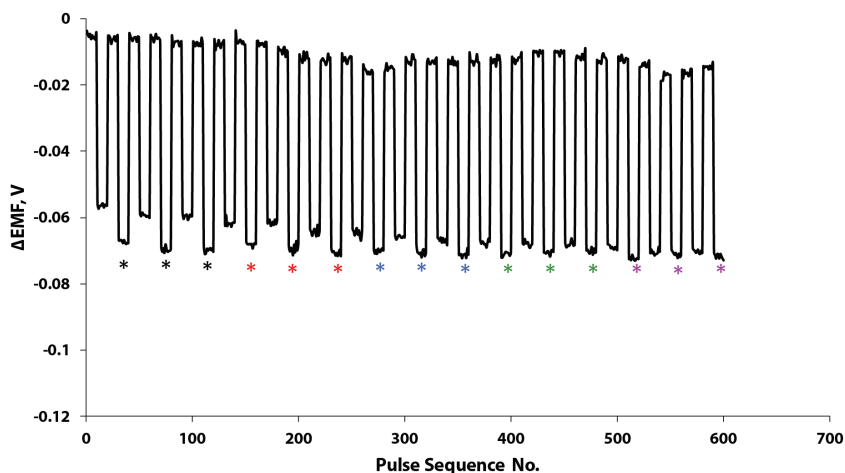
#### *6.2.5 Measurements Using Polymeric Membrane Configuration*

A conventional three-electrode set-up was used for the pulstrode measurements with the TDMA/DNNS-based polymeric membrane electrode serving as the working electrode and all electrodes were immersed in background/sample solutions. All experiments were carried out in 1 mM NaCl, 10 mM phosphate buffer, pH 7.4. The electrochemical measurements were conducted with an AFCBI bipotentiostat (Pine Instruments, Grove City, PA) controlled by a NI-DAQPad 6015 interface board and LabVIEW 8.6 data acquisition software (National Instruments, Austin, TX) on a PC computer. All measurements were carried out inside a Faraday cage to minimize electronic noise. Current (galvanostatic) pulse times of 1, 2, 3, 4, and 5 s and current magnitudes from 10-35  $\mu\text{A}$  were used for optimization experiments. Zero-current pulse lengths of 0.5, 1, 2, 5, and 10 s and a potentiostatic pulse of 0 V vs. Ag/AgCl (stripping potential) of 15 s were used. The potentials were sampled as the averaged data during the last 10% time period of the 0.5 s zero-current pulse. All experiments were carried out at room temperature (21-23  $^{\circ}\text{C}$ ).

### **6.3 Results and Discussion**

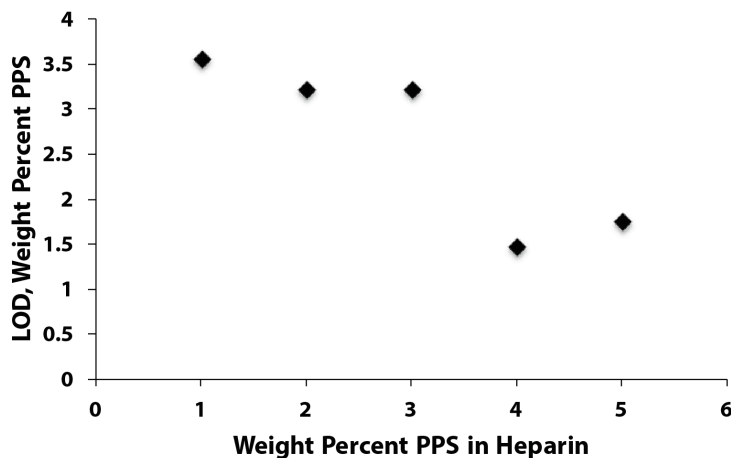
The initial parameters used for pulstrode experiments to detect PPS in heparin preparations are as follows: a 1 s, 20  $\mu\text{A}$  current pulse, a 0.5 s zero-current open-circuit pulse, and a 15 s 0 V potentiostatic pulse. Overall potential responses for pure heparin and pure PPS at 400  $\mu\text{g/mL}$  in 1 mM NaCl, 10 mM phosphate buffer, pH 7.4, were  $\sim$ -100

mV and  $\sim -220$  mV, respectively. Assuming a linear response to PPS, the detection limit for 10 wt % PPS spiked into 400  $\mu\text{g/mL}$  heparin under the above-mentioned conditions should be 0.6 wt% PPS. Limits of detection were calculated solving the following equation for X:  $3 \times \text{s.d.} = mX$ , where s.d. is standard deviation of the signal to pure heparin, m is the slope/sensitivity of signal vs. concentration of PPS contaminant, and X is the concentration. However, this method was not ultimately used to obtain the “true” LOD for PPS in heparin since as the concentrations of PPS decrease in heparin preparations, the degree of EMF difference between pure heparin and the contaminated sample does not have a linear dependence. Rather, the response to very low levels of PPS in the heparin is not actually discernible from the pure heparin signal, until a critical concentration of PPS is reached, at which point there is a clear difference in the EMF values for the pure heparin vs. the PPS contaminated heparin (see Fig. 6.1).



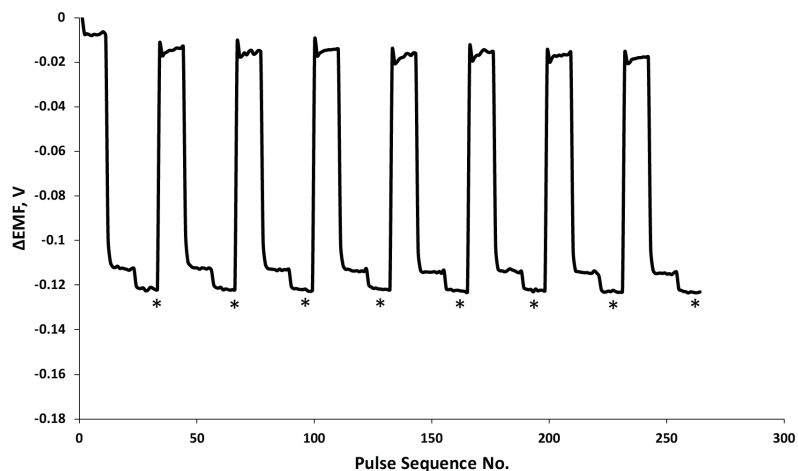
**Figure 6.1.** Potentiometric data for 5 (black asterisk), 4 (red asterisk), 3 (blue asterisk), 2 (green asterisk), and 1 wt% (purple asterisk) PPS in 400  $\mu\text{g/mL}$  heparin, 1 mM NaCl, 10 mM phosphate buffer. A 1 s, 10  $\mu\text{A}$  current pulse, 0.5 s open-circuit pulse, and 15 s potentiostatic pulse was applied.

Figure 6.2 displays the change in detection limits as the PPS concentration within 400  $\mu\text{g}/\text{mL}$  heparin increases. Detection limits calculated for 5 wt% PPS in heparin are half that calculated for 1%. This is likely due to the kinetic limitation of the pulstrode system (see below).



**Figure 6.2.** Detection limits for 1, 2, 3, 4 and 5 wt% PPS in heparin preparations. A 1 s, 10  $\mu\text{A}$  current pulse, 0.5 s open-circuit pulse, and 15 s potentiostatic pulse was applied. At 5 wt% PPS, the detection limits are half of what has been calculated for 1 wt%. No linearity is observed.

Pulstrode measurements of PPS concentrations  $\geq 10$  wt% in heparin gave intermediate (mixed) potential responses (see Figure 6.3). This is in contrast to the potential change observed during a simultaneous measurement of two different polyanions in single-use sensors, where the potential response is essentially governed by the polyion with the largest charge density at  $\geq 5$  wt%.<sup>1</sup> Typical reproducibility data for the measurement of pure heparin and 10 wt% PPS in heparin preparations using the pulstrode can be seen in Figure 6.3.



**Figure 6.3. Response to heparin and heparin spiked with PPS. Measurements for 400  $\mu\text{g/mL}$  heparin followed by heparin spiked with 10 wt% PPS (annotated with \*), where pulse sequence was a 1 s, 20  $\mu\text{A}$  current pulse, a 0.5 s open-circuit pulse, and a 15 s, 0 V potentiostatic pulse. Averages and standard deviations of measurements for heparin and 10 wt% PPS are -97.0 and  $\pm 0.693$  mV, and -106 and  $\pm 0.873$  mV, respectively. The average difference between pure heparin and PPS spiked heparin is -8.67 mV with standard deviation of  $\pm 0.473$  mV.**

As mentioned above, the difference in sensor behavior with higher concentrations of PPS in the heparin is due to the kinetics. The current pulse induces an ionic flux, driving all analytes with a complimentary charge toward and into the membrane.<sup>4-6</sup> It is not until the open-circuit pulse phase that the ion-exchanger in the sensing membrane can exchange less preferred analytes for the contaminant/target analyte (thermodynamics of cooperative ion pairing favors analytes with larger charge densities; in this case, heparin < PPS). The 0.5 s length of this pulse may not allow enough time for the ion-exchanger to completely exchange heparin for PPS before it is expelled back into the sample solution by the regenerative potentiostatic pulse. In single-use experiments, where concentrations of HCD species < 5 wt% can be readily detected, a potential drift down to the characteristic equilibrium EMF response is observed.<sup>1</sup> However, the time the sensor is allowed to equilibrate after injection of the polyion mixture is  $\sim 10$  min. Therefore,

experiments were carried out to extend the time length of the open-circuit pulse when using the pulstrode to assess whether better detection limits for PPS in heparin could be achieved. Time lengths of 1, 2, 5 and 10 s were studied, but results were not reproducible. For typical measurements with the 0.5 s open-circuit pulse, potentials are reproducible, and standard deviations are only 0.7% of the overall signal. However, with time periods longer than 0.5 s, the potentials generated exhibit relative standard deviations as large as 12% of the potentiometric signal. Measurements for all time periods can be seen in Figure 6.4.

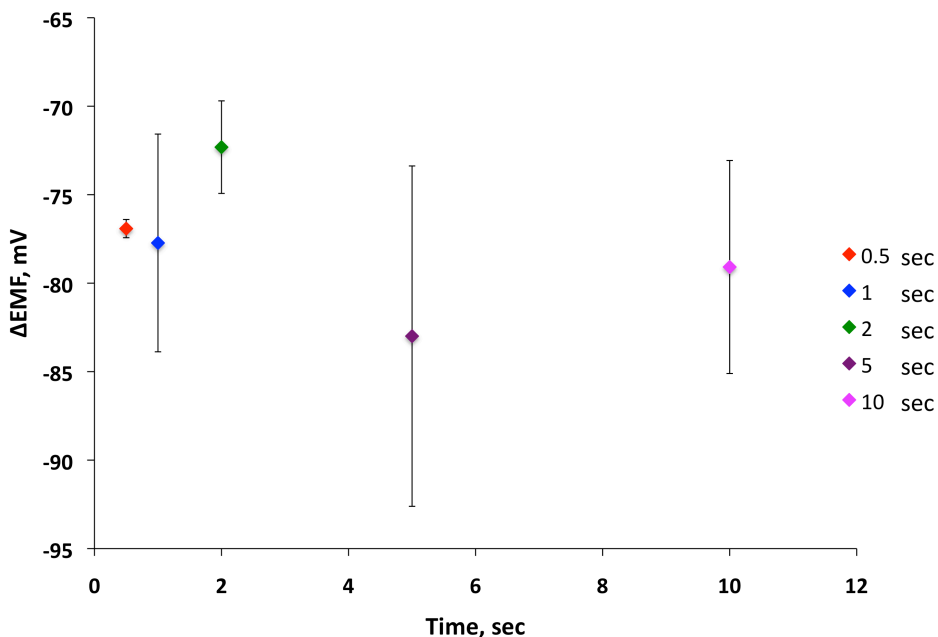


**Figure 6.4. Potential changes associated with different time lengths of open-circuit measurements. Each point represents the average potential change for a given time length. For the above points, standard deviations are as follows: (0.5 s) 0.515 mV, (1 s) 6.15 mV, (2 s) 2.62 mV, (5 s) 9.62 mV, and (10 s) 6.02 mV. A 1 s, 15  $\mu$ A current pulse and a 15 s potentiostatic pulse were applied.**

An explanation for this behavior may be clarified by studies reported by Lindner and co-workers.<sup>14</sup> The restoration of uniform equilibrium concentration profiles in

polyion sensing membranes is absolutely necessary if the sensor is intended to exhibit fully reversible and reproducible EMF functionality. The simplest restoration method is open-circuit zero-current relaxation, which is a diffusion-controlled process. Studies were carried out by Lindner and co-workers to determine the ideal method of membrane restoration in current-controlled membrane-based sensor systems. It was found that a minimum of 90 min was required for the open-circuit restoration method to obtain reproducible measurements,<sup>14</sup> and this is likely because the zero-current relaxation process following an applied current is very slow for most ISEs.<sup>15</sup> Hence, a reverse current was applied to speed up the restoration process (in contrast to studies carried out by Bakker and co-workers,<sup>4-6</sup> where a voltage pulse is used to restore the initial membrane composition). The 0.5 s time length of the open-circuit pulse is short enough to measure the sample/membrane interface potential reproducibly since any change in concentration profile within the 0.5 s is negligible.

Other factors were also taken into consideration regarding the membrane concentration profile during the current pulse. Hypothetically, the current pulse may not be sufficient in polarizing the lipophilic ion-exchanger salt within the membrane. By increasing the length of time of the current pulse, it was thought that increasing the concentration of ion-exchanger at the sample/membrane interface (see Figure 6.5) would increase the number of cooperative ion-pairs made at the surface. Therefore, optimization of the length of time for the current pulse was also pursued. All experiments were compared to results obtained using a 1 s 20  $\mu$ A current pulse. Other pulse lengths studied were 2, 3, 4 and 5 s. However, no detection limit improvement for HCD species was observed in comparison to results obtained in Figure 1. It is likely that

any improved polarization induced by increasing the time length of the current pulse was negligible.

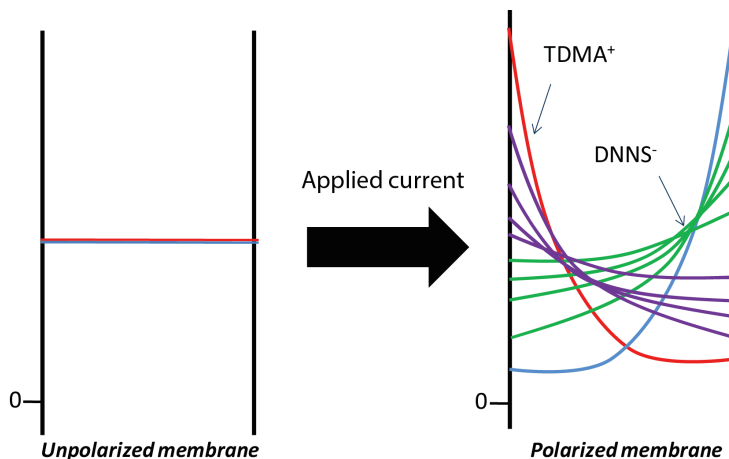


**Figure 6.5. Membrane concentration profile scheme.** As current polarizes the membrane, the concentration of salt components increase at opposite interfaces of the membrane. The purple and green traces represent  $\text{TDMA}^+$  and  $\text{DNNS}^-$ , respectively, migrating towards the opposite interfaces. The red and blue lines represent  $\text{TDMA}^+$  and  $\text{DNNS}^-$  at their final concentrations, just before the open-circuit zero-current pulse is applied.

The applied current magnitude can also be used to control the concentration of target analyte measured in pulstrode experiments,<sup>4-6</sup> and for that reason, optimizing the magnitude of current was also pursued. Intuitively, one would consider increasing the current magnitude to increase the concentration of the target HCD species within the membrane to improve detection limits for the HCD in heparin preparations. However, the literature suggests that lower current magnitudes are more beneficial in improving selectivity.<sup>6,7</sup> In addition, larger current magnitudes can destroy the membrane by permanently expelling portions of the lipophilic ion-exchanger salt. This is undesirable because the salt integrity (maintaining the 1:1 molar ratio of the TDMA/DNNS) is critically important to obtain reproducible EMF measurements. All experiments were compared to results obtained using a 1 s, 20  $\mu\text{A}$  current pulse and a 0.5 s open-circuit

pulse. Current magnitudes of 5, 10, 15, 25, 30, and 35  $\mu\text{A}$  were used to determine the optimal parameter. Note that the overall potential change to heparin increases as the current magnitude increases. However, detection limits of PPS in heparin do not improve when larger currents are applied. The optimal current magnitude was found to be 10  $\mu\text{A}$ , where a statistical significant difference was calculated at 2 wt% PPS (3 mV difference between heparin and heparin contaminated with 2 wt% PPS, Figure 6.1). However, in order for this method to have in-line applications, it would be desirable to have a larger potential difference. For example, a 3 mV shift in baseline may not be able to be differentiated from typical baseline drift if the pulstrode were used for in-line measurements during procedures that involve heparinization. Otherwise, special software would be needed to detect these smaller changes. Heparin preparations containing 4 and 5 wt% PPS gave signals that could be easily distinguished, with similar overall potential differences (subtracted from potentials of pure heparin) of -7 and -10 mV respectively. The results for heparin contaminated with 5 wt% PPS can be seen in Figure 6.6.

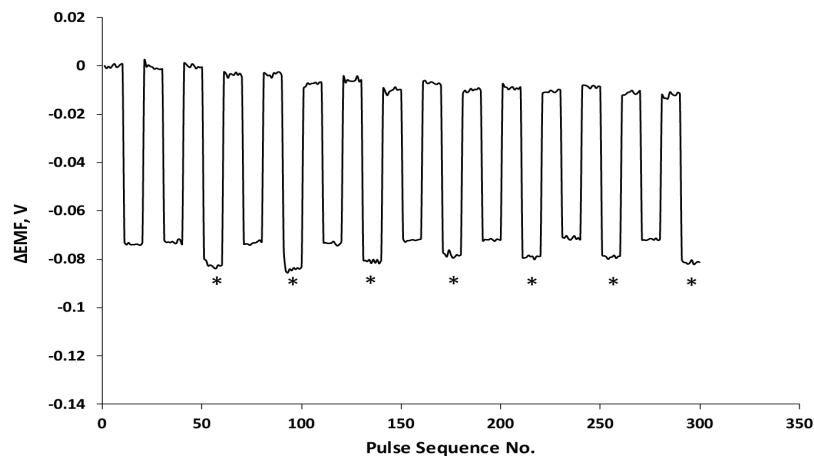


**Figure 6.6.** The dynamic response for 1 s 10  $\mu\text{A}$  current measurements for heparin and heparin samples spiked with 5 wt% PPS. Measurements of heparin spiked with 5% PPS are noted with asterisks (\*).

The potential change observed for 10 wt% PPS in heparin also increased (see Table 1), in comparison to other current magnitudes studied. Severe drift was observed for a current magnitude of 5  $\mu\text{A}$ , suggesting that the current magnitude is too low to maintain a stable baseline.

**Table 6.1.** Average potential change for heparin (0% PPS), 10 wt% PPS in heparin, and the average potential difference between the two measurements. For all measurements,  $n=3$ , except for 10 and 20  $\mu\text{A}$ , where  $n=7$ . The blue highlighted data represents the ideal current magnitude for detection of high charge density species (PPS) in heparin preparations with polymeric membrane compositions.

Current ( $\mu\text{A}$ )	Avg $\Delta\text{EMF}$		Avg $\Delta\text{EMF}$		Avg $\Delta\text{EMF}$	
	0% PPS	S.D	10% PPS	S.D	$\Delta\text{EMF}_{0-}$ $\Delta\text{EMF}_{10}$	S.D
10	-60.6	2.77	-87.3	3.52	26.9	1.58
15	-74.9	1.62	-86.6	2.43	11.8	1.05
20	-97.0	0.69	-106	0.87	8.67	0.47
25	-111	1.63	-121	2.00	9.53	0.76
30	-110	0.94	-122	1.76	12.2	0.88
35	-116	1.13	-130	2.89	14.6	1.10

## 6.4 Conclusions

Single-use polyanion sensors for the detection of high charge density contaminants have exceptional detection limits, where as little as 0.5 wt% of contaminant can be detected in heparin preparations.<sup>1</sup> Although the pulstrode configuration is not yet capable of such low detection limits, the reversible nature of the sensor would be much more desirable, especially as a commercial product. The pulstrode could potentially be used as an in-line system to monitor heparin during continuous infusion of heparin into a patient via a heparin drip line. Such a system could provide an alarm type system to alert medical personnel that some high charged contaminant is present in the heparin being given to the patient.

Further optimization of the pulstrode sensor for this application includes reformulating the membrane and improving polyanion detection in physiological NaCl levels, which is still an obstacle for the current pulstrode set-up. These ideas are discussed in more detail in Chapter 7.

## 6.5 References

- [1] Wang, L.; Buchanan, S.; Meyerhoff, M., *Anal. Chem.* **2008**, *80*, 9845-9847.
- [2] McKee, J., et. al., *J. Clin. Pharm.*, 2010, *50*, 1159-1170.
- [3] Kang, Y.; Gwon, K.; Shin, J. H.; Nam, H.; Meyerhoff, M. E.; Cha, G. S., *Anal. Chem.* **2011**, *83*, 3957-3962.
- [4] Shvarev, A.; Bakker, E. *J. Am. Chem. Soc.* **2003**, *125*, 11192-11193.
- [5] Makarychev-Mikhailov, S.; Shvarev, A.; Bakker, E., *J. Am. Chem. Soc.* **2004**, *126*, 10548-10549.
- [6] Shvarev, A.; Bakker, E., *Anal. Chem.* **2005**, *77*, 5221-5228.
- [7] Shvarev, A.; Bakker, E., *Anal. Chem.* **2003**, *75*, 4541-4550.
- [8] Makarychev-Mikhailov, S.; Shvarev, A.; Bakker, E., *Anal. Chem.* **2006**, *78*, 2744-2751.
- [9] Gemene, K.; Shvarev, A.; Bakker, E., *Anal. Chim. Acta* **2007**, *583*, 190-196.
- [10] Shvarev, A.; Bakker, E., *Talanta* **2004**, *63*, 195-200.
- [11] Perera, H.; Fordyce, K.; Shvarev, A., *Anal. Chem.* **2007**, *79*, 4564-4573.
- [12] Gemene, K.; Meyerhoff, M. E., *Anal. Chem.* **2010**, *82*, 1612-1615.
- [13] Kilgore, K. S.; Naylor, K. B.; Tanhehco, E. J.; et. al., *J. Pharmacol. Exp. Ther.* **1998**, *285*, 987-994.
- [14] Zook, J.; Lindner, E., *Anal. Chem.* **2009**, *81*, 5146-5154.
- [15] Pendley, B. D.; Gyuresanyi, R. E.; Buck, R. P.; Lindner, E., *Anal. Chem.* **2001**, *73*, 4599-4606.

## CHAPTER 7

### CONCLUSIONS AND FUTURE DIRECTIONS

#### **7.1 Summary of Results and Contributions**

Ion-selective electrodes (ISEs) have become important analytical tools for the detection and quantification of biomedically relevant ions due to their sensitivity, selectivity, and accuracy in measuring ion activities/concentrations. Although it was not considered possible to create ISEs for polyion detection, the breakthrough development of the single-use polymeric polyion selective (heparin) sensor opened the door to their application to many different biomedically important measurements.<sup>1-6</sup> The most notable being the quantitation of heparin in whole blood<sup>1-4</sup> and the detection of the contaminant/adulterant OSCS in commercially available heparins.<sup>5</sup> While the heparin sensor has been successfully applied in a variety of polyanion measurement applications, the reversible polyion selective pulstrode sensor was developed to address the irreversible nature of this single-use sensor. In addition, the pulstrode has provided a means to detect both polyanions and polycations with the same sensor/membrane device and has inspired a significant fraction of the research described in this dissertation.

In Chapter 2, a re-investigation into the working mechanism of the heparin sensor was initiated, and sufficient experimental evidence supports the previously reported

polyanion extraction mechanism.<sup>3,7</sup> Transport experiments were conducted using diffusion cells and varying polymeric membrane thicknesses, and diffusion coefficients of heparin within the polymeric membranes were calculated using equation 5 from Chapter 2 and determined to be reproducible. To verify this experiment, impedance spectroscopy was also carried out to determine the membrane conductivity, and as predicted, conductivity decreased as the target analyte migrated deeper into the sensing membrane. Gel electrophoresis was also employed to examine the polydispersity of low molecular weight heparin (enoxaparin), unfractionated heparin, and fractionated heparin. Based on the literature,<sup>8</sup> unfractionated heparin is void of LMW heparin species, and this was confirmed by the electrophoresis experiment.

In Chapter 3, the utility of the heparin sensor to detect OSCS in commercially available heparin preparations was evaluated. A blind study was carried out and heparin sensors were employed in screening a number of commercial heparin lots for OSCS that were provided by Baxter, Inc. After measurements were tallied, Baxter provided the relevant NMR data, which provided information regarding which samples were truly contaminated and the quantities of OSCS in each. As reported in Chapter 3, 100% of the sample measurements made with heparin sensors correlated with NMR data provided by Baxter, Inc. These sensor measurements did not provide any quantitative information, since in all cases the EMF change that was observed immediately went to the equilibrium/maximum value obtained for pure OSCS. However, such measurements can be readily used to determine qualitatively whether a sample is contaminated or not. Quantitative studies have been reported using the single-use sensor, but such experiments involve diluting heparin samples so the OSCS contaminant does not immediately induce

the equilibrium response. The rate of the EMF drift towards the larger EMF change for OSCS provides quantitative information for the contaminant.<sup>6</sup>

In Chapter 4, the use of a polyion selective pulstrode as a detector for FIA was explored and measurements were proven to be stable and reproducible. A thorough investigation into the longevity of the membrane composition within the flow-mode was carried out, and it was found that the leaching of the lipophilic cation-exchanger salt component (DNNS) was exacerbated by the constantly flowing the solution. Measurements made in static mode are stable for longer time periods; however, the pulstrode-FIA system has higher throughput capabilities. Five measurements per hour can be made in static mode, whereas the pulstrode-FIA was optimized to measure up to twenty samples per hour. Protamine was measured, heparin was titrated into the solution, and a decrease in sensor response to protamine was observed, suggesting that this FIA system could be used to detect heparin levels in a variety of samples.

In Chapter 5, the pulstrode was employed in monitoring polyanions/enzymatic activity degradation, where hexametaphosphate (substrate) and acid phosphatase (enzyme) were used as a model system. The EMF signal for the substrate was measured and enzyme was then added to the sample solution in which the pulstrode was placed in the polyanion sensing mode. A drift in potential towards the original baseline (in pure buffer) was observed and indicated substrate degradation by the enzyme. Reaction rates were calculated by measuring the slope of the EMF change during the first two minutes after enzyme injection. As expected, an increase in rate correlated with an increase in enzyme activity. Measurements were also made 24 h after the addition of enzyme to the substrate solution. No change in potential was observed when measurements of the

substrate-enzyme solution were subtracted from baselines generated by background buffer, indicating full the substrate degradation. In addition, studies were carried out to determine the effect of enzyme inhibitor (sodium tartrate) on acid phosphatase. As expected, a decrease in enzymatic activity rate was observed in proportion to the level of inhibitor present.

In Chapter 6, the polyion pulstrode system parameters were optimized for detection of high charge density contaminants in heparin preparations. Although detection limits of high charge density species in heparin with this system are not as low as those reported for the single-use polyion sensor, an overall improvement of the LOD for detecting PPS as a model polyanion impurity in heparin was achieved with the optimal parameters yielding a detection limit of 2 wt% PPS.

## **7.2 Future Directions**

In Chapter 3, the efficacy of the heparin sensor for the detection of OSCS was examined and a 100% correlation with NMR data provided by Baxter, Inc. was determined. The development of a commercial device for bench-top screening of commercially available heparin would be an obvious direction for this project. Recently, a single-use electrochemical strip-test device based on the principles of the heparin sensor has been developed and reported by Cha and co-workers,<sup>9</sup> but commercialization of this product has not yet been pursued.

Other applications for the single-use sensor include detection of fucoidan (Figure 7.1), a highly sulfated polysaccharide harvested from several species of brown seaweed,<sup>10,11</sup> which may have anti-inflammatory properties,<sup>12</sup> and may relieve pain

caused by osteoarthritis,<sup>13</sup> along with many additional medicinal applications.<sup>14-17</sup> Since there are both linear and branched structural variations and differing degrees of sulfation of fucoidan species,<sup>10,11</sup> it is important to have easy and cost-effective techniques to distinguish between the different variations so that further research can be pursued in determining the specific medicinal uses of each fucoidan variant. Extensive studies have been conducted by Prof. Kelly Mowery's group at Eastern University (Prof. Mowery is a former member of the Meyerhoff group), which yielded successful and comparable results with single-use polyanion sensors. Therefore, the reversible pulstrode technique may also have applications in fucoidan detection, and such pulstrode experiments should be carried out regarding the detection of this important high charge density polysaccharide.

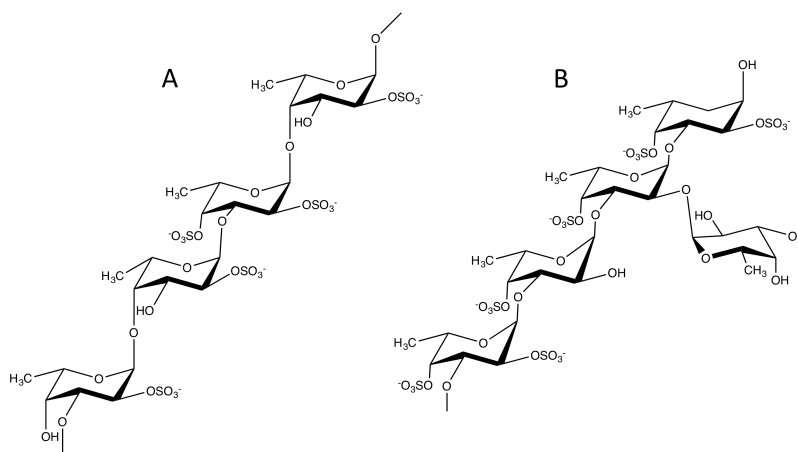


**Figure 7.1. Examples of structures of linear and branched fucoidans found in brown seaweed. (A) Linear fucoidan harvested from *fucus evanescens* (species of brown seaweed) and (B) branched fucoidan harvested from *chorda filum* (species of brown seaweed).**

Results reported in Chapter 4 suggest that there may be applications for monitoring protamine and heparin in whole blood using an FIA system. Preliminary experiments in whole blood have been carried out, but large background EMF changes prevented protamine peaks from being distinguished. One approach to improving protamine detection in whole blood when using the pulstrode as a detector in FIA would be to decrease the current pulse magnitude. Successful protamine detection in whole blood has been reported by Bakker and co-workers in static mode.<sup>18,19</sup> In these experiments,<sup>19</sup> a -2  $\mu\text{A}$  current was used to induce the ion flux and polarize the membrane. This smaller current magnitude may be key in reducing the large background response (physiological matrix). Therefore, optimization of current magnitudes  $< -12 \mu\text{A}$  should be pursued to achieve detection of protamine in whole blood samples using the FIA pulstrode arrangement. If significant EMF changes can be observed, then indirect detection of heparin levels in whole blood would be possible using a reagent stream of protamine at a fixed concentration to merge with the sample stream consisting of the injected whole blood sample.

Other potential pulstrode-FIA applications include additional studies of enzymatic reactions in the flow mode. Some preliminary experiments have been carried out using trypsin and protamine as a model system and have been successful (see Chapter 4). Slight modifications were made to the pulstrode-FIA system. Two carrier streams were employed: one containing protamine, and the other the background buffer, while the protamine concentration was held constant throughout. Different concentrations of trypsin were injected into the sample port, and both streams met at a mixing triangle. For increasing trypsin activity, an increasing inverted peak deviation from the protamine

baseline was observed. This set-up provides rapid measurements for enzyme assays, and additional studies should be carried out regarding alternate enzymatic systems (e.g., heparin/heparinase and DNA/DNases).

The higher sample throughput of the pulstrode-FIA method could also be improved by further reducing the length (time) of the potentiostatic pulse (described in detail in Chapter 4). The potentiostatic pulse must be sufficient in completely restoring the membrane back to its initial state in order to obtain reproducible EMF measurements. Therefore, reformulating the membrane to improve diffusion/ion mobility rates within the membrane phase could allow for even shorter potentiostatic pulse times, leading to an increase in the overall samples per hour measured (in comparison to the 20 samples/h reported in Chapter 4). A newer membrane formulation pioneered by Bakker and co-workers (discussed in Chapter 1) may provide enhanced membrane diffusion coefficients. The membrane is fabricated by impregnating the pores of a 25  $\mu\text{m}$  thick, porous polypropylene film with plasticizer doped with an ion-exchanger salt. This membrane is more fluid-like in comparison to the plasticized polymeric membrane used for pulstrode studies in this dissertation. Hence, diffusion coefficients and mobility of ions within such membranes should be much more rapid. With this newer membrane formulation, it may be possible to restore the initial ion concentration profiles more quickly and to further decrease the potentiostatic pulse length.

Reformulating the membrane, mentioned above, may also have an impact on monitoring enzymatic reactions in static mode as well. In Chapter 5, the pulstrode was not capable of monitoring enzymatic activity above 0.75 U/mL due to signal discontinuity. If the pulse sequence (17.5 s) can be shortened (minimizing time length of

potentiostatic pulse), it may be possible to diminish the signal discontinuity and expand the enzyme activity range the sensor can measure.

Another shortfall of the pulstrode system is that polyanions could not be measured in physiological NaCl background (i.e., 0.1 M NaCl). In contrast to results reported for protamine in whole blood,<sup>18,19</sup> heparin has yet to be detected in physiological matrices, even at large concentrations (> 400 µg/mL). Recently, improved detection limits for protamine in physiological background were reported.<sup>20</sup> Chronopotentiometric measurements employing a 2:1 DNNS/TDDA ion-exchanger salt doped into a thin porous polypropylene membrane allowed for a lower LOD. The Bakker group carried out such experiments for direct heparin detection. However, these experiments were unsuccessful. It was hypothesized that the energy output from the potentiostatic pulse (for membrane regeneration) was too weak to reverse the cooperative ion-pair formed by heparin and TDMA<sup>+</sup>. The protamine/DNNS complex is much weaker than the heparin/TDMA complex, simply because the absolute value of charge density for protamine is much smaller than heparin (20 vs. 70). In addition, smaller polyions are less thermodynamically preferred by the ion-exchanger (e.g., protamine is actually much shorter in length than heparin). Therefore, the 2:1 DNNS/TDDA doped membrane system was more successful in directly measuring protamine, since the potentiostatic pulse more easily regenerates initial membrane concentration profiles.

Various ion-exchangers were evaluated during the development of the single-use heparin sensor. Polymeric membranes doped with TDMACl gave the best responses, and this was likely because heparin forms the strongest cooperative ion-pair with TDMA<sup>+</sup>.<sup>1</sup> However, several ion-exchangers gave mid-range EMF responses to heparin in phosphate

buffered saline. These responses may have resulted from weaker ion-pairing with heparin. This weaker ion-exchanger/heparin complex is desirable for chronopotentiometric measurements so that the energy provided by the regenerative potentiostatic pulse is sufficient to reverse the cooperative ion-pair. A membrane formulation containing a cationic ion-exchanger other than TDMA<sup>+</sup>, in 100% molar excess to DNNS<sup>-</sup>, may improve heparin detection limits in physiological matrices, such as whole blood. This opens the door also for improving the pulstrode approach for the detection of HCD contaminants in heparin preparations. With this new membrane formulation, it may be possible to attain detection limits for pulstrode/chronopotentiometry as low as ones for single-use polyion sensors. This sensor would also improve the likelihood that the pulstrode could be used as an in-line monitor for clinical applications.

Lastly, miniaturizing the pulstrode may have the added benefit of measuring smaller sample sizes. Currently, static mode pulstrode measurements are carried out in 10 mL sample sizes. Miniaturizing the sensor size and the double junction reference electrode could enable new applications, such as detection in microfluidic devices, etc. Of course, smaller area electrodes, such as micro ion-selective polymer membrane electrodes<sup>21,22</sup> might be employed to achieve this goal, although with the much smaller membrane surface area comes much higher resistance, which could complicate things, but this may be overcome by reducing the membrane resistance (as mentioned above, e.g., using more liquid membranes).<sup>21,23</sup>

Overall, new fundamental and applied studies of both single-use and reversible pulstrode type polyion sensors have been reported in this dissertation. These devices

provide stable and reproducible EMF measurements proportional to polyion concentrations. The field of polyion detection regarding potentiometric and chronopotentiometric (pulsed) techniques has many potential biomedical/clinical and analytical applications. With more development and optimization, commercial products based on this technology may be possible and will provide industry and clinicians with convenient, rapid, and cost-effective means to measure/monitor important polyions.

### 7.3 References

- [1] Ma, S.; Yang, V.; Meyerhoff, M., *Anal. Chem.* **1992**, *64*, 694-697.
- [2] Ma, S.; Yang, V.; Fu, B.; et. al., *Anal. Chem.* **1993**, *65*, 2078-2084.
- [3] Fu, B.; Bakker, E.; Yun, J.; et. al., *Anal. Chem.* **1994**, *66*, 2250-2259.
- [4] Fu, B.; Bakker, E.; Yang, V.; et. al., *Macromolecules* **1995**, *28*, 5834-5840.
- [5] Wang, L.; Buchanan, S.; Meyerhoff, M., *Anal. Chem.* **2008**, *80*, 9845-9847.
- [6] Wang, L.; Meyerhoff, M. E., *Electroanalysis* **2010**, *22*, 26-30.
- [7] Bell, A.K.; Höfler, L.; Meyerhoff, M. E., *Electroanalysis*, **2012**, *24*, 53-59.
- [8] Bertini, S.; Bisio, A.; Torri, G.; Bensi, D.; Terbojevich, M., *Biomacromolecules*, **2005**, *6*, 168.
- [9] Kang, Y.; Gwon, K.; Shin, J. H.; Nam, H.; Meyerhoff, M. E.; Cha, G. S., *Anal. Chem.* **2011**, *83*, 3957-3962.
- [10] Zhang, J.; Tiller, C.; Shen, J.; Wang, C.; Girouard, G. S.; et. al., *Can. J. Physiol. Pharmacol.* **2007**, *85*, 1116-1123.
- [11] Cumashi, A.; Ushakova, N. A.; Preobrazhenskaya, M. E.; D'Incecco, A.; et. al., *Glycobiology* **2007**, *17*, 541-552.
- [12] Thring, T. S.; Hili, P.; Naughton, D. P., *Altern. Med.* **2009**, *9*, 27-27.
- [13] Myers, S. P.; O'Connor, J.; Fitton, J. H.; Brooks, L.; et. al., *Biologics.* **2010**, *4*, 33-44.
- [14] Hayashi, S.; Itoh, A.; Isoda, K.; Kondoh, M.; et. al., *Eur. J. Pharmacol.* **2008**, *580*, 380-384.
- [15] Levitskaia, T. G.; Creim, J. A.; Curry, T. L.; Luders, T.; et. al., *Health Phys.* **2010**, *99*, 394-400.
- [16] Juffrie, M.; Rosalina, I.; Rosalina, A.; Damayanti, W.; et. al., *Indones. J. Biotechnol.* **2006**, *11*, 908-913.
- [17] Bojakowski, K.; Abramczyk, P.; Bojakowska, M.; Zwolinska, A.; et. al., *J. Physiol. Pharmacol.* **2001**, *52*, 137-143.
- [18] Shvarev, A.; Bakker, E., *J. Am. Chem. Soc.* **2003**, *125*, 11192-11193.
- [19] Shvarev, A.; Bakker, E., *Anal. Chem.* **2005**, *77*, 5221-5228.
- [20] Bakker, E.; Crespo, G. A.; Afshar, M. G.; Saxer, T.; Bendjelid, K., *Chimica*, **2013**, *67*, 350-350.
- [21] Ammann, D.; Pretsch, E.; Simon, W., *Anal. Chim. Acta* **1985**, *17*, 119-129.
- [22] Morf, W. E., *The Principles of Ion-Selective Electrodes and of Membrane Transport*; Elsevier Scientific: New York, 1981
- [23] Crespo, G. A.; Afshar, M. G.; Bakker, E., *Angewandte* **2012**, *51*, 12575-1257.